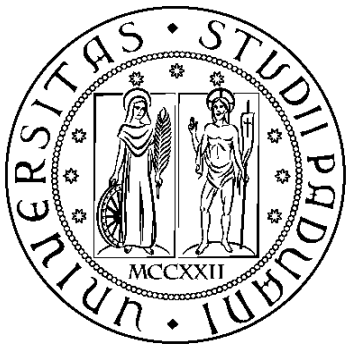

UNIVERSITY OF PADUA

DEPARTMENT OF INDUSTRIAL ENGINEERING

Master Thesis is Environmental Engineering

MONITORING AND MODELING NITROGEN DYNAMICS AT THE TIDAL SCALE IN A SALT MARSH OF THE VENICE LAGOON

Supervisor
Prof. Luca Palmeri

Co-supervisor
Dr. Damiano Baldan

Student
Luca Bomben

ACADEMIC YEAR 2016-2017

Abstract

The Venice Lagoon is a delicate ecosystem, whose equilibrium is threatened by many factors, such as industrial and fishing activities, deep channel excavation, subsidence and eustatism. One of the most damaged part of its ecosystem are the salt marsh, which are constantly being loss due to erosion. In order to understand better their role in the lagoon, a long series of sampling campaigns (April – October 2017) is carried on during single tide events, which is the first one, to our knowledge, carried on in a salt marsh of the lagoon. Water samples are collected inside and outside the salt marsh and analyzed to obtain ammonium (NH_4^+), nitrate (NO_3^-) and dissolved organic nitrogen (DON). Moreover, temperature, dissolved oxygen (DO) and salinity are registered using WTW multiparametric probes. The results indicate a heterogeneous and complex behavior of the salt marsh in the different analyzed tidal cycles, typical of mature ecosystems, and it is possible to partially detect a general trend. Successively, a mass balance model for the salt marsh is calibrated using the observed concentration values, a selection for the best model is carried on and the annual fluxes in import and export are then evaluated. Lastly, the nitrogen loads reduction ecosystem service provided by the salt marsh is calculated. A total annual import of 12.37 gN m^{-2} y^{-1} is obtained, for an economic value of 1170 € ha^{-2} y^{-1}.

Summary

1. Introduction

1.1 Aim and outline of the thesis

The Venice Lagoon sustained for centuries and still sustains the life of the people that live in Venice and in all the small islands of this basin. The old Venetians knew the importance of the preservation of the peculiar characteristics of this coastal wetland, but in the last century, this attention was lost. In Porto Marghera, a huge industrial area was built, the channels of the lagoon were deepened to allow the passage of big ships, the disruptive fishing activities increased and subsidence and eustatism are increasingly greater concerns. All these actors damaged the environmental status and quality of the whole Lagoon (D'Alpaos, 2010).

The loss of coastal ecosystem is a worldwide problem and the lagoon is no exception, due to the already mentioned anthropic pressures. One of the most affected ecosystems in the lagoon is the salt marshes, with a loss of circa 72% of their surface between 1901 and 2003 due to erosion (D'Alpaos, 2010). They are characterized by a great ecological importance and a high economic value because of the ecosystem services they provide (Costanza et al., 1998; Clarkson et al., 2013), given that they are among the most productive ecosystem worldwide (Hopkinson and Giblin, 2008). In this framework, the LIFE VIMINE Project (www.lifevimine.eu) aims to protected the salt marshes with small soil bioengineering works, including, in an integrated perspective, also the people of the lagoon and other different stakeholders.

In this thesis work an existing mathematical model for nitrogen cycling salt marsh at subtidal time scale (Baldan, 2015)has been improved, to obtain an evaluation of the nitrogen mass balance and of the nitrogen cycling ecosystem service provided by this ecosystem. This nutrient is chosen because it is a sensitive element for the lagoon trophic state, due to its high loads from the surrounding areas, which are still higher than the fixed quality levels for the basin (ARPAV, 2012) and the existing regulation limits its load to the lagoon (Regione Veneto, 2000). Also dissolved phosphorus phosphorus was analyzed toghether with nitrogen but not modelled, due to the constant low concentrations.

A long set of sampling campaigns was carried on between April 2017 and October 2017, covering spring and summer, when biological activity is higher due to the temperature. Water samples were collected inside and outside of a marsh creek and later analyzed in the laboratory for ammonium (NH_4^+), nitrate (NO_3^-) and dissolved organic nitrogen (DON). Two WTW probes were installed in a marsh creek to measure temperature, salinity and dissolved oxygen (DO) along the tidal events and water samples were taken also outside of the salt marsh. The geometry of the salt

marsh was finally measured. This amount of data was then used to improve the hydraulic of the system and to assess the seasonal behavior of the salt marshes and its related the nitrogen dynamics, along with a literature research on previous salt marshes mass balances or kinetic rates of different biochemical processes. The model was calibrated at the subtidal time scale using all these dataset in order to obtain an optimal set of parameters describing the nitrogen dynamics within the salt marsh. A choice of a best version of the model was carried out using Nash-Sutcliffe efficiency and Akaike's information criterion as indicators of the model efficiency and goodness of fit. Finally, the best model's results was at the monthly time scale were used to obtain an annual mass balance and an economic evaluation in terms of nitrogen cycle regulation ecosystem service provided by the salt marsh was performed.

1.2 The Venice Lagoon

The Lagoon of Venice is a shallow water body that covers an area of around 550 km^2 of the north coast of the Adriatic Sea and is the largest wetland in the Mediterranean Basin (Figure 1.1). It

Figure 1.1 View of the Venice Lagoon (Google Earth, 2017).

is characterised by a length of 50 km, a width of around 10 km and mean depth of 1.1 m circa. It has three outlets (from north to south: Lido-San Nicolò, Malamocco and Chioggia) that connect the lagoon with the sea and only the 8% of the total surface is occupied by islands and by Venice. The main freshwater tributaries are the Dese River and the Marzenego River (through the Orsellino channel), which naturally discharge a great amount of nutrients in the lagoon water, coming from wash-out and run-off of agricultural soils and diffused emissions.

Since the Roman times, the population of the surrounding territories moved into the lagoon, attracted by the protection that it gave from barbaric invasions, but also by the food source that it can provide. This started the first city nucleus that, later in the centuries, became the city of Venice and the Serenissima Republic.

For this reason, the lagoon has been influenced by the anthropic presence since long time (D'Alpaos, 2010). However, its maintenance was always a priority for the Venetian Republic, because the peculiar characteristics of this area were well known and protected: an example is the decision to banish fishing activities that damaged the natural resources in 1173 (Solidoro et al., 2010). The Republic also diverted the Brenta and the Sile Rivers directly into the Adriatic Sea, because they were filling the lagoon with their sediment transport. In addition, the Po River was diverted southward, in order to prevent it to fill the coastal area near the lagoon.

In the 20th century, a new industrial area was built in Porto Marghera, which caused a great pollution in particular in the central part of the lagoon, and created a strong environmental pressure upon the basin and its ecosystem (Pastres et al., 2004). This pressure was worsened by other factors, like:

- Fishing activities, which destroy the lagoon bottom with the dredging action, increasing sediment resuspension and nutrient release in the water column;
- Subsidence, eustatism and groundwater extraction, which change the morphology of the area, lowering the bottom level and increasing the mean sea level, causing more frequent flooding events (during the daily tidal cycle);
- Erosion of specific areas of this ecosystem, like salt marshes (see Paragraph 1.3);
- Pollutants emission from sewage discharge from Venice and the urban areas that surround the lagoon.

The pollutants generated by Porto Marghera were mainly nutrients (ammonium, nitrate and phosphorus) and heavy metals (Hg, Pb, As, Cd, Zn, and Ni), but also organic pollutants (POPs), polychlorinated biphenyls (PCBs), hexachlorobenzene (HCB), and polycyclic aromatic hydrocarbons (PAHs) are emerging concerns (Solidoro et al., 2010).

All these pressures strongly contributed to move away the ecosystem from a natural trophic state. Due to increasing environmental attention, the situation was improved from the ‘70s, when some industries were closed, new wastewater treatment plants were built and phosphorus content in domestic detergent product was decreased (Pastres et al., 2004). In this way, the trophic state of the Lagoon has improved but this area has not yet reached a satisfactory ecosystem steady state (Bendoricchio and De Boni, 2005). Indeed, in 2012 the nitrogen loads were still above the fixed quality levels of the regional legislations (Regione Veneto, 2010): 4 500 ton/y against the 3000 ton/y of the limit (ARPAV, 2012). These data, though, do not take into account the discharges coming from the city of Venice and the atmospheric deposition, which increase the total annual nitrogen loads.

Despite the abovementioned pressures the Lagoon of Venice is still an exceptional site because of the variety of ecosystems, of the high biodiversity and of lasting historical successful co-existence of nature and society. For all this reasons, the Lagoon of Venice falls within the Site of Community Importance IT3250031 “Laguna Superiore di Venezia” (Northern Venice Lagoon), as per the European Commission Habitats Directive (92/43/EEC), and within the Special Protection Area IT3250046 “Laguna di Venezia”, as per the Birds Directive 2009/147/EC of the European Parliament. It is also one of the World Heritage Site of UNESCO from 1987.

Figure 1.2 View of Venice lagoon salt marshes (Google Earth, 2017).

1.3 The salt marshes

Salt marshes are an important feature of the coastal lagoons and constitute a transitional ecosystem between the inland and the sea being formed from tidal and river sediments and populated by different plants species that are halophytes (salt tolerant,(Spohn and Giani, 2012). They are characterized by the presences of meandering marsh creeks, causing a huge exchanging surface between the tidal water and soil (Figure 1.2). The vegetation presence is fundamental for the marshes, since the plants increase flow resistance, increase sedimentation rates and so they contribute to the marsh accretion and evolution (D'Alpaos and Marani, 2015).

Salt marshes can be found along the Atlantic coastline and the Gulf of Mexico, in the Pacific area, in Australia and New Zealand and in tropical environments. However, around the world, the loss of coastal habitats is a widespread problem (Barausse et al., 2013). Erosion is the main factor but these ecosystems are also threatened by increasing rates of relative sea level rise and limited sediment supply (D'Alpaos and Marani, 2015).

Salt marshes are among the most productive ecosystems in the world (Hopkinson and Giblin, 2008) and they provide a substantial ecological and economic value, classified as ecosystem services (Costanza et al., 1997; Clarkson et al., 2013). The provided ecosystem services are numerous:

- Provisioning services, like food source, freshwater supply and raw materials and in the Lagoon they also provide havens for many fish species juvenils;
- Regulating services, which means, for example, moderation of extreme event (in the lagoon, tidal peaks smoothening in particular), regulation of water flows, water treatment, erosion prevention; moreover, they have been identified as carbon sinks and nitrogen reservoirs and play an important role in mitigating climate change due to their high carbon sequestration rates (Chen et al., 2017), which is confirmed also in lagoon;
- Habitat or supporting services, like lifecycle maintenance and gene pool protection;
- Cultural services, as aesthetic value, recreation/tourism, spiritual experience and cognitive information: for example, the cultural value of Torcello's basilicas.

All these provided services generate a high economic value, which can vary, according to different estimations, between 10 000 \$ ha^{-1} y^{-1} (Costanza et al., 1998) and 214 000 \$ ha^{-1} y^{-1} (Clarkson et al., 2013).

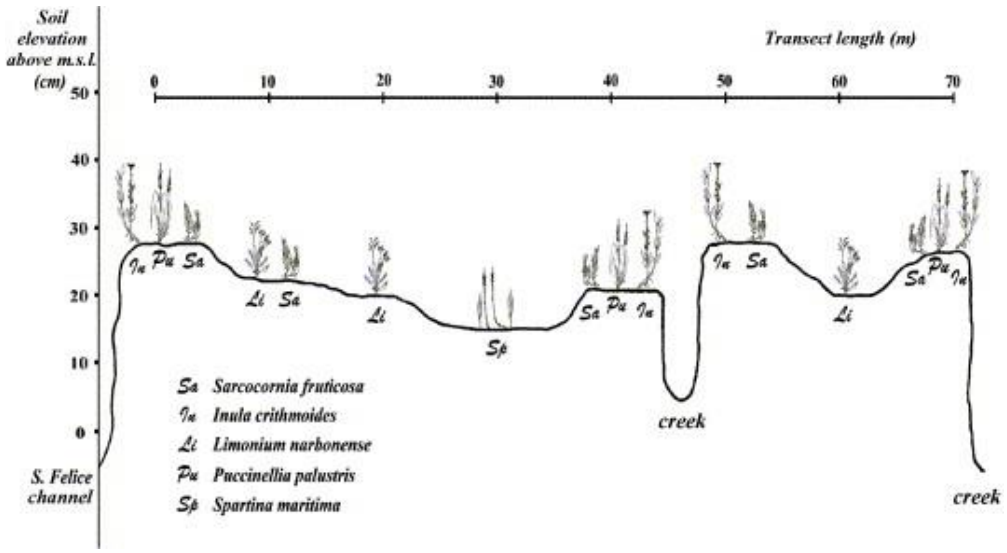

Figure 1.3 Example of vegetation distribution (Silvestri et al., 2005

Sal marshes are exposed to a unique combination of environmental variables, including strong salinity gradients, fluctuating water levels and anaerobic, waterlogged sediments. A rich biogeochemical diversity is commonly present and this leads to a wide array of possible N transformations but complicates the full quantification of the marsh N cycle (Hopkinson and Giblin, 2008).

In the Venice lagoon, salt marsh cover around 47 km^2, with an higher abundance in the northern part of the lagoon, better preserved. Salt marshes are characterized by an elevation of 20÷40 cm above the mean sea level. Only on the borders it is possible to observe higher elevations, up to 50 cm (Bonometto, 2013). Different types of halophytic vegetation are present and the main plant species are *Spartina maritima*, *Sarcocornia fruticosa*, *Salicornia veneta* and *Limonium narbonense*. A visible spatial variability in the plant distribution is recognisable, due to the slightly different salt tolerance of the plants (Figure 1.3). For example, *S. maritima* tends to grow in the central and lower part of the salt marsh, while the other species tend to be found on the marsh edges or along the marsh creek borders (Silvestri et al., 2015).

1.4 The LIFE VIMINE Project

Salt marshes in the Venice Lagoon are undergoing an intensive erosion process, which is unfortunately common to many coastal ecosystems around the world.

The causes are numerous, of both natural and anthropic origin. Among the first ones, it is possible to recognize the effect of tidal currents and wind-induced waves, whose combined effect results in the resuspension and transport of sediments out from the lagoon, into the sea. However, the waves generation depends of wind speed and fetch length, but the last one depends also on the presence of the salt marshes themselves; thus, the erosion and disappearance of salt marshes is a cascading, self-reinforcing process (D'Alpaos, 2010).

As far as anthropic causes are concerned, the absence of riverine sediment and freshwater inputs, the construction of long jetties and excavation of deep lagoon channels (which have modified the lagoon currents) are among the most important and significant. Moreover, motor boats generate waves that erode bottoms and salt marshes borders; clam fishing resuspends sediments and destroys microphytobenthos film; subsidence of lagoon bottom and sea level rise can generate higher tidal processes, which concur to the disruptive erosive action (Barausse et al., 2013).

Over the past decades, the surface of salt marshes has strongly decreased, from 170 km^2 in 1901 to 47 km^2 in 2003 (-72%; D'Alpaos, 2010). Comparing bathymetric maps of 1927, 1970 and 2002, erosion rate shows an acceleration: from a loss of 0.3 $Mm^3\ y^{-1}$ between 1927-1970 to a value of 0.8 $Mm^3\ y^{-1}$ between 1970 and 2002. It is also possible to see the difference in the channel size in 2002 and in 2017 in Figure 1.4.

To stop this process, the LIFE VIMINE Project aim to protect salt marshes border from erosion using soil bioengineering techniques, with very low environmental and landscape impact (Barausse et al., 2013).

Biodegradable fascines made up by wooden branches and vegetable nets are placed along the marsh borders and the space between the fascines and the marsh border is filled with sediments, so

Figure 1.4 Differences in a channel between marshes due to erosion (Google Earth, 2017).

that this area works also as a sediment trap. Other applied techniques are the utilization of groynes and wind barriers. The first ones are made of fascines and placed perpendicular to the marsh borders, in order to modify local hydrodynamics by slowing down water velocity and fostering sedimentation. The second ones are fascines placed perpendicular to the main wind direction, in order to slow down wind-induced currents.

Other important aspects of this project are the integrated approach and the prevention, which are developed through the involvement of local communities and stakeholders, so that the operations could be economically viable beyond the end of the project. Moreover, local communities are necessary, due to their knowledge of the lagoon and ability to recognize rapidly the points where erosive process is starting, in order to prevent the damages to become irreversible.

Furthermore, a short supply chain for the fascines construction is created, because the wood comes from the pruning of vegetation along the Dese and Zero Rivers and from lagoon islands, thus reusing a material that would become a waste.

The chosen area for the development of this project is located in the northern part of the Venice Lagoon, between Dese River estuary, the group of islands north of Mazzorbo, and the mudflats area in front of Tesséra airport. The selected salt marshes are located immediately south of Palude dei Laghi and adjacent to Mazzorbo Channel.

2. Materials and methods

2.1 Site description

The selected salt marsh for the field surveys carried out in this thesis is located in the northern part of the Venice Lagoon, near the Dese River estuary, along the Dese channel and near Palude dei Laghi (Figure 2.1). It was selected for different reasons:

- it is easy to reach using a boat;
- it is a relatively high marsh, respect to the surrounding salt marshes, which delete the risk that tidal water may flood the whole marsh too frequently (avoiding hydraulic disturbance and different water input);
- it has a central and big marsh creek, which ensure that the water flows into the marsh only through it, and it also defines a central basin, which is related to this creek (Figure 2.2);
- the salt marsh is relatively compact, with few inputs and few outputs, which allow to sample in a single point which is very likely representative of that specific input (or marsh creek);

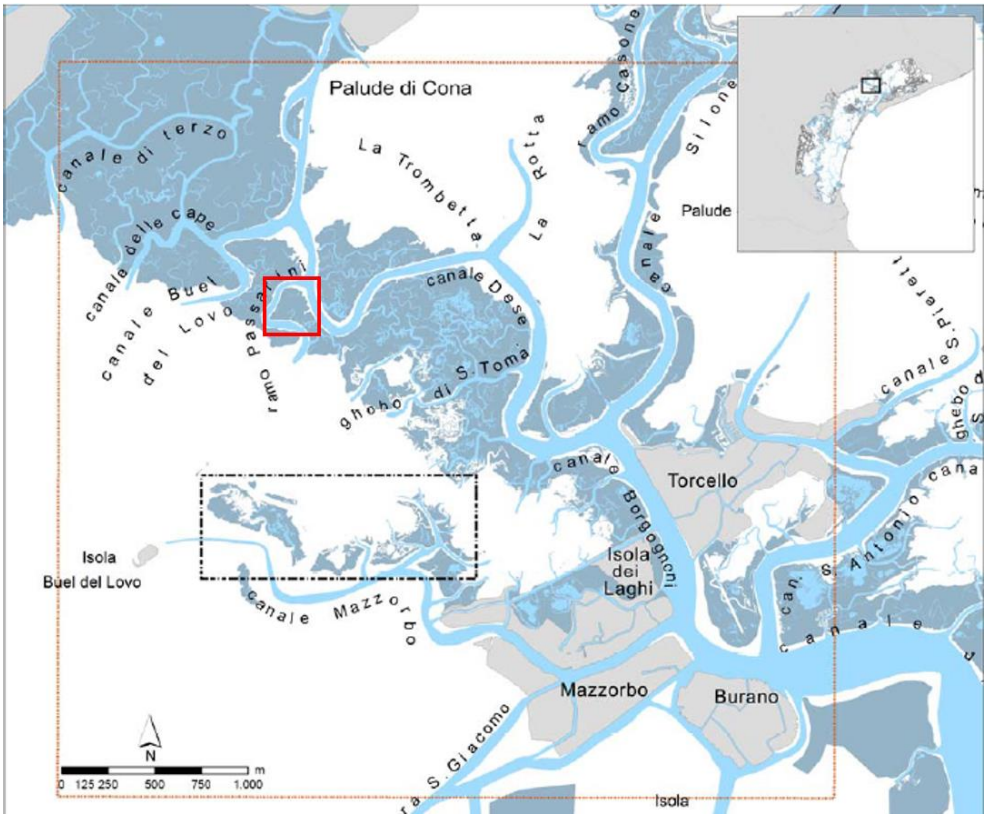

Figure 2.1 In the red box, the location of the selected marsh; in the black box, the LIFE VIMINE project selected area

Figure 2.2 View of the selected salt marsh (Google Earth, 2017). Red arrow indicates the direction that the tide follows, red circle indicates roughly the basin connected to the salt marsh creek.

- the presence of a palafitte with a “bilancia”, a big net used to fish in the near channel, which allows to keep the instruments and the samples safe (and in the shadow during the summer period) and also allows to keep the feet upon a solid basis and not on the mud for hours.

2.2 Monitoring description

The selection of the correct tidal and meteorologicalconditions for the monitoring and sampling campaign is based upon the astronomical tide prediction made by the CSPM (“Centro Previsioni e Segnalazioni Maree”, center for the prediction and signaling of tide). The predicted tide event must be not too low (the water must enter into the marsh creek and reach the sampling point; point 1 in Figure 2.3) and not too high (the water must not submerged the whole salt marsh). The prediction is referred to a fixed point or a mareographic zero, called VPS (Venezia Punta della Salute), obtained at the end of the XXI century. Due to subsidence of the lagoon bottom and eustatism, this reference system is now lower of 26 cm and this correction must be taken into account when the tide event is referred to the mean sea level. A suitable tide event for a sampling campaign is characterized by a minimum of 50 cm and a maximum of 70 cm and it usually lasts 6 hours.

The selection of the day must also take into account other factors:

- The chosen day cannot be during the weekend, for practical reasons, and the Friday, if it is not possible to filter the samples the next day;
- The weather conditions must be suitable for the campaign; rain tends to make the ground more "muddy" but also it becomes another nitrogen input to the salt marsh, which disturbs the analysis;
- The wind condition must be suitable, no strong Sirocco or Bora must be present because these winds can foster or prevent the flux of water into the marsh creek and can anticipate or delay the tide peak;
- The predicted tide peak must be not too early during the morning or too late during the afternoon, for practical reasons; the peak must be approximately between the 10:00 and the 15:00 and it is predicted using the CPSM analysis adding a delay of 1 h 15 min / 1h 30 min due to the meandering structure of the lagoon channels and to the shear stress between the water and the bottom; the daylight saving time must be also taken into account, because the CPSM prediction is based on the winter time.

The municipality of Venice provide the tide prediction combined with the forecasted meteorological conditions but only on the short term, which means for the subsequent two days.

Figure 2.3 Location of sampling points (Google Earth, 2017).

The monitoring period went from April 2017 to October 2017. The aim of the sampling campaigns is to collect several water samples inside the salt marsh creek and outside of the salt marsh (respectively in point 1 and 2 in Figure 2.3). The samples are collected during the flood (3 samples), at the tidal peak (1 sample) and during the ebb (3 samples), in order to observe the tendency of the nitrogen compounds during the tidal cycle. the time interval for samples collection is 45-60 min, depending on the tidal cycle duration and height of the peak. Sometimes, in the field it is not so easy to catch the tidal peak, due to different conditions that control the tidal cycle, which cannot allow a perfect estimation of the peak moment. For this reason, it is easy that only 5, 6 samples are collected during a field survey, which means the first 3 samples for the rising tide and the last 3 samples for the descending tide (or 2 for the rising tide, one for the peak and two for the ebb). This has no effect on the successive data analysis and on the significance of the observed trend along the tidal cycle.

Samples outsidethe salt marsh, are collected at the surface (10-20 cm from the free water surface) and at the bottom (circa 50 cm from it) of the channel, in order to appreciate concentrations differences due to channel stratification. A couple of samples (surface and bottom) is collected when the tide is rising, the second couple at the tide peak and the last couple then the tide is going down. Therefore, a total number of six samples was collected from the channel in a single campaign.

Figure 2.4 Location of the graduated stick (left) and the multiparametric probes (right).

Figure 2.5 View of the five analyzed cross-section (Google Earth, 2017).

All these samples are stored in a container with ice to keep the temperature low (slow down kinetics) and are then alanyzed in laboratory to get the concentrations of ammonium nitrogen (NH_4), nitrate (NO_3^-), dissolved organic nitrogen (DON) and orthophosphate (PO_3^{-4}).

To obtain data on the real tidal event in the marsh, the water level was measured every time a sample was collected from the marsh creek, with a graduated stick posed in the center of the marsh creek (Figure 2.4).

Moreover, during the whole field survey, two multiparametric probes (WTW Multiprove, Figure 2.4) were attached to two different sticks and posed in the center of the marsh creek. They were used to measure salinity, dissolved oxygen (DO) and temperature continuously, with a time interval of 5 minutes. WTWs were at the beginning of the tidal cycle, but the sensors are located a few centimeters from the bottom of the marsh creek, so the first and last few values must be deleted because they do not refer to real water parameters measurement.

Five cross sections were considered in order to assess the behavior of the free water surface along the small channel (Figure 2.5). This was important to improve the hydraulics input data for the hydraulic submodel (see Paragraph 2.5.2).

2.3 Sampling procedure

The sampling procedure involves different techniques and several instruments. As far as the sampling in the marsh creek is concerned, the samples were taken with two different procedures, depending on the water level inside the creek.

If the water level is very low (few centimeters), a vacuum pump was used (Figure 2.6; Figure 2.7). It is made of an electric pump, connected to a Büchner flask, which create the vacuum inside it. A small plastic tube with little holes is connected to the flask, and is used to suction the water from the creek (Figure 2.7). This system is used in order to create the smallest possible disturbance to channel bottom.

When the water level is higher, a plastic becher is fixed at the extremity of a rod and it is used to take the water samples, avoiding generating disturbance in the creek bottom.

The samples are stored inside plastic bottles (500 mL and 1000 mL)primed with a little amount of the same water (Figure 2.6).

Figure 2.6 From top left to bottom right: the vacuum pump used for sampling, the Niskin bottle and the "messaggero" (between the two caps), the two WTW multiparametric probes, the 1000 mL bottles used to contain the samples.

Figure 2.7 Sampling in the marsh creek using the vacuum pump and the pierced plastic tube.

During the last campaigns, though, the vacuum pump was always used to sample the water inside the salt marsh, to be consistent with the same sampling methodology.

In the channel outside the salt marsh, a different procedure was applied. For the surface samples, the plastic bottles are used directly (prior priming of the container) to take a water sample. For the bottom ones, a Niskin bottle was used (Figure 2.6). This is a plastic cylindrical instrument, which has two opening (on the top and on the bottom) with two separate covers that are connected with each other using some rubber bands. The Niskin bottle is lowered using a rope keeping the covers open, so that the internal part is primed during the descent, and with the rubber bands under tension. A series of weights is attached to the bottle, in order to facilitate its descent. The covers can be closed with a "messenger" (a small lead counterweight), which slides along the rope to hit a sort of switch. This "switch" release a snap-hook, which is connected to a metallic cable connected to the covers that keeps them open. In this way, the elastic rubbers enter in action and close the two covers, collecting the water inside the bottle.

Due to some problems with this instrument (one of the supports for the switch broke), another instruments to take deep samples was built: a 1000 mL plastic bottle was mounted on a rod and a

Figure 2.8 On the left, the positioning of the rope perpendicular to the creek for the cross section analysis; on the right, vertical measurements are taken.

rope was attached to the cap. The rod is then lowered into the channel and the rope is pulled, in order to open the cap and fill the bottle.

All the samples are collected into a camping fridge with iced water bottles, in order to keep them fresh and avoiding process of degradation inside them, especially in summer time. They are then transported into a real fridge in the laboratory and filter the next day.

Other analysis of the salt marsh regarded the geometry of the creek in different sections. To get these data, two poles were driven into the marsh ground, one for each side of the creek, and then a measuring rope divided into centimeters (one notch every 10 cm) was stretched between the poles (Figure 2.8) and the inclination was controlled centering the bubble. For every notch, a vertical measurement was taken (in cm) between the rope and the marsh bottom using a measuring tape (Figure 2.8). Then the marsh creek bottom was reconstructed using AutoCAD software (https://www.autodesk.it/products/autocad/overview).

Other instruments that were used or it is important to have in the campaigns are:

- WTW probes manual;

- Manual vacuum pump (as a reserve);
- Zip ties (to fix the probes to the plastic tubes);
- PVC tubes;
- Toolbox and scissors;
- Permanent markers and pens (to order the samples and write down data and notes);
- Field survey notepapers (printed before the campaign);
- Folder to keep the notepapers and the probes manual;
- Bottles with freshwater (to clean the instruments);
- Paper towel (to clean the instruments);
- 9V battery for the pump (as a reserve);
- Weights for the Niskin bottle;
- Plastic container to keep all the instruments and facilitate the transport.

2.4 Laboratory procedure

The samples, after being collected in and outside the salt marsh, are transported in the laboratory and put into the fridge. The next day, all the sample are filtered using a 45 μm glass fibers filter. Filtered samples are then frozen to wait for the chemical analysis, which are carried on following procedure described by APAT, CNR-IRSA, 2003; Grasshoff et al. (1983) and Greenberg et al. (1992).

For the phosphate (PO_4^{-3}), 10 mL of samples are taken and 400 μL of mixed reagent and 400 μL of ascorbic acid are added. The mix is then analyzed with the spectrophotometer (Figure 2.9), adding also a blank solution to the samples list, which is purified water with the same reagents used for the water sample.

Starting from the value given by the instrument, to all the values must be subtracted the value of the blank solution and then the concentration [mg/L] is calculated as:

$$P - PO_4 = X * \frac{30.97}{1000} \quad (1)$$

where X is the value given by the spectrophotometer, 30.97 is the molecular weight of the phosphorus and 1000 is a value to transform from μg/L to mg/L.

Figure 2.9 Top: spectrophotometer used for the chemical analysis. Bottom: reduction column used in the chemical analysis for nitrate and TDN.

For the ammonium (NH_4^+), 10 mL of samples are taken and mixed with 400 µL of phenol and 400 µL of potassium ferrocyanide. Then 1 mL of oxidizing solution is added and the mix is analyzed with the spectrophotometer. In this case, no blank solution is needed. The concentration value is then obtained as:

$$N - NH_4 = X * \frac{14}{1000} \quad (2)$$

where 14 is the molecular weight of the nitrogen.

For the nitrate (NO_3^-), 20 mL of samples are taken and diluted to 100 mL using ammonium chloride. The mix is then passed through a reduction column (Figure 2.9), made of chromium grains covered with copper, and a peristaltic pump. The first 50 mL are discarded, and then 10 mL are taken, mixed with 400 µL of sulfanilamide and 400 µL of NED and analyzed with the spectrophotometer. Moreover, other samples, which are blank solutions and standard samples of a solution with a known concentration (after passing through the column), are analyzed. These two are used to determine the reduction yield of the column: indeed, different samples are taken at

different moments during the usage of the column, to calculate at the end an average value. The reduction yield R is then calculated as:

$$R = \frac{\overline{ST} - \bar{B}}{20} \tag{3}$$

where $\overline{ST}$ is the average value of the standard samples, while $\bar{B}$ is the average value of the blank solution and 20 is the known concentration of the standards. The concentration of nitrate is then calculated as:

$$N - NO_3 = \left(\frac{X - \bar{B}}{R} * 5\right) * \frac{14}{1000} \tag{4}$$

where 5 is a dilution ratio (20 mL of water samples into 100 mL after the dilution).

For the dissolved organic nitrogen (DON), the total dissolved nitrogen (TDN) analysis is required. This follows a similar procedure to the one of the nitrate. 20 mL of samples are taken and added to 20 mL of oxidizing solution (potassium persulfate in basic environment), digested in autoclave for 45 minutes and neutralized with concentrated sodium hydroxide. Then, the chlorine in excess is removed in the gaseous form by agitation and the samples are diluted to 100 mL using ammonium chloride. Eventually, the procedure follows the same steps of the one for the nitrate, including the creation of samples for blank solutions and standards samples to calculate the reduction yield (using again Eq. 4). In this case, though, two sets of blank solutions are created, one with digested purified water ($\overline{B_{DIG}}$) and one with the purified water after the reduction column ($\bar{B}$). The concentration of TDN is then evaluated as:

$$TDN = \left(\frac{X - \overline{B_{DIG}}}{R} * 5\right) * \frac{14}{1000} \tag{5}$$

The DON concentration is calculated as:

$$DON = TDN - (N - NO_3) - (N - NH_4) \tag{6}$$

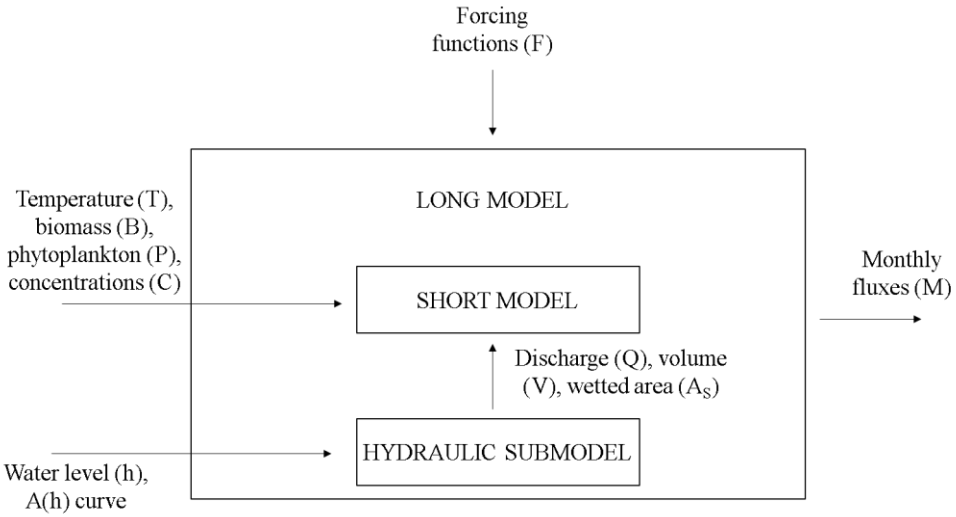

Figure 2.10 CSTR model conceptualization and considered processes.

2.5 Model description

The developed conceptual model for the salt marsh mass balance is composed by two different ones. The hydraulic model and transforms the data of the water level of the tide event into values of discharge, volume and submerged area. The water level behavior is recreated using the data collected inside the marsh creek (with the graduated stick) and fitting them with a sinusoid.

The second model solves the mass balance equations for the different nitrogen compoundswith a time scale lower than the duration of the tide event. All the process occurring in the salt marsh are included and it is used to describe all the biochemical reactions that are active during the flooding of the marsh creek (nitrification, denitrification, release from the sediment, hydrolysis, exudation, uptake, etc.).

This model is then calibrated using the data obtained during the sampling campaigns. At first, it is calibrated focusing on the single datasets, to obtain a best set of initial data that can furnish sufficiently good calibration efficiencies. Successively, it is calibrated using all the dataset at the same time, to obtain a set of best values for the different model parameters.

The calibrated model is then integrated into the long scale one. This solves the equations for the monthly time scale and it is applied with forcing functions that vary according to the selected month. This allows obtaining an annual trend for the nitrogen compounds and a value for the total input and output (and a net value with their difference) on a year.

All the computations have been carried on using scripts on MatLab software (https://it.mathworks.com/products/matlab.html), which can be found in the appendix.

2.5.1 Model conceptualization and structure

The studied and modelled portion of the salt marsh goes from the sampling point in the salt marsh until the end of the marsh creek, and identifies a specific basin with an area of 2331.12 m^2 (Figure 2.11). It is conceptualized as a continuous stirred tank reactor (CSTR), assuming that the input and output water enters and exits with the same concentration. This allows to assume that concentration and forcing functions values are not space dependent and to pass from partial derivative differential equations (PDE) to ordinary differential equations (ODE), which means that the processes are zero dimensional and only dependent upon time.

The CSTR model approach (Figure 2.10) implies that parameters are lumped all over the considered area. However, the salt marsh presents two different parts, which are the salt marsh creek, where the water flows (therefore flooded very frequently), and the marsh surface, where halophytic vegetation is present and is flooded only during exceptionally high tide. In these two zones, the involved processes are different: for example, denitrification ix expected to be higher in the marsh creek, while plant uptake could be more intensive in the salt marsh ground. For this reason, the resulted kinetic constant of this model could be not significative or representative of the real constant of the physical processes occurring at the marsh level. To better represent the real conditions, it would be necessary to subdivide the model into different submodels for every marsh sub-habitats.

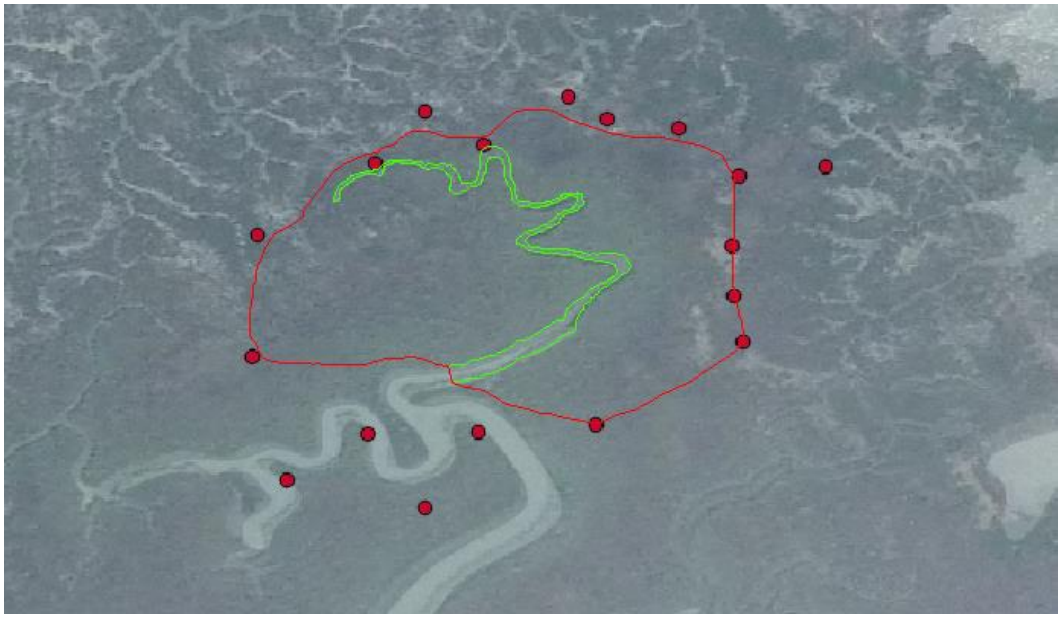

Figure 2.11 Basin related to the studied marsh creek (Baldan, 2015).

2.5.2 Hydraulic submodel

The hydraulic submodel is divided into different conceptual steps, which lead to obtain values of discharge, volume and submerged area that relate to that specific field campaign.

The first step is the definition of the tide trend, starting from the water level data registered at every collected sample. This data are used to fit a sinusoidal curve, which general formula is:

$$h(t) = a * \sin(b * t + c) \tag{7}$$

where a is half of the amplitude (m), c is the relative sea level (m), b is the pulsation (min^{-1}) and t is the time.

After obtaining the equation, it is applied to create the tide event with a time step of one minute. After assessing the temporal scale, these data are used as input to the hydraulics submodel.

This model is obtained from the water mass conservation principle. Commonly, it is applied to reservoirs in order to determining the input and output flows as a function of water level value $h(t)$ and basin physical characteristic. The formula is:

$$Q(t) = A(h)\frac{dh(t)}{dt} \tag{8}$$

where $Q(t)$ is the discharge, which is function of time, $A(h)$ is an experimental curve that describes the superficial area occupied by the water at a certain water level h (see Figure 3.7 in Paragraph 3.2.1), while the derivative term expresses the velocity of water level increase or decrease. The temporal behavior of Q is assumed to be symmetrical (see Figure 3.8 in Paragrapg 3.2.). This model is applied also in other studies on salt marshes hydraulic (Fagherazzi et al., 2013).

The values of wetted area $A(t)$ is obtained interpolating the data of $A(h)$ with h, while the volume data $V(t)$ are the result of:

$$V(t) = \int_0^{A(t)} h(A)dA \tag{9}$$

The volume curve has a similar behavior to the one of $A(t)$.

2.5.3 Short scale model

The model on the short time scale analyzes the dynamics of the nitrogen compounds on a temporal scale lower than the duration of the tidal cycle. The dynamics can be important; therefore, differential equations are required to portray correctly the problem.

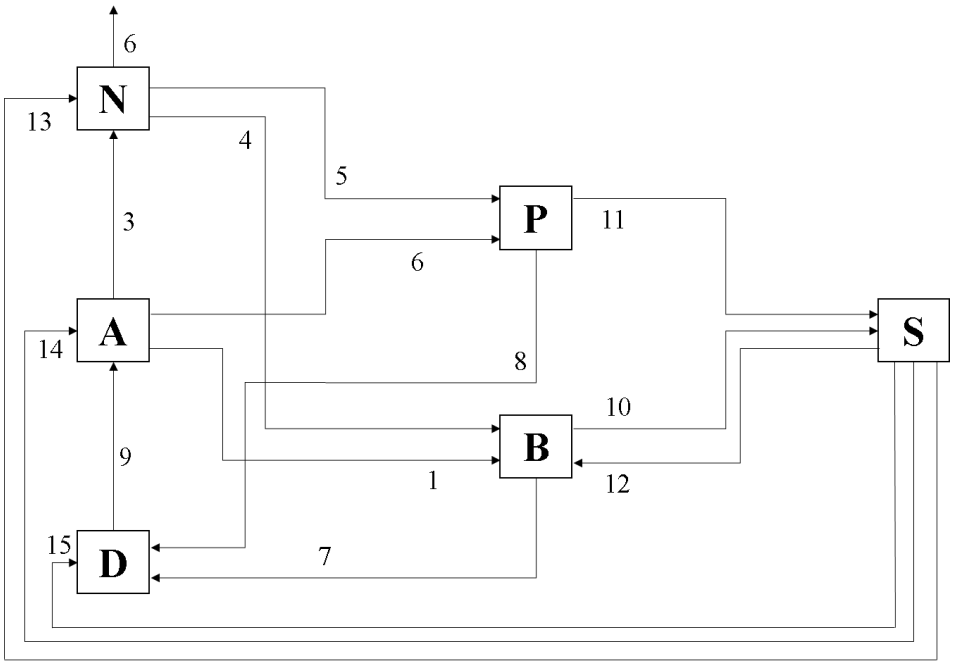

Figure 2.12 Graphical schematization of the processes occurring in the salt marsh. State variables are ammonium(A), nitrate (N), dissolved organic nitrogen (D). Forcing functions are plant biomass (b), phytoplankton (P), sediment concentration (S). Considered processes are: ammonium uptake from vegetation (1), ammonium uptake from phytoplankton (2), nitrification (3), nitrate uptake from vegetation (4), nitrate uptake from phytoplankton (5), denitrification (6), DON exudation from vegetation and transformation of dead biomass (7), DON exudation from phytoplankton and transformation of dead biomass (8), ammonification (9), nitrogen transfer in sediments mediated by vegetation (10), phytoplankton sedimentation (11), uptake of sediment from vegetation (12), nitrate release from sediment (13), ammonium release from sediments (14), DON release from sediments (15).

The considered nitrogen compounds are ammonium (A), nitrate (N) and DON (D), which are the state variables of the model (Figure 2.12). Particulate organic nitrogen (PON) has not been considered, because it is mostly associated with living matter and detritus and its modelling could be very complex.

The equations set that solves the nitrogen mass balance is represented by Eq. (10), (11) and (12). The analysis is not performed on concentration, because the variability of volume with time cannot allow taking it out from the derivative sign.

$$\frac{d(VA)}{dt} = A_{in}Q_{in} - AQ - k_{AU}BAV - k_{AUP}PAV - k_{nitr}AV + k_{hydrD}DV + k_{RA}SA_SH \qquad (10)$$

$$\frac{d(VN)}{dt} = N_{in}Q_{in} - NQ - k_{NU}BNV - k_{NUP}PNV + k_{nitr}AV - k_{denitr}NV + k_{RN}SA_SH \qquad (11)$$

$$\frac{d(VD)}{dt} = D_{in}Q_{in} - DQ + k_{DEXB}BA_S + k_{DEXP}PV - k_{hydrD}DV + k_{RD}SA_SH \qquad (12)$$

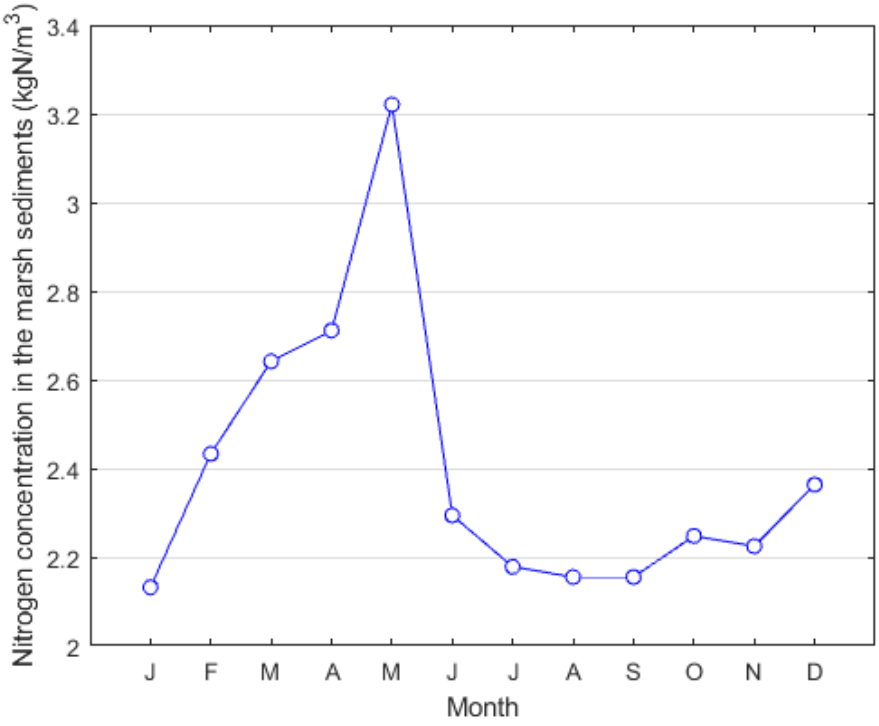

Figure 2.13 Nitrogen stock in the marsh sediment.

As it is possible to observe, the equations contain the related consumption or production rates and the advective fluxes, positive if they represent a source or negative if they represent a sink. Differently from Baldan (2015), in this case no equation for the sediment mass balance is considered, because the nitrogen concentration in sediment is kept constant on a monthly time scale and does not vary on a tidal scale. The sediment concentration is then implemented as a forcing function: so processes 10, 11 and 12 in the schema in Figure 2.12 are not modelled, but are reported in the image for completeness. The monthly values of nitrogen concentration in marsh soil are taken from Baldan (2015), where these data were given by Sfriso A. and Facca C. as personal communication. The values referred to an analyses carried out on June 2014 for a salt marsh soil sample and from March 2010 to February 2011 on tidal flats. It is then assumed a similar behavior of concentration data for salt marshes. The analyzed nitrogen concentration in the marsh is 2.294 kgN m_{soil}^{-3} and it is used to create a seasonal variability (Figure 2.13). Another important parameter is the thickness of the active soil layer, fixed to 10 cm and not varied, due to the fact that some processes in the rhizosphere occur also when no water is present in the marsh creek (or in salt marsh).

Equations (10), (11) and (12) are coupled with Eq. (13), which solves the water mass balance:

$$\frac{dV}{dt} = Q_{in} - Q \tag{13}$$

The considered processes inside Equations (4), (5) and (6) and in Figure 2.12 are here briefly described:

1. Ammonium uptake from vegetation is modelled as a first order kinetic:

$$R = k_{AU}ABV \tag{14}$$

where k_{AU} is the ammonium uptake from vegetation kinetic constant [L^2 M^{-1} T^{-1}], A is the ammonium concentration [M L^{-3}], B is the plant biomass concentration [M L^{-2}] and V is the volume occupied by water [L^3];

2. Ammonium uptake from phytoplankton is modelled as a first order kinetic:

$$R = k_{AUP}APV \tag{15}$$

where k_{AUP} is the ammonium uptake from phytoplankton kinetic constant [L^3 M^{-1} T^{-1}] and P is the phytoplankton biomass concentration [M L^{-3}];

3. Ammonium nitrification is modelled as a first order kinetic:

$$R = k_{nitr}AV \tag{16}$$

where k_{nitr} is the nitrification kinetic constant [L^3 M^{-1} T^{-1}];

4. Nitrate uptake from vegetation is modelled as a first order kinetic:

$$R = k_{NU}NBV \tag{17}$$

where k_{NU} is the ammonium uptake from vegetation kinetic constant [L^2 M^{-1} T^{-1}], N is the nitrate concentration [M L^{-3}];

5. Nitrate uptake from phytoplankton is modelled as a first order kinetic:

$$R = k_{NUP}NPV \tag{18}$$

where k_{NUP} is the nitrate uptake from phytoplankton kinetic constant [L^3 M^{-1} T^{-1}];

6. Nitrate denitrification is modelled as a first order kinetic:

$$R = k_{denitr}NV \tag{19}$$

where k_{denitr} is the denitrification kinetic constant [T^{-1}];

7. DON exudation from vegetation (and transformation of dead biomass) is modelled as a zero order kinetic:

$$R = k_{DEXB} B A_S \quad (20)$$

where k_{DEXB} is the DON exudation from vegetation kinetic constant [T^{-1}] and A_S is the area occupied by water time t [L^2];

8. DON exudation from phytoplankton (and transformation of dead biomass) is modelled as a zero order kinetic:

$$R = k_{DEXP} P V \quad (21)$$

where k_{DEXP} is the DON exudation from phytoplankton kinetic constant [T^{-1}];

9. DON hydrolysis to ammonium (ammonification) is modelled as a first order kinetic:

$$R = k_{hydrD} D V \quad (22)$$

where k_{hydrD} is the DON exudation from phytoplankton kinetic constant [T^{-1}] and D is the DON concentration [$M\ L^{-3}$];

10. Nitrogen fixation mediated by plants is not modelled in this thesis;
11. Sedimentation of phytoplankton is not modelled in this thesis;
12. Uptake by plant roots is not modelled in this thesis;
13, 14, 15. Releases from sediments are modelled as first order kinetics. This processes are due to transfer of nitrogen from interstitial water in the sediments to the tidal water due to concentration gradients. Because redox conditions in the soil could vary and so oxidized and reduced nitrogen compounds could be present, three term are implemented:

$$R_A = k_{RA} S A_S H \quad (23)$$

$$R_N = k_{RN} S A_S H \quad (24)$$

$$R_D = k_{RD} S A_S H \quad (25)$$

where k_{RA} is the ammonium release kinetic constant [T^{-1}], k_{RN} is the nitrate release kinetic constant [T^{-1}], k_{RD} is the DON release kinetic constant [T^{-1}] and S is the sediments nitrogen concentration [M L^{-3}].

In addition to these reactions terms, also advective process are taken into account, which are modelled as follows:

$$ADV = Q_{in}C_{in} - QC \tag{26}$$

where Q_{in} is the input discharge when the tide is rising [L^3 T^{-1}], C_{in} is the generic input concentration in input, equal to the concentration in the water surrounding the salt marsh [M L^{-3}] and Q is the output discharge during the ebb [L^3 T^{-1}]. Furthermore, C is the concentration of the generic nitrogen compound at the time t [M L^{-3}], which is equal to the concentration inside the salt marsh at same moment, due to the CSTR hypothesis.

All the kinetic parameters are then corrected with the temperature values (interpolated from the data of the WTW probes) using the Van't Hoff – Arrhenius exponential relationship:

$$k_T = k_{T_{ref}}\theta^{(T-T_{ref})} \tag{27}$$

where k_T is the kinetic constant at the temperature T [°C], while $k_{T_{rif}}$ is the value of the parameter at the reference temperature, which is equal to 20°C. The value of θ, the Van't Hoff – Arrhenius constant, can vary from process to process, so it should be changed for every kinetic parameters or should be calibrated. However, in the calibration step, it is impossible to calibrate both the kinetics and the θ values, so it has been fixed equal to 1.01.

To sum up, all the model parameters are shown in Table 2.1.

Table 2.1 Synthesis of the model kinetic parameters.

KINETIC PARAMETERS	UNIT OF MEASUREMENT	PROCESS
k_{AU}	$[L^2\ M^{-1}\ T^{-1}]$	Ammonium uptake by biomass
k_{AUP}	$[L^3\ M^{-1}\ T^{-1}]$	Ammonium uptake by phytoplankton
k_{NU}	$[L^2\ M^{-1}\ T^{-1}]$	Nitrate uptake by biomass
k_{NUP}	$[L^3\ M^{-1}\ T^{-1}]$	Nitrate uptake by phytoplankton
k_{DEXB}	$[T^{-1}]$	DON exudation by biomass
k_{DEXP}	$[T^{-1}]$	DON exudation by phytoplankton
k_{nitr}	$[T^{-1}]$	Nitrification
k_{hydrD}	$[T^{-1}]$	DON hydrolysis
k_{denitr}	$[T^{-1}]$	Denitrification
k_{RA}	$[T^{-1}]$	Ammonium release from sediments
k_{RN}	$[T^{-1}]$	Nitrate release from sediments
k_{RD}	$[T^{-1}]$	DON release from sediments

2.5.4 Long scale model

The long scale model is an integration of the short scale one, applied on a monthly time scale. In this case, some of the forcing functions are not constant as in the short scale model but change during the different months. Later in this paragraph, these forcing functions are listed and described.

This model, in practical terms, solves the mass balance one time for each month, using the characteristic forcing functions, it calculates the input and output fluxes of nitrogen compounds and then multiplies these values for 2 (because there are two tidal events in a day) and for 30 (30 days in a month).

The generic flux F_i [gN/tidal cycle] is computed as:

$$F_i = \int_0^t Q(t)C_i(t)dt \tag{28}$$

where $Q(t)$ is the discharge at the time t and $C_i(t)$ is the concentration of the i-th nitrogen compound. For input fluxes, input discharge Q_{in} and input concentration C_{in} are used, while for

output fluxes output discharge Q and output concentration C are utilized. The net flux of a single compound is calculated as the difference between the input and the output flux.

It is computed also the denitrification flux, which express the quantity of gasified nitrogen in output from the salt marshes, by solving the ODE related to the denitrification term only:

$$\frac{dDenitr}{dt} = -k_{nitr}NV \tag{29}$$

The flux is then expressed as $Denitr(t)$.

Also the monthly fluxes of nitrogen uptake and release from the biomass and the sediment is computed, for very month, as:

$$F_{bio}(i) = \big(B(i) - B(i-1)\big)A_S \tag{30}$$

$$F_{sed}(i) = \big(S(i) - S(i-1)\big)V_{soil} \tag{31}$$

where i is the month, $S(i)$ is the sediment concentration and $B(i)$ is the biomass concentration [M L^{-2}] at the i-th month.

As far as the forcing functions are concerned, they are specific values that do not change with a tidal cycle (with the exception of the temperature), but change along the different months.

The forcing functions are:

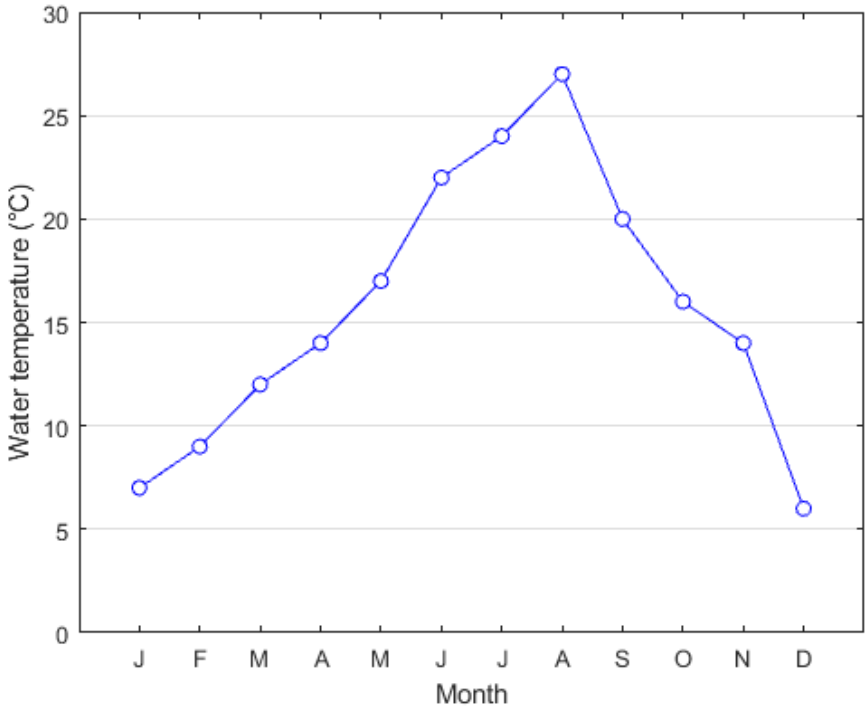

Figure 2.14 Average monthly temperature

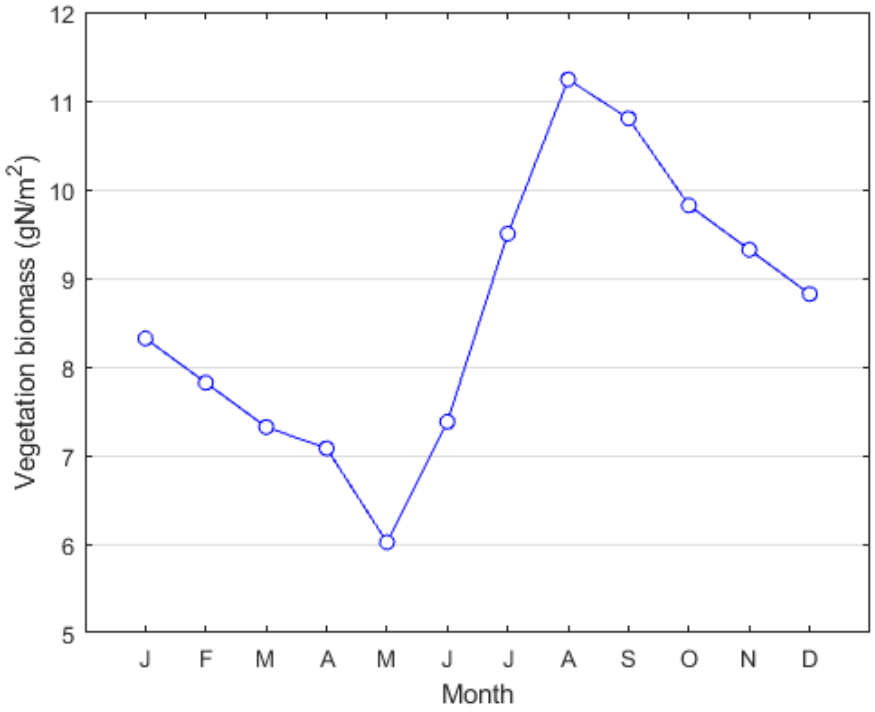

Figure 2.15 Monthly vegetation biomass

- Water temperature monthly averaged values (Figure 2.14), which are obtained from Solidoro et al. (2005). The data ranges between 6°C in December to 27°C in August. Differently from the short scale model, whose temperature data vary along a tidal cycle and are, for this reason, interpolated while solving the mass balances, for the long scale these temperature data are kept constant for a single month, due to the fact that is complex from a computational point of view, maybe not significative and not easy to use real data that changes day by day or hour by hour;
- Vegetation biomass is obtained from literature data (Scarton, 2006). Biomass data (Figure 2.15) are available for the period March – October, and for the winter time it is assumed that no new biomass production is produced (only degradation occurs). The gaps have been filled using linearly interpolated values. Moreover, the used data are expressed in mass of nitrogen per unit area, and so the literature values are multiplied by the average nitrogen content in halophyte vegetation, equal to 0.02 gN gDW^{-1} (Davy et al., 2001);

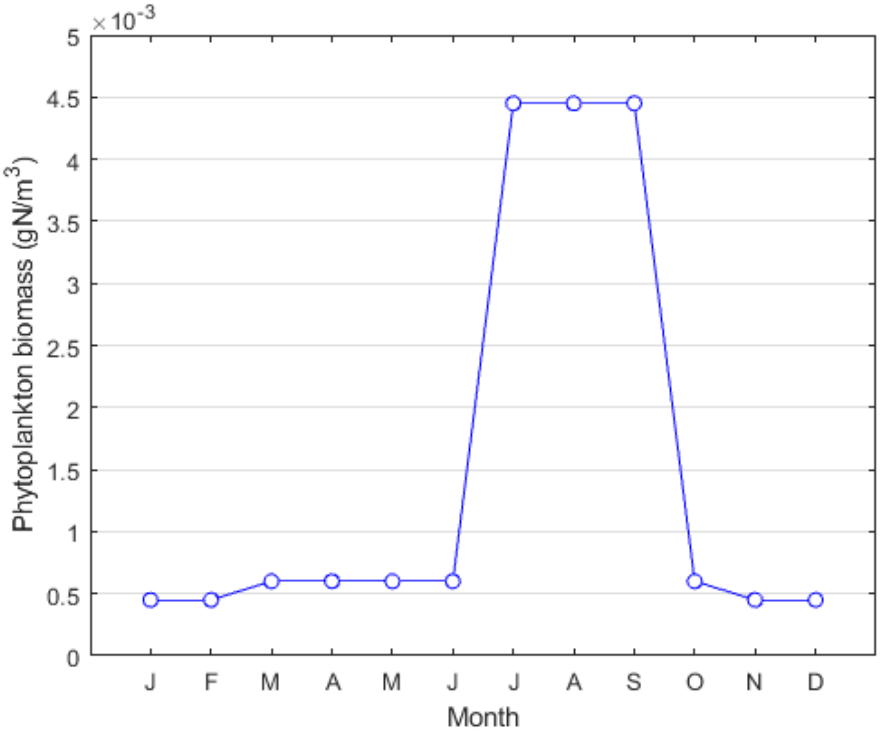

Figure 2.16 Phytoplankton biomass monthly values

- Phytoplankton biomass is obtained from ARTISTA data on trophic network modelization (Bendoricchio and Palmeri, 2005). In this case, no data for every month is available but only values for the winter, spring and summer time. No interpolation is possible, so values from winter time are used for November, December, January and February, data for spring time for March, April, May, June and October and data for July, August and September are the one of summer time (Figure 2.16). The assumption of spring values used for October is not so strong, because some articles reports increase of phytoplankton or chlorophyll *a* during the autumn time due to a second yearly bloom (Solidoro et al., 2004). Eventually, a carbon/nitrogen Redfield ratio of 10 gC gN^{-1} is assumed to transform literature data unit of measurement (gC m^{-3}) into the one used in the model (gN m^{-3});

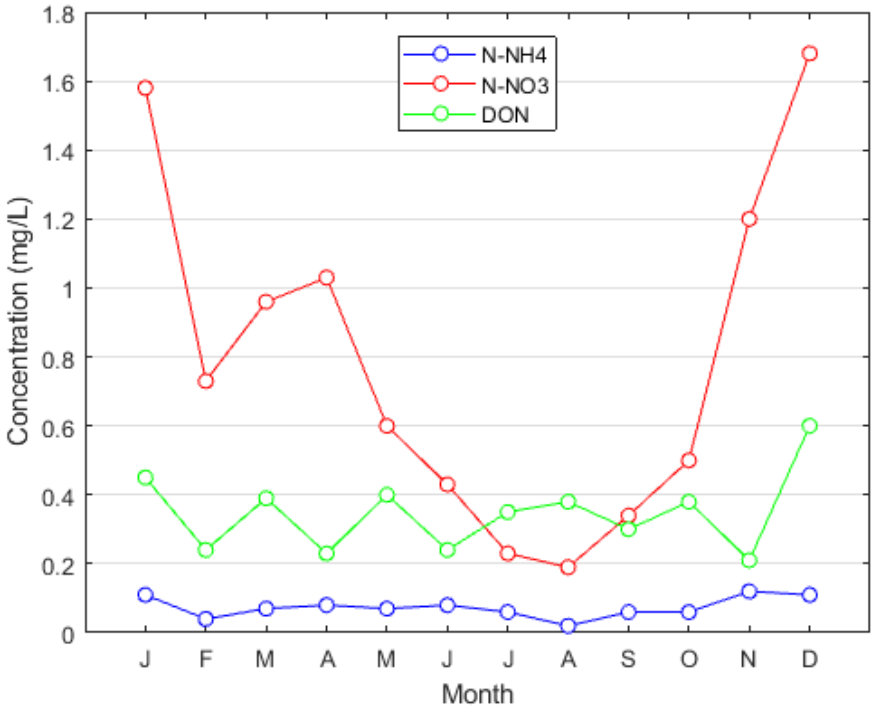

Figure 2.17 Average monthly values for nitrogen compound concentration

- Concentration of nitrogen outside the salt marsh (Figure 2.17) are obtained by averaging field data measured near the salt marsh (station 1B of the studies) for the years, 2003, 2004, 2005, 2007 and 2008 (Rapporto tecnico I anno (MELa2); Rapporto tecnico II anno (MELa2); Rapporto tecnico finale sulle attività di monitoraggio della qualità delle acque Volume 1. Rapporto di sintesi (MELa3); data kindly provided by Ministero delle Infrastrutture e dei Trasporti – Provveditorato Interregionale alle OO. PP del Veneto – Trentino Alto Adige – Friuli Venezia Giulia).

Another forcing function, that deserves a separate analysis, is the average tidal cycle used as input to the long scale model. Due to issues of computational demand, it was not recreated a monthly trend of the tide and not implemented in the model. For this reason, a statistical analysis of 10 years of water level (2005 - 2014) recorded at “Punta della Salute” meteorological station was performed by Baldan (2015), studying data of minimum and maximum for each tidal cycle.

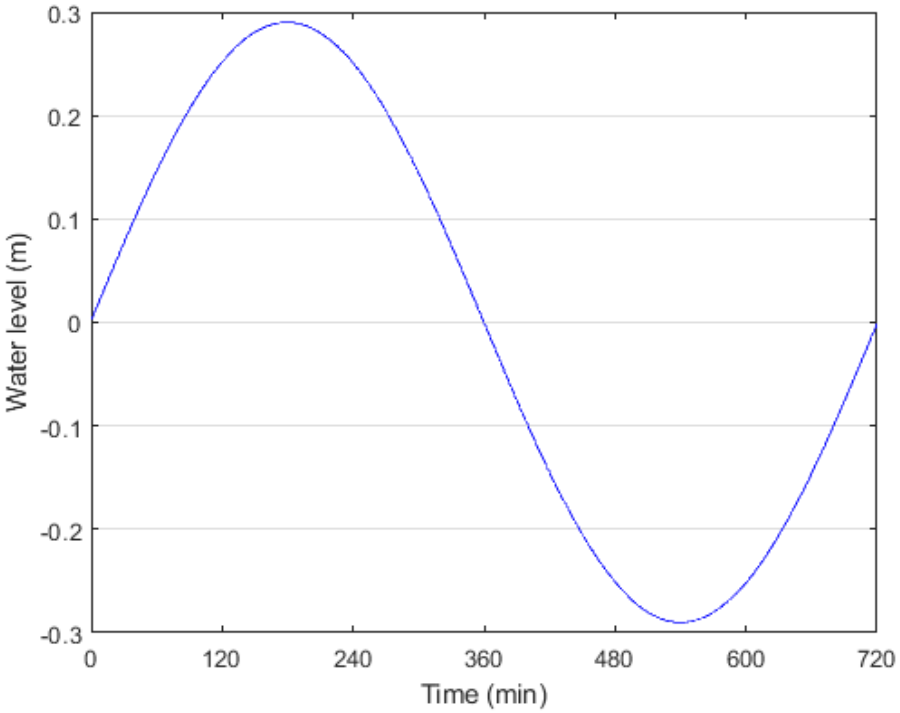

Figure 2.18 Average tidal cycle used for the long scale model

An average minimum of 0.01, an average maximum of 0.62 m and an average amplitude of 0.60 m have been obtained. These data have been used to create an average tidal event as forcing function with a period of 12 hours. Using again Eq. 7, where a is equal to 0.29 m, c is equal to 0.26m and b is equal to 0.523 h^{-1} or 0.00871 min^{-1}. The result is shown in Figure 2.18.

The long scale model, applied to a whole year, also takes into account other processes that involves nitrogen dynamics in the salt marsh, but happen very slowly and then their effect is significant only on the long time scale. These processes are:

- Atmospheric deposition, which is composed by a wet and a dry deposition. The first one is due to the nitrogen present in the rainwater, while the second one is due to nitrogen adsorbed to particles and to gaseous aerosol deposition. This flux can be a not-negligible nitrogen input in costal system and a study in Venice shows that there is a great variation in bulk deposition, with high values near Porto Marghera and lower values in the most peripheral zones (Rossini et al., 2005). It has been assumed that atmospheric deposition is 1.5 gN m^{-2} y^{-1} (0.12 gN m^{-2} $month^{-1}$), the value of the paper for the city of Venice, which has almost the same distance from Porto Marghera of the studied salt marsh.

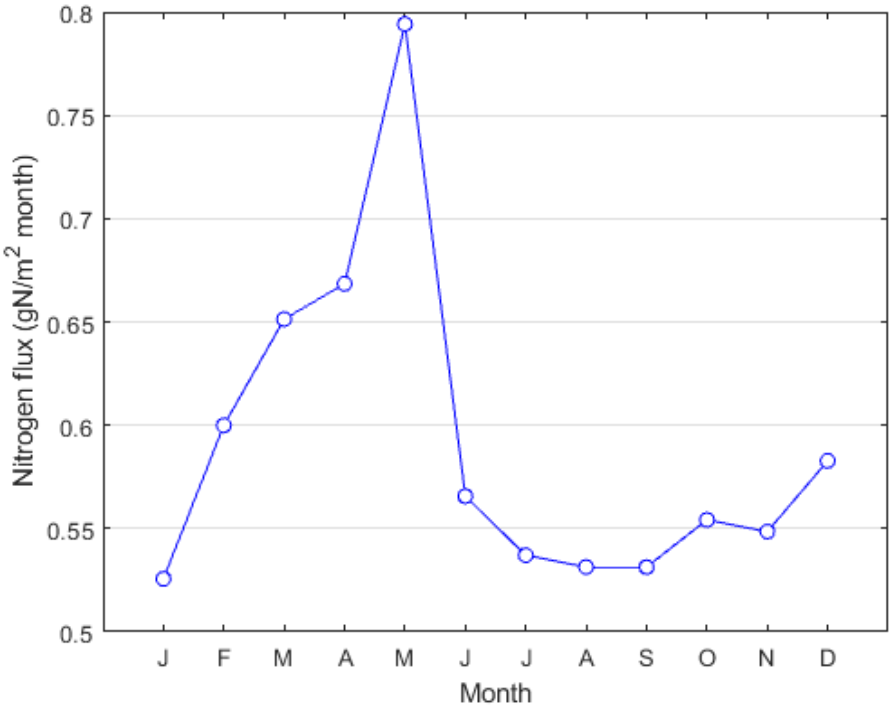

Figure 2.19 Sediment accretion flux

- Fixation of atmospheric nitrogen, generated by blue-green algae, rhizosphere and non-rhizosphere bacteria. In the salt marsh analysis, this process is considered to be mostly related to soil processes, due to the fact that the marsh creek occupies only 1/10 of the entire marsh surface. This flux, though, has not been considered because it is assumed that the input given by fixation is contained in the yearly vegetation biomass dynamics (all nitrogen fixed in the rhizosphere is uptaken directly by plants).
- Accretion, which means nitrogen acquisition through sediment deposition, is determined equal to 0.5 gN m^{-2} y^{-1}. This value was obtained assuming a detritus settling rate of 0.1 d^{-1} and N/C ratio of 0.08 (Jorgensen, 1979) and a detritus concentration obtained from ARTISTA food web datasets (Bendoricchio and Palmeri, 2005). However, deposited matter becomes rapidly part of the sediment and, for this reason, it is possible to assume that the concentration in the new sediment is the same of the marsh soil; therefore, this flux can be calculated as the product between the nitrogen sediment concentration and the flux of sediment, equal to 0.3 cm y^{-1} (Grechi, 2015). Results are shown in Figure (2.19).

There are also neglected fluxes, for different reasons. The first one is the ammonium stripping process, not considered due to the scarce influence to the nitrogen mass balance (Valiela and Teal,

1979), and the second one is the input due to animal dejections, which is assumed to be very low, too. Another neglected flux is the loss of nitrogen due to eroded soil, because the selected marsh is not near a lagoon channel, and so no erosive process of marsh border is currently ongoing. This last flux, though, can be a very important flux, because of the high nitrogen concentration in the soil, and erosive process is also one of the biggest threat to salt marshes in the Venice lagoon (see Paragraph 1.4).

2.5.5 Calibration

Calibration of the model is necessary in order to obtain the best kinetic parameters that better fit the observed concentrations data. Not all the parameters undergo to the calibration process, only the ones that show the highest sensitivity. However, no sensitivity analysis is done in this thesis, because the focus is onto the analysis of the different trends of the nitrogen compounds in different seasons and onto the improvement of the model, calibrating it with a bigger set of concentrations data. The calibrated parameters are then chosen based on the sensitivity analysis made by Baldan (2015) and assuming similar results for our datasets.

The calibration procedure is carried out by minimization of an objective function (optimization problem), using as constraints the variation ranges for each parameter (Jørgensen and Bendoricchio, 2001). This function can be a scalar or a vector one, and aims to find a parameter vector that minimizes the residues between the output model and the observed data, between all the possible vectors that can be generated inside the variation ranges. In this thesis, the selected function is the negative likelihood: along with the procedure, the likelihood of the data is calculated for the different parameters vectors and the best one is then identified.

The likelihood function, for a competing hypothesis θ given the data Y, is proportional to the probability of the data given the hypothesis (Hobbs and Hilborn, 2006.), i.e. it is possible to write that:

$$L(\theta|Y) \; \alpha \; P(Y|\theta) \tag{32}$$

where θ represents a set of parameters values specifying a particular model and the interest is to know the probability of observing output Y, given those parameters values.

For a single observation, the likelihood of the prediction of the model is proportional to the probability of making that observation conditional on the model's parameters (it is common practice to assume a constant proportionality equal to one in Eq. 32):

$$L(\theta|y_i) \; \alpha \; g(y_i|\theta) \tag{33}$$

where g is the probability density function. If multiple observations are independent with each other, it is possible to use a factorization:

$$L(\theta|Y) = \prod_{i=1}^{n} g(y_i|\theta) \tag{34}$$

The best parameters values are then the one that maximizes the likelihood. For practical reasons, it is useful to modify Eq. 34, inserting the logarithm of the likelihood function, in order to obtain a sum of terms and not a product of a sequence of terms:

$$\ln\big(L(\theta|Y)\big) = \sum_{i=1}^{n} \ln\big(g(y_i|\theta)\big) \tag{35}$$

This function can easily sum together multiple observations, taking advantage of the logarithm additivity property:

$$\ln\big[\big(L(\theta|X,Y,Z)\big)\big] = \ln\big[\big(L(\theta|X)\big)\big] + \ln\big[\big(L(\theta|Y)\big)\big] + \ln\big[\big(L(\theta|Z)\big)\big] \tag{36}$$

To implement the likelihood function to the calibration procedure, it is assumed that the residues, defined as the difference between the observed and the modelled output values, are normally distributed. For this reason, the likelihood function, for a single parameters vector output, can be calculated as:

$$L_i = \frac{1}{\sqrt{2\pi\sigma^2}} e^{-\frac{1}{2}\left(\frac{Y_{i,obs}-Y_{i,mod}}{\sigma}\right)^2} \tag{37}$$

where σ, the variance of the residues, is calculated as:

$$\sigma^2 = \sum_{i=1}^{N} \frac{1}{N}\big(Y_{i,obs} - Y_{i,mod}\big)^2 \tag{38}$$

Using the same properties of Eq. 35, the negative logarithm of total likelihood (the sum of likelihoods from multiple time series) can be defined as:

$$-\ln(L) = -\sum_{i=1}^{N} \ln(L_i) \tag{39}$$

The choice of the likelihood function is made because of the property of additivity of likelihood logarithm (valid only in case of independent events), which allows to calculated the total likelihood for a set of multiple field data. Moreover, the likelihood results can be used to obtain the Akaike's information criterion (see Paragraph 2.5.6).

2.5.6 Best model selection

It is possible to define a good model as a balance between complexity and capacity of observed data prediction (Jørgensen and Bendoricchio, 2001). This is not so difficult to understand, since a complex model, with a great number of parameters, may be connected with high uncertainty of data, because numerous observations are necessary in order to calibrate all the model parameters. On the other hand, a too simplistic model may not take into account important processes and therefore badly estimate the field results. For all these reasons, a good balance must be found in the formulation a model.

The best model selection is carried on analyzing the prediction capacity of the model, using the Nash-Sutcliffe efficiency (McCuen et al. 2006), and obtaining other information from information theory (i.e. implementing the Akaike's information criterion or AIC).

The Nash-Sutcliffe efficiency is calculated as:

$$EFF = 1 - \frac{\sum_{i=1}^{N}\left(Y_{i,obs} - Y_{i,mod}\right)^2}{\sum_{i=1}^{N}\left(Y_{i,obs} - \widehat{Y_{i,obs}}\right)^2} \tag{40}$$

where $Y_{i,mod}$ is the output of the model, $Y_{i,obs}$ is the observed value, $\widehat{Y_{i,obs}}$ is the time averaged value of observed data and N is the number of observations.

The efficiency result may vary as a numerical value between $-\infty$ and 1, and has then different meaning:

- If it is equal to 1, the model perfectly fits the data;
- If it is equal to 0, it means that the residues between the model output and the observed data are equal to the ones between the mean of the observed values and the observed values themselves. This also means that the mean works as well as the model in terms of prediction capacity;
- If it less than 0, it means that the fit is not good and the more the value is negative, the worse is the fit.

As far as the AIC is concerned, this index takes into account both the goodness of the fit and the complexity of the model (Anderson, 2008). It is formulated as follows:

$$AIC = -2\ln\left(L\left(\tilde{\theta}\middle|data\right)\right) + 2K \tag{41}$$

where $L\left(\tilde{\theta}\middle|data\right)$ is the likelihood of the calibrated parameters $\tilde{\theta}$, given the observed data, while K is the number of calibrated parameters.

Being this indicator a measure of information lost when approximating reality with a model, the best model is the one that minimized the AIC. So bad-fitting models does not give good AIC values, but also too complex model.

To the Eq. 41, a correction must be applied when the sample size is limited to N observations, to obtain:

$$AIC_C = -2\ln\left(L\left(\tilde{\theta}\middle|data\right)\right) + 2K\left(\frac{N}{N-K-1}\right) \tag{42}$$

The minimum AIC variation of significance is 2, that is the change in AIC due to removal of a parameter (Anderson, 2008).

Different models, with different umber of parameters are tested and the one with a good balance between simplicity and goodness of the fitting capacity is chosen to run the yearlong mass balance evaluation for the salt marsh.

3. Results and discussion

3.1 Literature research

A literature research has been carried on in order to find some kinetic parameters values for biochemical processes occurring in the salt marsh. It was not possible to find values for every parameter, since it is likely that not every considered process in the model has been analyzed in scientific papers and because some of the processes considered are lumped. Many analyses have been done about nitrogen in costal lagoons because of the relationship between this nutrient and eutrophication (Solidoro et al., 2005; Pastres et al., 2005). However, these studies focus only on the processes in the water column, and not on the ones that occur in areas of the lagoon that are periodically flooded. Moreover, a research about nitrogen mass balances in salt marshes was also carried on, which ended up with only two complete balances (Valiela and Teal, 1979; Pomeroy and Wiegart, 2012), highlighting a lack of literature data on this topic. Above all, for the Venice Lagoon only few other studies have been found (Eriksson et al, 2003; Solidoro et al., 2004).

The kinetic parameters that have been found are:

- Ammonium and nitrate uptake by plants (Table 3.1), which can be described by a semisaturation equation and can be transformed into a second order kinetic if substrate concentration is low. Researches show how ammonium uptake is faster in oxic conditions than in aerobic conditions and it varies from 0.014 and 0.125 gN/l.

Table 3.1 Literature research for ammonium and nitrate uptake (V_{MAX} is the maximum reaction velocity, K_M the half saturation constant).

V_{MAX} (mgN gRDM^{-1} h^{-1})	K_M (mgN l^{-1})	Other information	Location	Reference
0.180	0.014	Oxygen saturation, ammonium uptake	Laboratory experiments	Bradley and Morris, 1990
0.113	0.035	Anoxic conditions, ammonium uptake		
0.11	0.057	Ammonium uptake	Laboratory experiments	Morris, 1980
	0.124	Nitrate uptake		

From these data, first order kinetic can be obtained by dividing the maximum reaction velocity by the half saturation constant.

- Ammonium release, which is lower for vegetated soils (perhaps due to vegetation uptake) and higher for unvegetated creeks that are a more-reducing environment. Values range between 1 and 3.5 mgN m^{-2} h^{-1}. Literature data are presented in Table 3.2.

Table 3.2 Literature results for ammonium release.

Release (mgN m^{-2} h^{-1})	**Other information**	**Location**	**Reference**
1	Vegetated ponds	Marsh close to Campalto, Venice Lagoon	Eriksson et al., 2003
3.5	Creeks		

- Inorganic nitrogen uptake rates (Table 3.3), which are higher in the rhizosphere than at the surface of the salt marshes and ranges between 0.1 and 4 mgN m^{-2} h^{-1}. They are also higher in natural marshes than in constructed marshes.

Table 3.3. Literature data for inorganic nitrogen uptake rates.

Uptake (mgN m^{-2} h^{-1})	**Other information**	**Location**	**Reference**
3.97	/	Marsh in Georgia	Hopkinson and Schubauer, 1984
0.196 - 0.635	Constructed marsh, at the surface	Marsh in California	Langis et al., 1991
0.345 - 1.665	Natural marsh, at the surface		
1.347 - 3.524	Constructed marsh, in the rhizosphere		
0.104 - 2.48	Natural marsh, in the rhizosphere		

- Bacterial and blue-green algae ammonium uptake, which are shown in Table 3.4, and values vary between 0.05 and 5 mgN m^{-2} h^{-1}. There can be also a term of ammonium release from them, in anaerobic conditions. However, it is very improbable that, in the

marsh creek, anaerobic conditions occur when water is present, with the only exception of the anoxic sediment.

Table 3.4 Bacterial and blue-green algae ammonium uptake process in salt marsh from literature.

Ammonium uptake (mgN m^{-2} h^{-1})	**Ammonium release (mgN m^{-2} h^{-1})**	**Other information**	**Location**	**Reference**
0.049 - 5.27	/	Lower in presence of bare mud, higher in pools dominated by blue-green algae	Marsh in England	Jones, 1974
1.82	1.28	Uptake in aerobic conditions, release in anaerobic conditions	Tidal freshwater estuary in Massachusetts	Bowden, 1986

- Nitrification rates, which are dependent on the location inside the marsh, because higher values are observed in creeks, while lower values characterize the vegetated area. Results are presented in Table 3.5 and ranges between 0.9 and 5 mgN m^{-2} h^{-1}.

Table 3.5 Nitrification rates literature results.

Nitrification rate (mgN m^{-2} h^{-1})	**Other information**	**Location**	**Reference**
2 - 5	Higher in creeks, lower in vegetated area	Marsh close to Campalto, Venice Lagoon	Eriksson et al., 2003
0.875 – 3.73	Computed as difference between mineralization and ammonium in the output	Coastal lagoon in Virginia	Anderson et al., 2003
0.014 – 0.022	Vegetated area	Marsh in Georgia	Dollhopf et al., 2005
8.68 – 8.86	Creek banks		

- Denitrification rates, for which many literature results can be found. Results are presented in Table 3.6 and vary between 0.0002 and 3 mgN m^{-2} h^{-1}.

Table 3.6 Denitrification rates in literature.

Denitrification rate (mgN m^{-2} h^{-1})	**Other information**	**Location**	**Reference**
0-2.5	Denitrification of nitrate in the water column	Marsh close to Campalto, Venice Lagoon	Eriksson et al., 2003
0-1	Coupled nitrification - denitrification		
0.34 – 1.59	/	Marsh in Georgia	Hopkinson and Schubauer, 1984
1.09 – 3.01	Computed as difference between nitrification and nitrate out	Coastal lagoon in Virginia	Anderson et al., 2003
0.038 – 0.061	Higher in vegetated area, lower in creeks	Marsh in Georgia	Doolhopf et al., 2005
0.0002 – 0.001	Laboratory analysis	Marsh in St. Lawrence Estuary, east Canada	Poulin et al., 2007
0.5	/	Marsh in Schiermonikoog island, The Netherlands	van Wijnen and Bakker, 2000

Another literature research has been carried on in order to find the forcing functions for the long scale model, as explained in Paragraph 2.5.4.

As far as the mass balances in literature are concerned, only two studies have carried on a complete analysis, by Valiela and Teal (1979) and by Pomeroy and Wiegart (2012).

The first one focuses on the Great Sippewisset marsh in Massachusetts. This salt marsh presents a great capability in capturing nitrogen loads from the surrounding water and displays a positive sediments budget, indicating that nitrogen is fixed inside the sediment. Another important process withinthe marsh appears to be the internal recycling : the majority of nitrogen sources are endogenous from the recycle of already present nitrogen forms. This also suggest that, despite the capacity to capture nitrogen form the tidal water, these inputs have a limited effect on the total salt marsh nitrogen mass balance.

The second study analyzed a salt marsh in Sapelo Islands, Georgia, which is characterized by groundwater springs that operate as nitrogen input. In this case, output water during the tidal cycle

are enriched in nitrogen respect to the entering water when the tide is rising. However, the quality of exiting nitrogen is changed: the marsh exports PON (particulate organic nitrogen), while it consumes nitrate. This process has an important effect on the food web and the trophic chain, because disadvantage primary producers and advantage filter feeders.

To sum up the results of these two studies, both salt marshes have an important role in the ecosystem as nitrogen processors, involving a great quantity of transformed nitrogen, and are evolving ecosystems, since they accrete representing a sink for sediments and for nitrogen. In particular, they reduce the nitrogen loads, transforming the ozidation state. They retain nitrogen during the summer (sinks), while releasing it during the winter (sources), acting as buffers (Valiela and Teal, 1979). Internal cycling may appear to have a great effect in the marsh nitrogen budget, so that high consumption rates should not be common. However, these results are still a subject of discussion.

The complex flow, stage and nutrient dynamics that result from the influence of tides makes quantifying nutrient uptake in tidal marshes a challenge (Etheridge et al., 2017). Moreover, as it is possible to notice from the above mentioned studies, salt marshes can have different behavior and role in ecosystem according to the geographical position. There are also opposite results in some researches about the salt marshes function: for example, Teal (1962) proposed the idea that salt marshes are exporters of organic matter and providers for food resources that support marine productivity. However, other studies concluded that marshes act as organic and nutrients sinks or that, in hypernutrified conditions, sediments can have the capacity to become sinks for nitrate, as benthic denitrification responds to high nitrate concentration and then acts as nitrogen buffer (Simas and Ferreira, 2007).

3.2 Results of field campaigns

In this paragraph, results of the marsh creek cross sections and the hydraulic analysis are reported. toghether with the results of the chemical analysis of the creek and channel samples with a final discussion about salt marsh and nitrogen compounds behavior and on mass balances for the single sampling campaigns, taking into account also two field surveys of June 2016 and August 2015. Detailed numerical data are shown in Appendix 7.12.

Figure 3.1 Location of the five analyzed cross-section (Google Earth, 2017).

3.2.1 Cross sections results

As explained in Paragraph 2.3, five different cross sections have been taken along the salt marsh creek (Figure 3.1) in order to increase the understanding of the hydraulic inside this small channel and to improve the A(h) curve, necessary for the hydraulic submodel (Eq. 8).

The first point coincides with the sampling point in the salt marsh creek, while the others are taken at similar distance from each other or at significative points. The progressive distances from section 1 are shown in Table 3.7.

Table 3.7 Progressive distances of the cross sections.

Section	Progressive distance (m)
1	0
2	17
3	29
4	29.5
5	55

The data collected are then analyzed using AUTOCAD software and the graphical results are shown in Figure 3.2, 3.3, 3.4, 3.5 and 3.6.

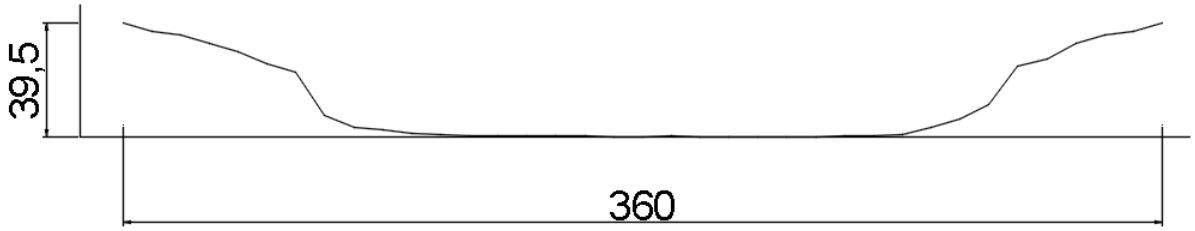

Figure 3.2 Section number 1. Values are in cm.

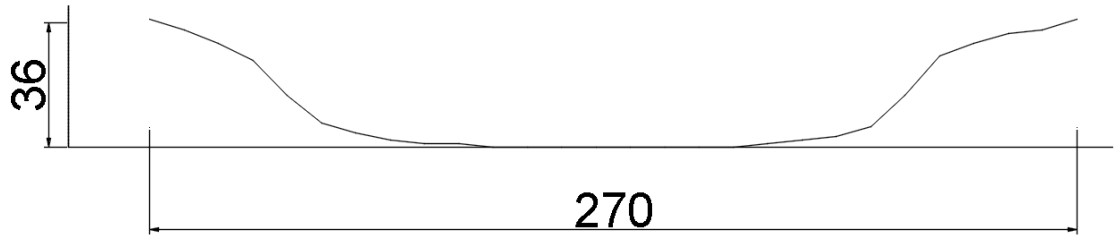

Figure 3.3 Section number 2. Values are in cm.

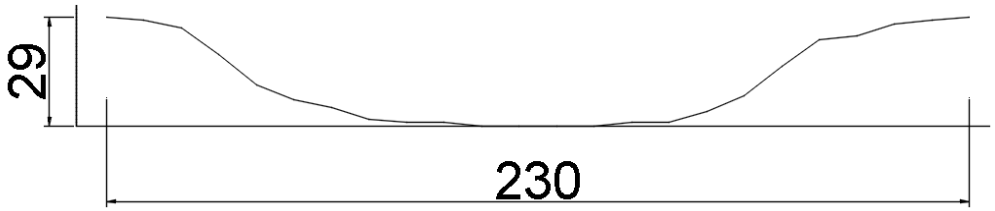

Figure 3.4. Section number 3. Values are in cm.

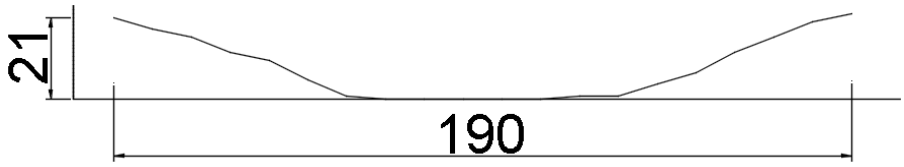

Figure 3.5 Section number 4. Values are in cm.

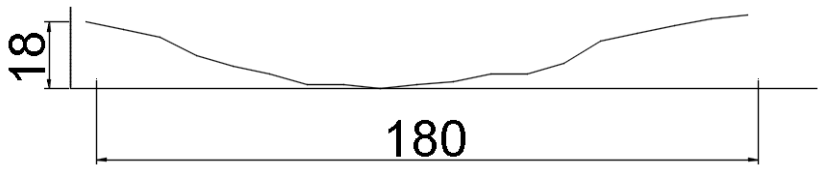

Figure 3.6 Section number 5. Values are in cm.

Moreover, an analysis of the slope was carried out by registering water level values in the five sections at the same moment: by assuming that the absolute water level was the same in all the considered sections, it has been possible to assess the relative difference on elevation of their bottoms. Results are shown in Table 3.8.

Table 3.8 Analysis of water level to obtain the slope on the salt marsh creek

Section	Water level at the same instant (cm)
1	15
2	10
3	6
4	2.5
5	0.5

From these data it is possible to obtain an average slope of $2.73*10^{-3}$ m/m.

The entire marsh creek is 94 m long, but the last part (from section 5 until the end) presents a constant section and a geometry not particularly similar to the main part of the creek (as it possible to notice from the comparison of Figure 3.6 with the others). In other words, the creek in the last part becomes very flat and without distinct sloping borders. This result shows two things: the first one is that it is concordant with the morphological properties of the salt marsh, since it is higher than the surrounding marshes (so higher tidal events are needed to constantly carve the final part of the creek, as water does frequently in the first part). Indeed, if we take the peak of the average tidal event used for the long scale model and we analyze it using the slope, we obtain a water value in section 5 of 14 cm. This results may show that the limit of the normal cross sections is in a sort of equilibrium with the effect of the erosion by the tide, and the final part of the marsh creek is flooded (and so carved) only in the higher tidal events. This is an interesting results, but the assumptions are strong and other marshes and creeks must be analyzed in order to demonstrate this point.

On the other hand, the second result from the cross section analysis indicates that this final part of the creek is able to contain around 10-15 cm of water, before it becomes too high and floods the surrounding marsh soil. This means that, in the accounting for the A(h) curve, this flooding tendency must be taken into account for high water level.

In order to obtain this curve, the trend of the width of the free water surface at different water level is studied for the five sections (Table 3.9). Results are then compared with each other, taking into account also the slope and the differences in the simultaneous water level in the different sections (Table 3.8).

Table 3.9 Values of free water surface for different water level (h) in the five sections.

Water level (cm)	SECT. 1 (cm)	SECT. 2 (cm)	SECT. 3 (cm)	SECT. 4 (cm)	SECT. 5 (cm)
1	160				
2	179				
3	193				
4	203				
5	209	70			
6	214.6	100			
7	220	120			
8	223	135			
9	226	143.3			
10	229	150	70		
11	231	156.7	83.3		
12	233.4	161	90		
13	235	163.5	96.7	70	
14	236	166	102.5	75.8	
15	237.7	168	110	81.7	30
16	239	170.6	117.5	87.5	43.3
17	240.6	173	122.5	93.3	51.7
18	242	175.3	126.3	98.7	70
19	243.4	177.6	130	104	78.3
20	245	180	133.8	108	86.7
21	246.3	182	136.3	112	93.3
22	247.7	183.7	138.8	116	98.3
23	250.5	185.6	141.3	123	103.3
24	254.6	187.5	143.8	130	107
25	260.3	189.4	146.3	135	110.7
26	267.3	191	148.9	140	114.3
27	274	193	151.6	145	118
28	278	195	154.3	150	125
29	282.4	197	157.1	157.5	135
30	287	198.7	160	165	145
31	292.3	201.6	162.9	170.8	155
32	297.4	205.4	165.7	176.7	
33	303.3	210.3	177.1		
34	310	215	181.9		
35	316.7	220	186.7		
36	330	226	195		
37	343.3	231.7			
38	350	237.5			

The area for a certain water level h is then calculated just treating horizontal area between two sections as a trapezoid, where the two free water surface width value are the two bases and the distance between the two sections the height. When water level reaches all the sections, the area is calculated with the same procedure but summing the results for every couple of sections, and the final part of the creek is considered as a rectangle (due constant section). As it possible to notice, when the tide reaches the value of circa 30 cm, it pours out from the last section, which indicates the flooding of the last part, as stated previously. In this case, it is assumed an increasing percentage of flooding of the total basin area (2331.12 m^2; see Figure 2.11).

The obtained values are shown in Table 3.10 and in Figure 3.7. Also, in Baldan (2015), it is assumed a difference in 3 cm between the beginning of the marsh creek and the section 1, which is maintained also in this thesis and corrects the water level value.

Table 3.10 Values of areas for different water level. Corrected values take into considereation the difference of 3 cm between the beginning of the marsh creek and the sampling point within it.

Water level (m)	**Corrected water level (m)**	**Area (m^2)**
0	0.03	0.0
0.01	0.04	4.4
0.05	0.08	23.7
0.1	0.13	58.6
0.13	0.16	73.8
0.15	0.18	81.6
0.2	0.23	116.5
0.22	0.25	124.3
0.25	0.28	135.3
0.27	0.30	166.5
0.29	0.32	217.7
0.31	0.34	339.7
0.35	0.38	769.4
0.4	0.43	1218.3
0.5	0.53	2331.1

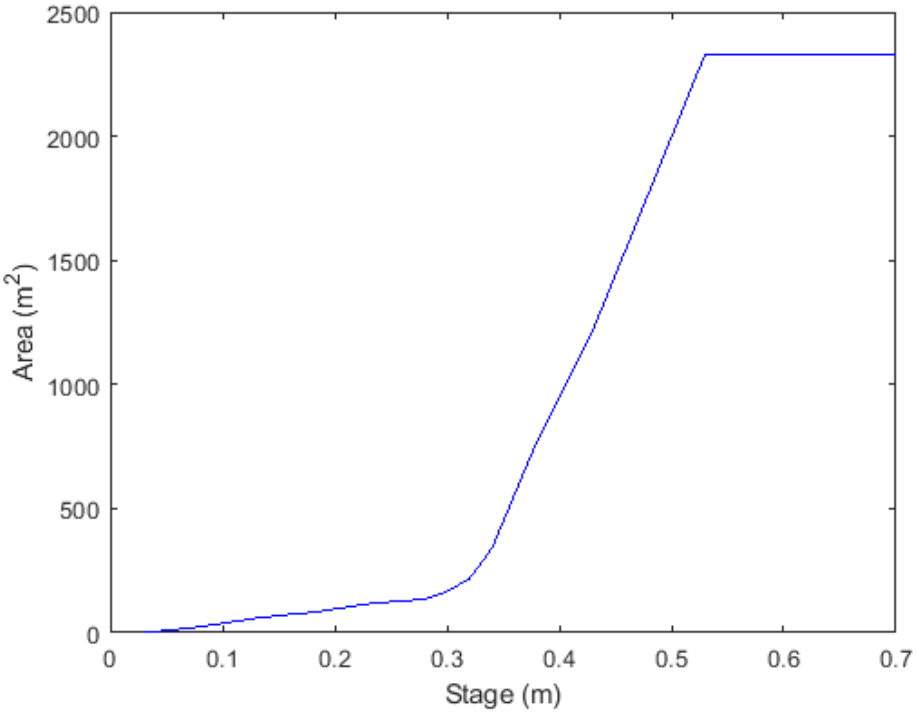

Figure 3.7 A(h) curve.

As it possible to notice from Figure 3.7, the curve has a sudden increase of flooded area at about 32-33 cm of water level at section 1. This indicates that the final part of the creek was

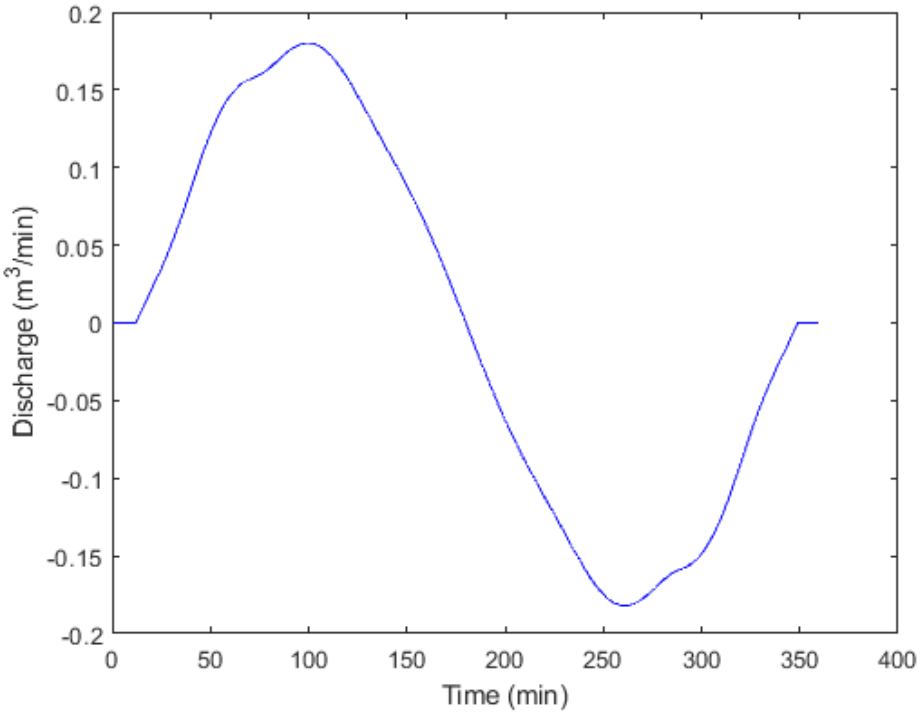

Figure 3.8 Average trend of the discharge during a tide event.

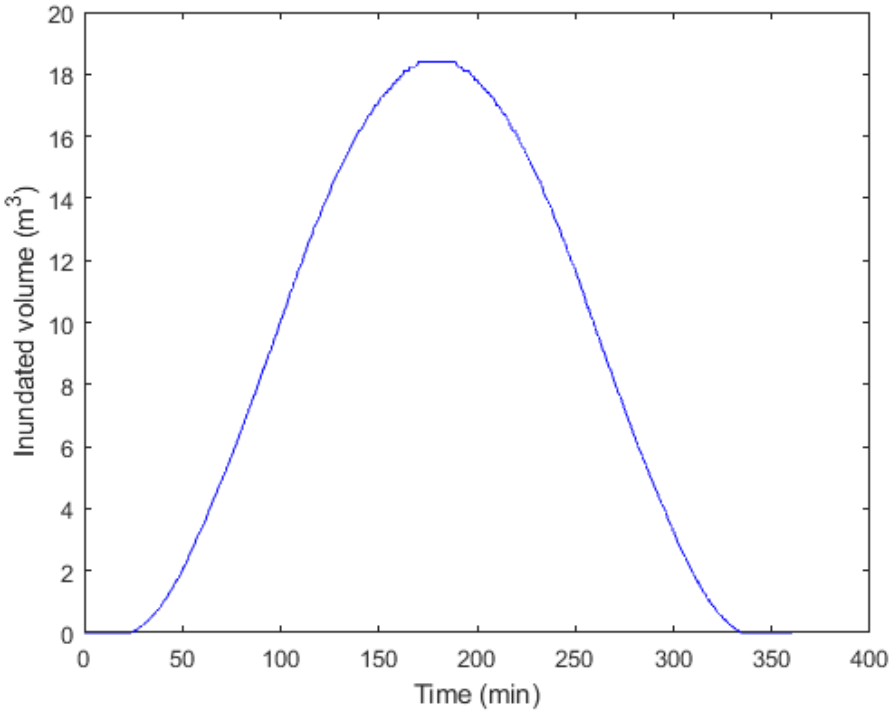

Figure 3.9 Average trend of the volume during a tide event.

completely submerged by the tide and a certain part of the basis begins to be flooded. From that point, for a small increase of water level corresponds a great increase in the submerged surface, until the marsh is considered completely flooded for water levels equal or greater than 50 cm.

To sum up all the results, it is possible to understand that the marsh creek could be in a sort of equilibrium with the tide events that characterize a certain salt marsh. It is well studied in literature that the system of marsh creeks is generated, during the life of the salt marsh, by the tide. It starts with a small perturbation in a certain point, that can allow the tide to enter, and then the shear stress and the consequent erosion begin to carve the creek. This happens until a sort of equilibrium between the tide erosive effect and the vertical growth of the salt marsh due to accretion, which tends to fill the creeks, is reached. For this reason, the shape of the cross section is function of the creek history and the area is dictated by the discharges (D'Alpaos et al., 2006) (Figure 3.8). Moreover, it is possible to notice that the creek is capable of containing high levels of tide, before starting to flood the marsh surface. This can be an indicator of the importance of the marsh creek in the nitrogen balance, since it is the most frequently flooded are of the salt marsh and therefore can process important volumes of water (Figure 3.9).

3.2.2 Results of April 2017

The results of the sampling campaign of April 2017 are presented in this paragraph. It was carried out on the 27/04/2017 and it was characterized by a tidal event with a height of 0.42 m (Figure 3.10).

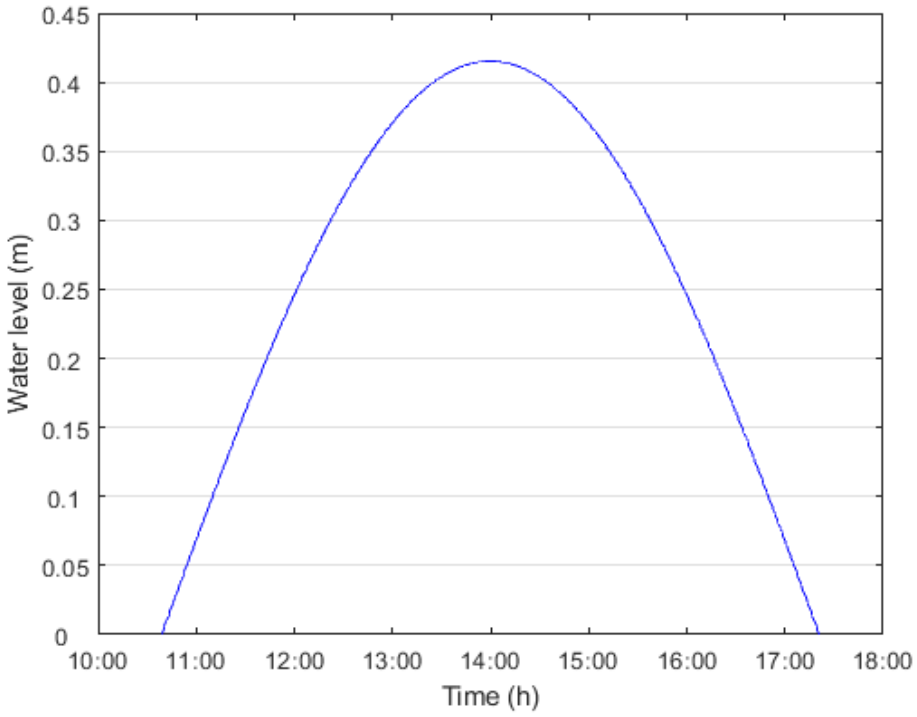

Figure 3.10 April tide event.

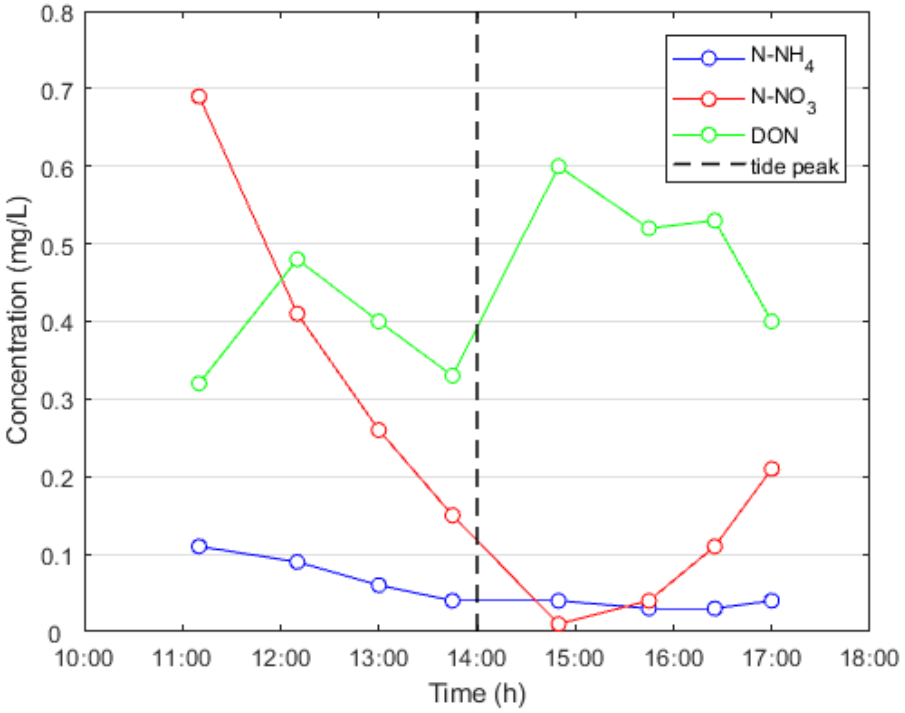

Figure 3.11 Concentration of nitrogen compounds inside the marsh creek.

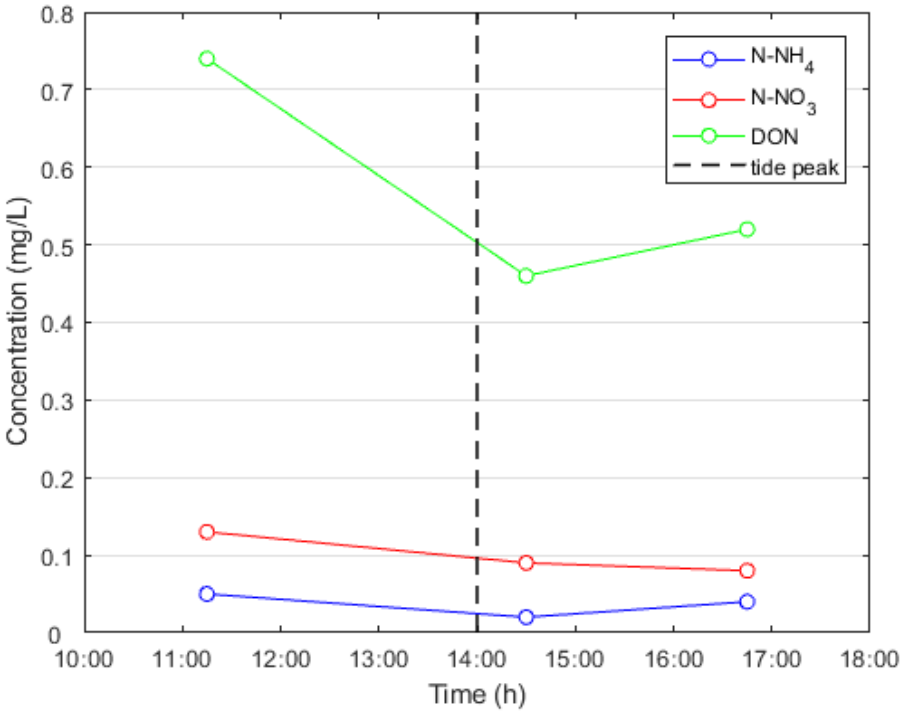

Figure 3.12 Concentration of samples taken at the surface of the channel outside the salt marsh.

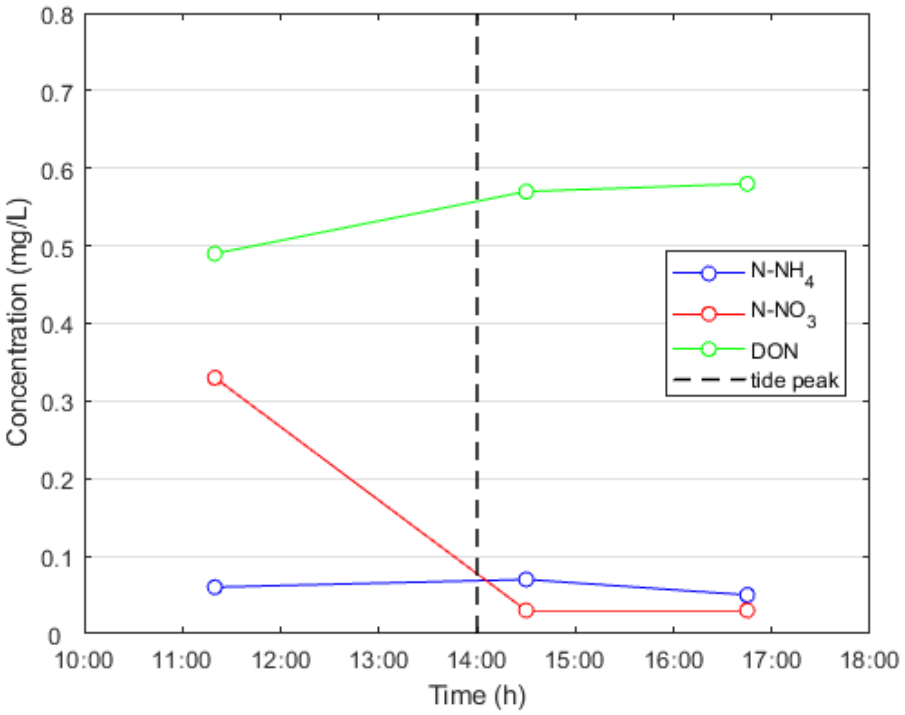

Figure 3.13 Concentration of samples taken at the bottom of the channel outside the salt marsh.

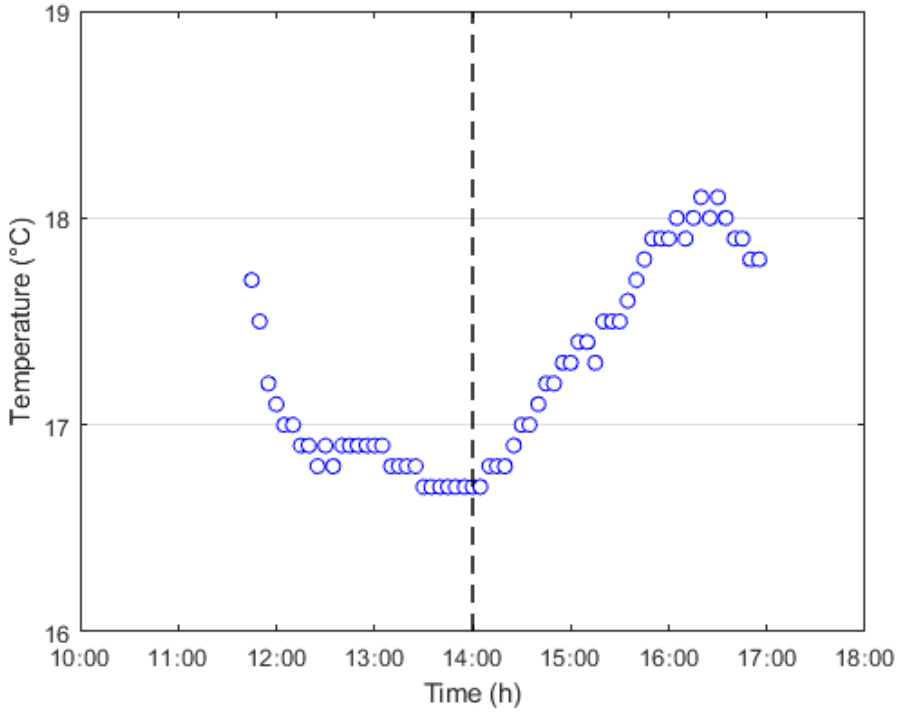

Figure 3.14 Temperature data from the WTW probe.

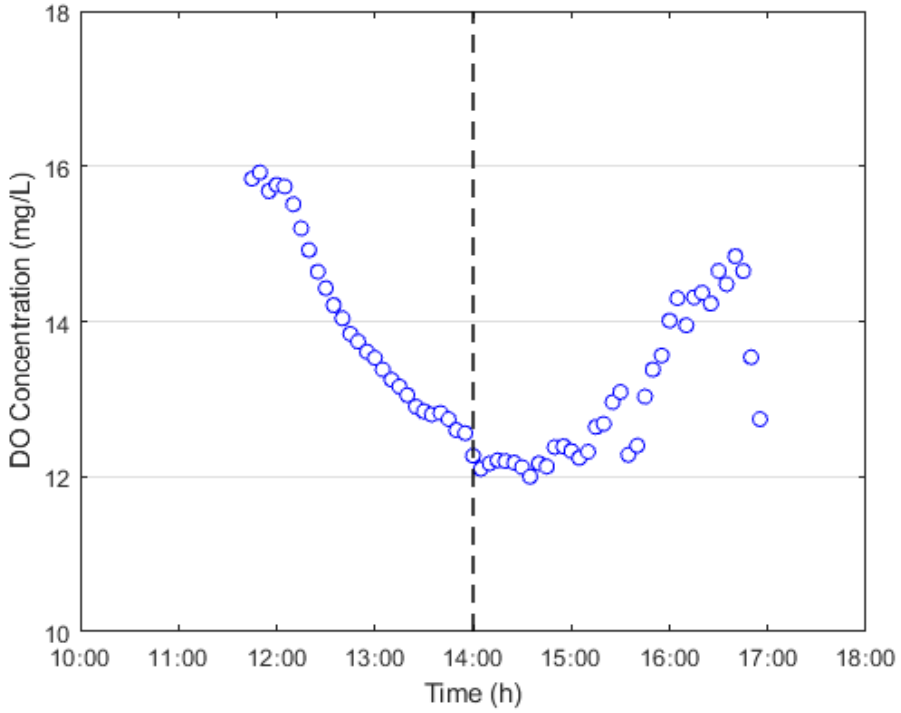

Figure 3.15 Dissolved oxygen data from WTW probe

.

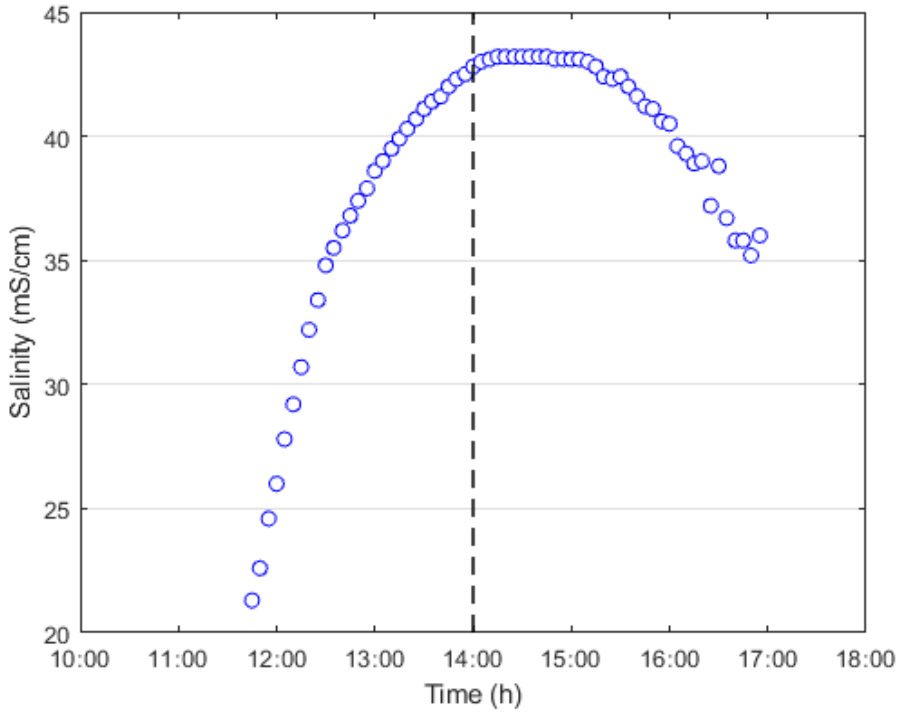

Figure 3.16 Salinity data from the WTW probe

From Figure 3.11, it is possible to notice how ammonium is characterized by constant low values, along the entire tide event.

The nitrate concentration decreases with the water entering in the salt marsh, but during the ebb, the values tend to increase again. This can be due to different factors, such as release from the sediment, not complete consumption of the entire input mass of nitrate or other biochemical factors. It must be pointed out that this campaign was characterized by great amount of rainfall in the days before the field survey and during that precise day. This led to stratification of fresh- and seawater, as it is possible to notice from the differences in concentration between surface and bottom of the channel in Figure 3.12 and 3.13. This can explain the high concentration in input of nitrate, as the freshwater discharge to the lagoon may have washed out the agricultural soil (during a period of fertilization of fields), and, standing the freshwater above the salty one, it entered in the first moments in the salt marsh, which is explained also by the initial low value of salinity. As far as the DON (dissolved organic nitrogen) is concerned, it does not have a constant trend: for the increasing tide, it increases and then decreases and the same happens for the ebb. This result can be due to the combined effect of many factors: the decrease can be the consequence of dilution happening with the increasing tide or by hydrolysis, and the increase can be due to release from sediment, maybe generated by concentration gradient.

Analyzing the temperature and DO (dissolved oxygen) concentration, it is interesting to notice that at the increase of the first one corresponds an increase in the second one. This points out the beginning of biological activity triggered by the temperature, which may be correlated with the difference in initial and final concentration of ammonium and nitrate during the tide event, which have been degraded biologically. However, it is possible that the low temperature and the high initial concentration mat have partially inhibited this activity but further data are necessary to address this point.

Interesting is also the trend of the salinity. As it is possible to notice, the salinity at the beginning is increasing, which indicates the passage from freshwater to more seawater entering. During the ebb, though, the salinity tends to decrease, reaching values higher than the initial ones. This shows a mixing of the freshwater, entered at the beginning, with the tide water, in the last part of the salt marsh creek.

Finally, it possible to notice a decrease in nitrate concentration in the channel outside the salt marsh, which is in concordance with the decrease observed in the creek. While ammonium remains almost constant, it is noteworthy how the concentration of DON slightly increases, in contrast with the decreasing values in the creek. Anyway, DON is the nitrogen compound, which, in average, has the highest concentration in the lagoon water

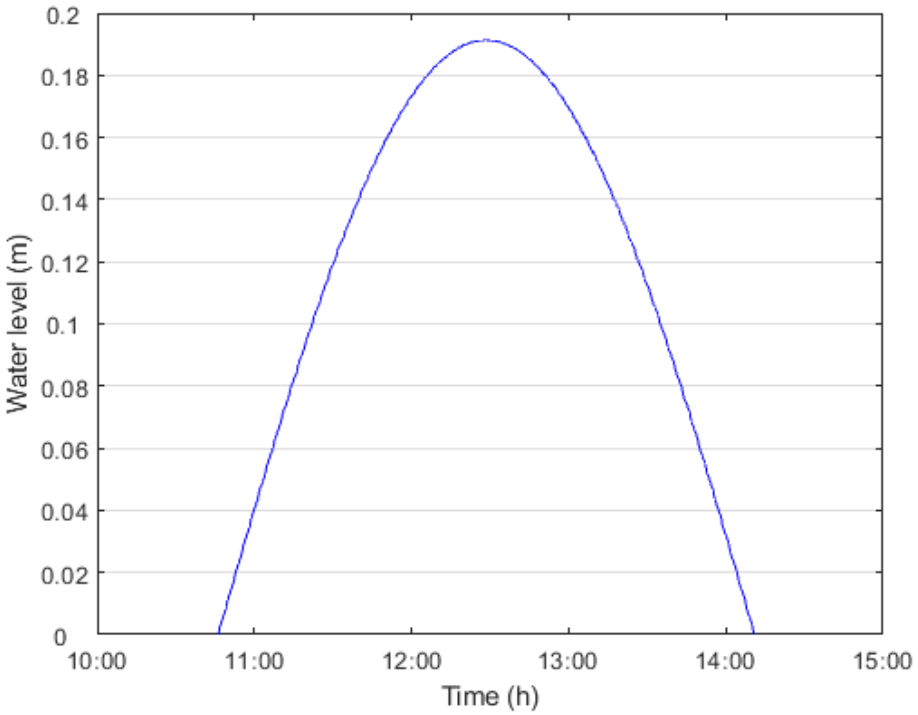

Figure 3.17 May tide event.

3.2.3 Results of May 2017

In this paragraph, the results of the sampling campaign of the 25/05/2017 are presented. A particular issue characterized this campaign: The tide was charactherized by an elevation of 19 cm and a duration of 205 min (Figure 3.17), which allowed to take only few samples. Moreover, at different points the sampling activity was carried on both with the vacuum pump and with the plastic becher attached to a rod, in order to analyze possible differences. No particular change in results is observed between the two methods.

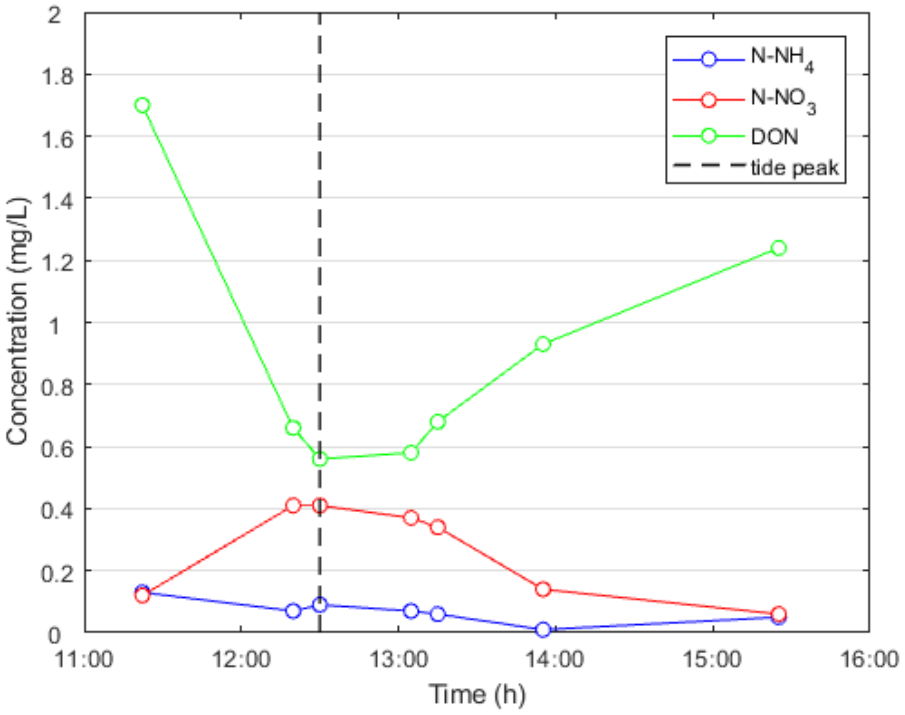

Figure 3.18 Concentration of nitrogen compounds inside the marsh creek.

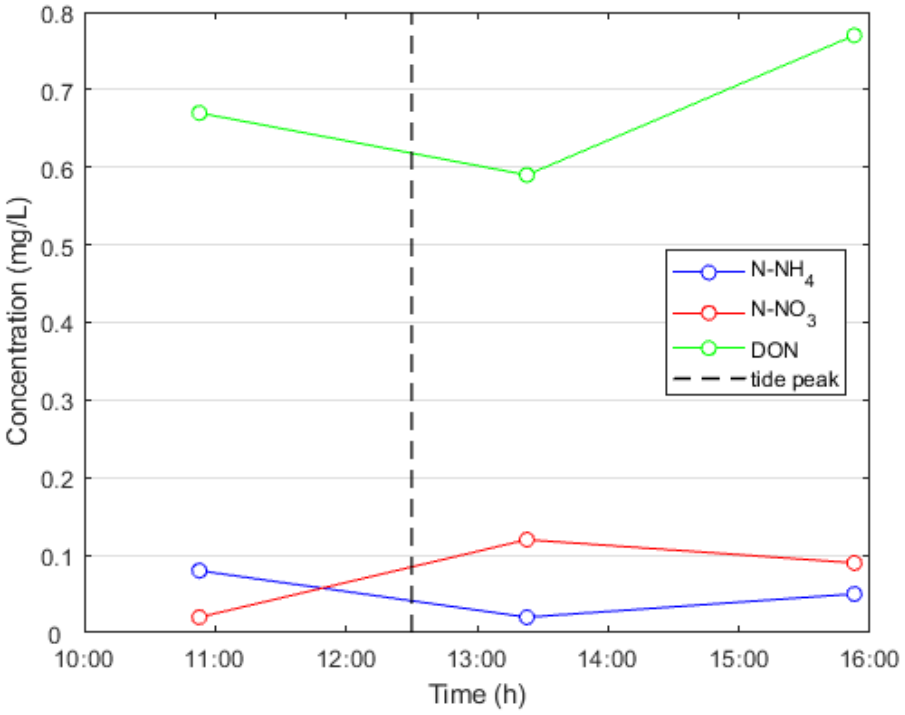

Figure 3.19 Concentration of samples taken at the surface of the channel outside the salt marsh.

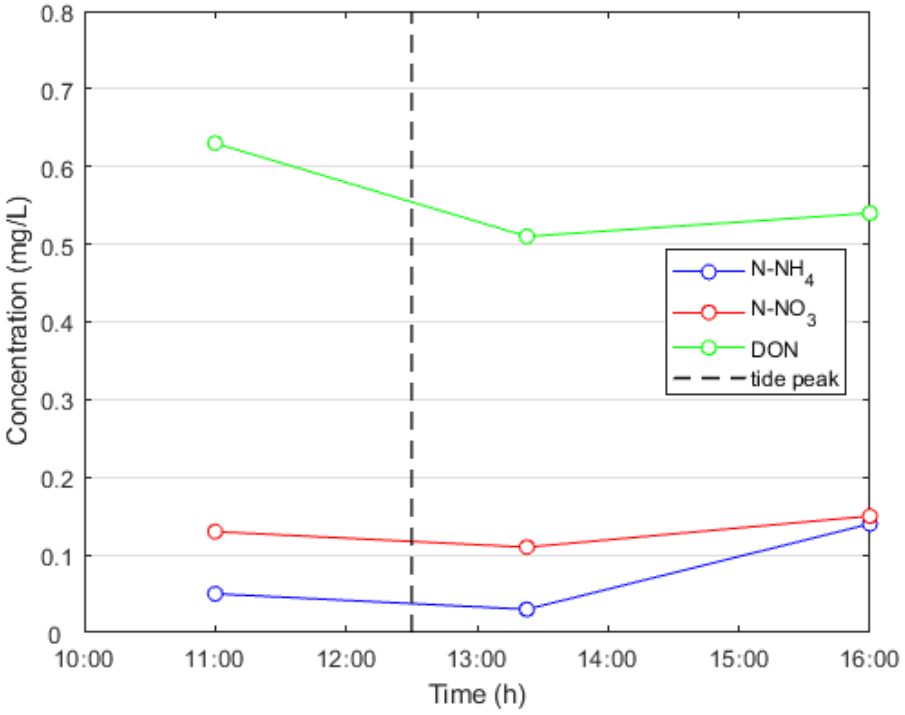

Figure 3.20 Concentration of samples taken at the bottom of the channel outside the salt marsh.

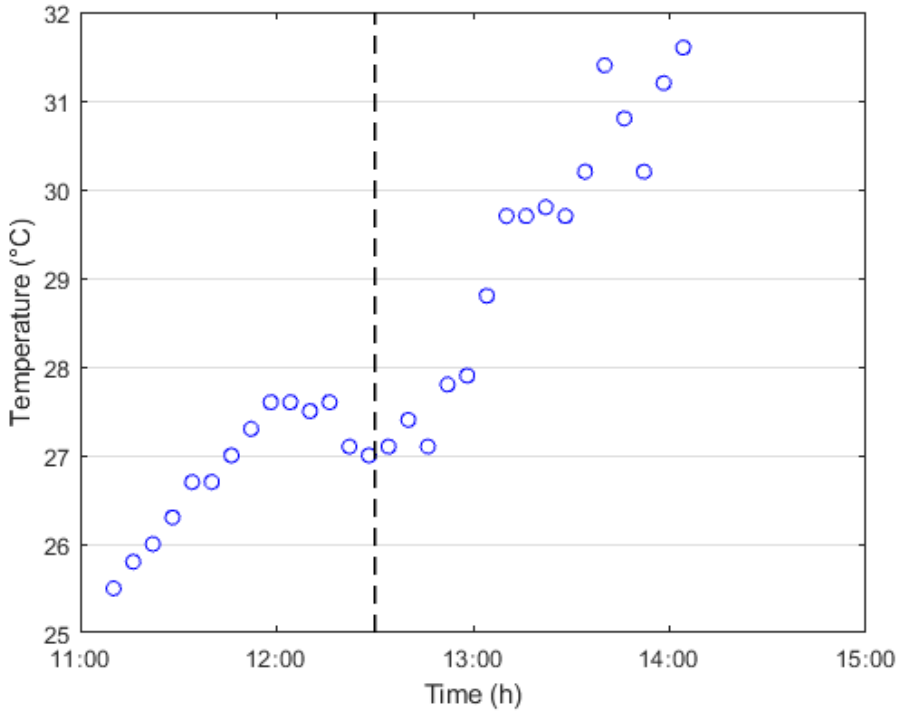

Figure 3.21 Temperature data from the WTW probe.

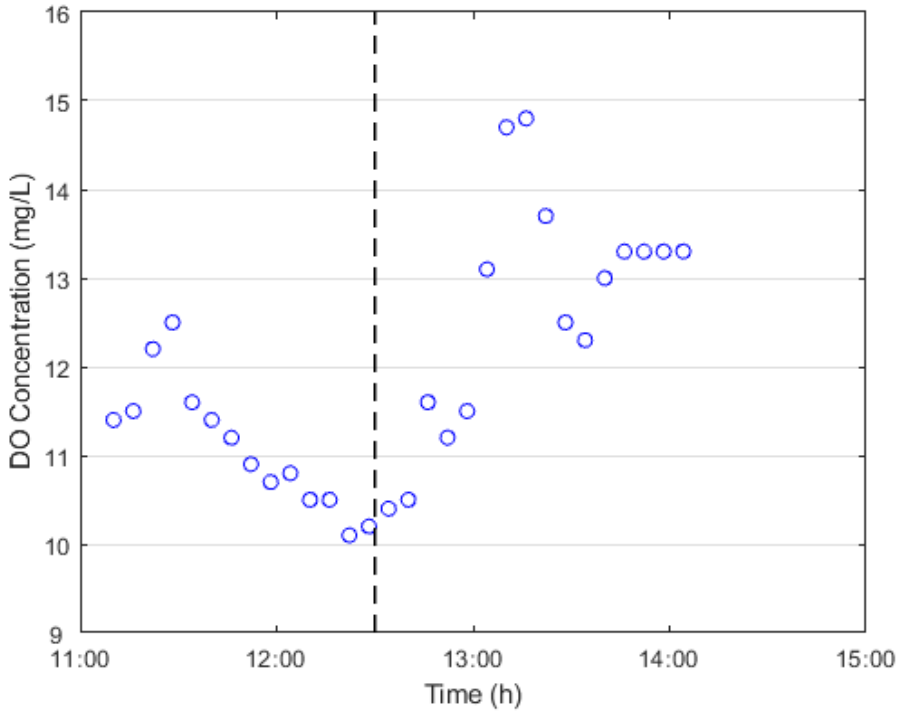

Figure 3.22 Dissolved oxygen data from WTW probe.

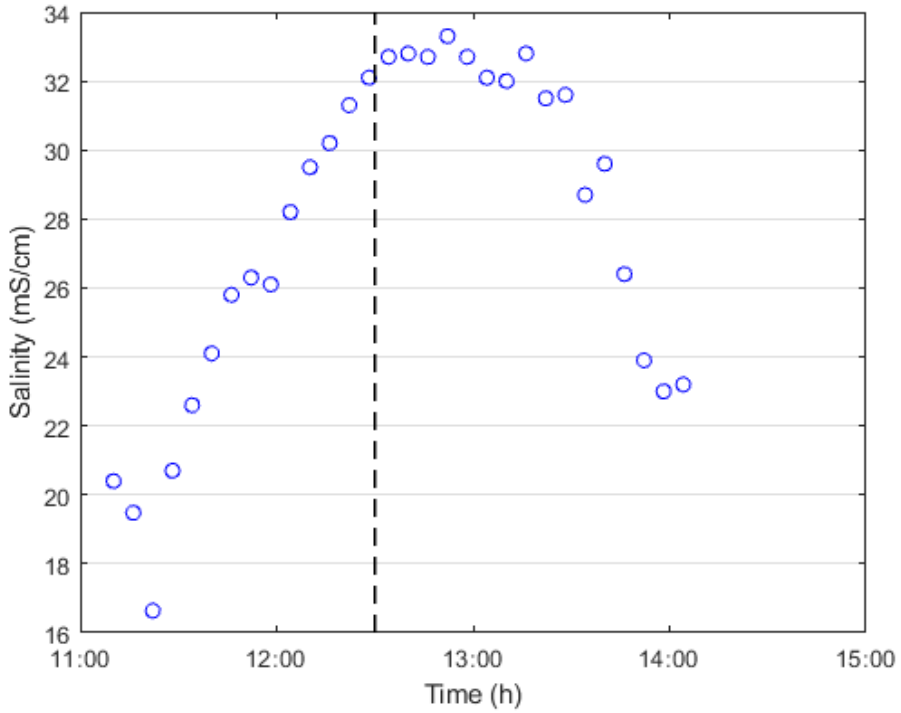

Figure 3.23 Salinity data from the WTW probe.

In this case, it is important to point out that the last samples in the creek are taken after the end of the tidal cycle, trying to collect the seepage water released by the sediment (Figure 3.18).

As it possible to notice, DON is the nitrogen species that presents the higher concentrations, characterizing the lagoon water. Results of the campaign show a more constant concentration trend, despite the first value, showing a release of DON by the salt marsh. This can also be connected to the increase in DON concentration evaluated in the samples outside the salt marsh, more significative for the surface samples (Figure 3.19).

Ammonium presents again low concentrations, which indicates that this nitrogen compound may not contribute significantly to the marsh mass balance. Despite the low values, it tends to decrease inside the creek, indicating a consumption or uptake of ammonium.

As far as nitrate concentrations are concerned, despite the first low value, they show a increase in concentration respect to the input water before the tide peak, which may be connected with transformations in the first part of creek, and a decrease during the ebb, indicating a constant degradation. In this case they show lower concentrations respect to April, which may indicate that the rainfall event in the previous days of the April survey could have an important effect on the nitrate concentration in the lagoon.

It is possible to notice again, analyzing the probes data, an interesting relationship between the increase of the temperature and the increase of dissolved oxygen. In this case, temperature

values increases with a constant trend (Figure 3.21), while the dissolved oxygen firstly decrease to invert later the trend (Figure 3.22). This could highlight again a relationship between the biological activity (connected to DO) and temperature, and could be connected to the decrease of ammonium and, above all, nitrate in the marsh creek.

The salinity starts with low values, pointing out the presence of freshwater at the beginning of the tidal event (Figure 3.23). The values tends to increase due to the higher input of seawater, but then tends to decrease more than in April during the ebb. This could be connected to the low peak and the short tide event: a smaller amount of salty water entered the salt marsh and, in the mixing process, the freshwater still constitutes for the greater part, generating a final values of salinity which are more similar to the initial ones respect to the peak one (considered pure seawater). This time, though, there is no correlation between the initial freshwater and high concentrations of nitrate, which may indicate that the source of nutrients could be the seawater itself and not the river water.

This event, despite the low and short tide, shows some similarities and some differences from the previous sampling campaign, giving a first indication of the important differences that a salt marsh can show in different moments of the year.

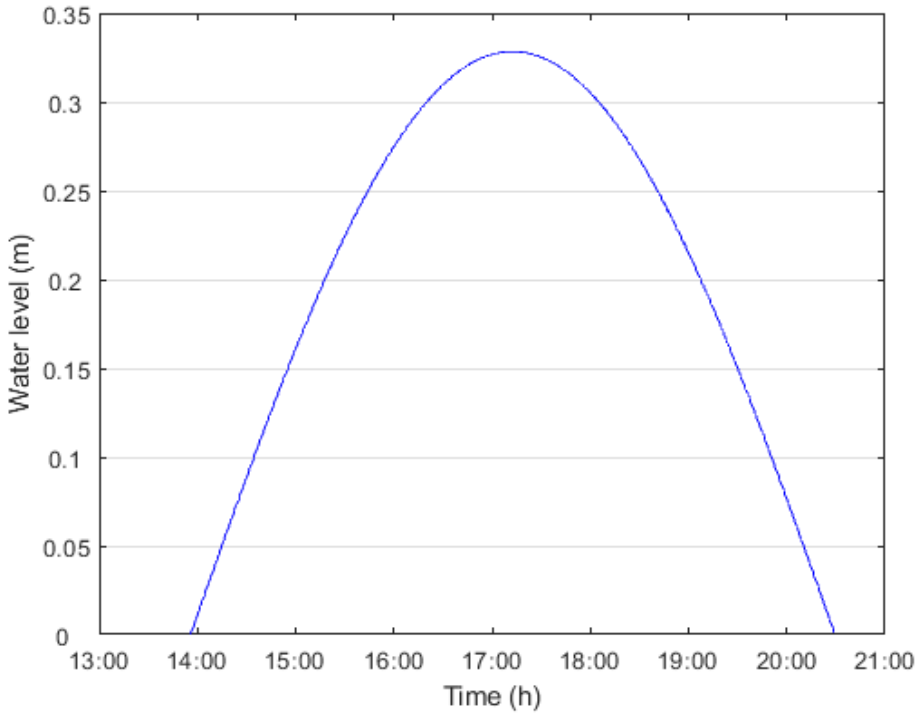

Figure 3.24 June 2016 tide event

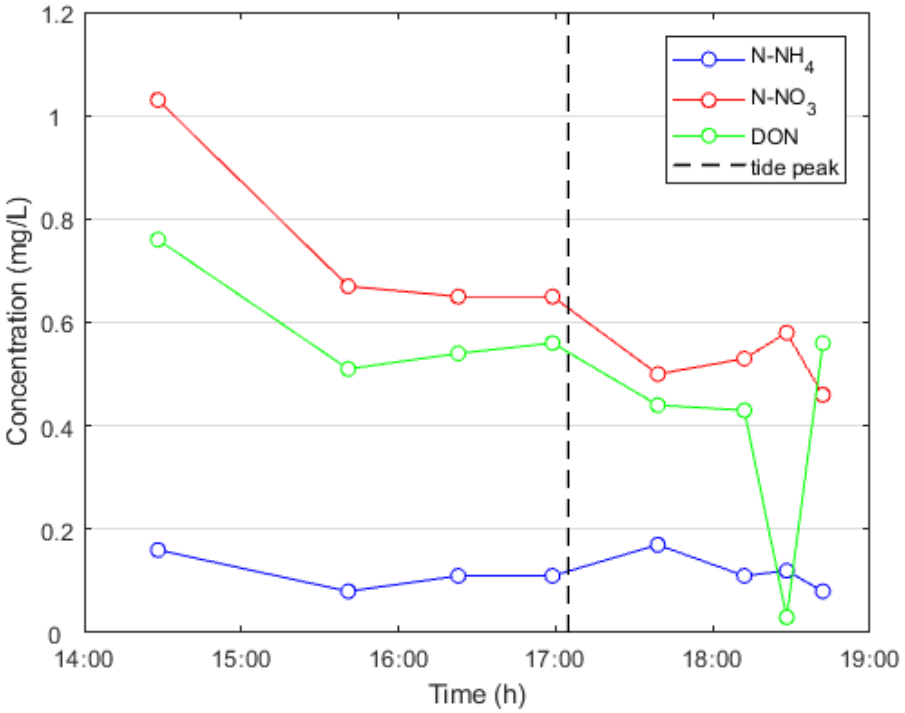

Figure 3.25 Concentration of nitrogen compounds inside the marsh creek.

3.2.4 Results of June 2016

This sampling campaign is prior to this thesis work and its field surveys (10/06/2016), but it was analyzed to have a better understanding of the seasonal salt marsh behavior. This campaign was also characterized by important rainfall events the previous days and no samples for the channel bottom were collected. Moreover, only one WTW probe was present: since it was not possible to continously analyze DO, temperature and salinity, data were collected directly from the bottles with the tide water samples.

An important tide event was registered (peak of circa 32 cm and a duration of 393 min), as well as high concentrations of nitrate, both in the creek (Figure 3.25) and in the channel outside the salt marsh (Figure 3.26). This is, like in April 2017, a correlation between rainfall events and high nitrate concentration. Also ammonium presents higher values than in the previous field surveys and does not show a constant decreasing trend, even if the final concentration value is lower that the first one (indicating a consumption).

As in April, DON tends to decrease as the water enters and then to increase near the tide peak, to repeat again the same trend during the ebb (the penultimate low value may be caused by some error in the sampling moment or during the chemical analysis). This trend is very peculiar and may be caused by many different factor, as stated in Paragraph 3.2.2.

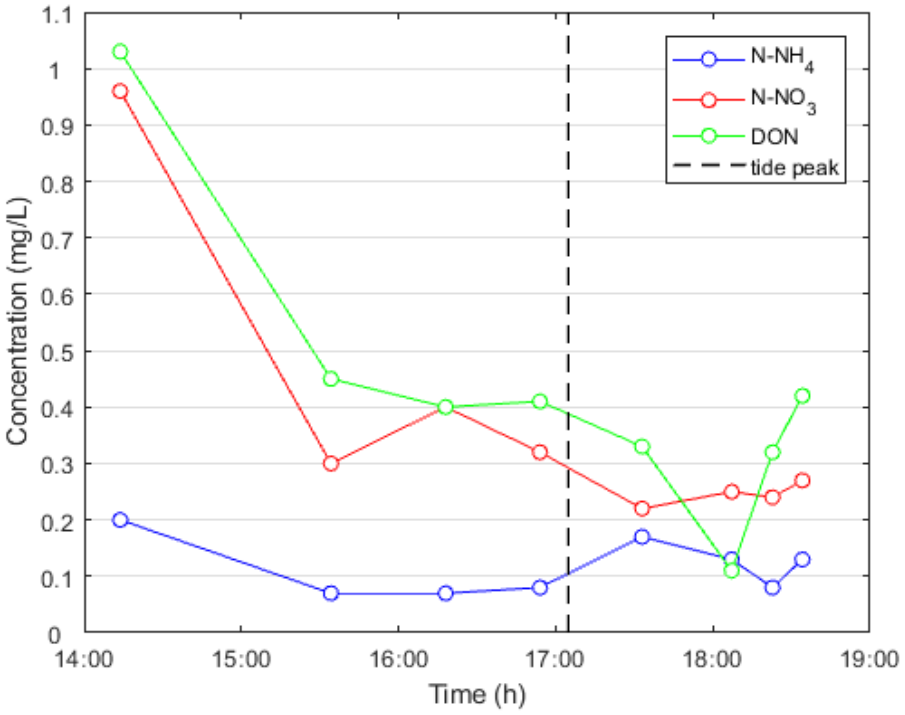

Figure 3.26 Concentration of samples taken at the surface of the channel outside the salt marsh.

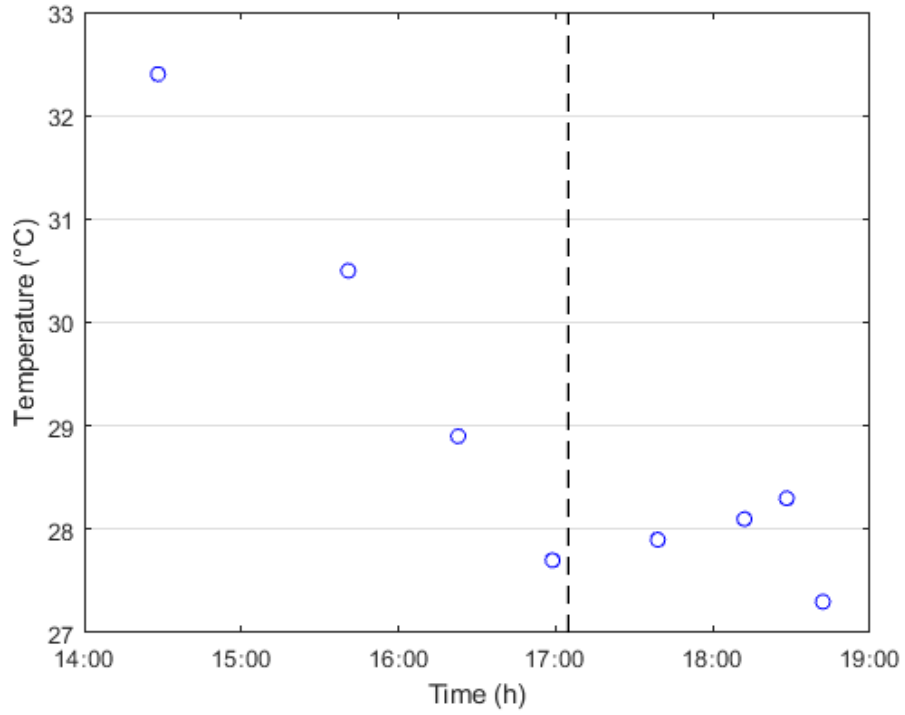

Figure 3.27 Temperature data from the WTW probe.

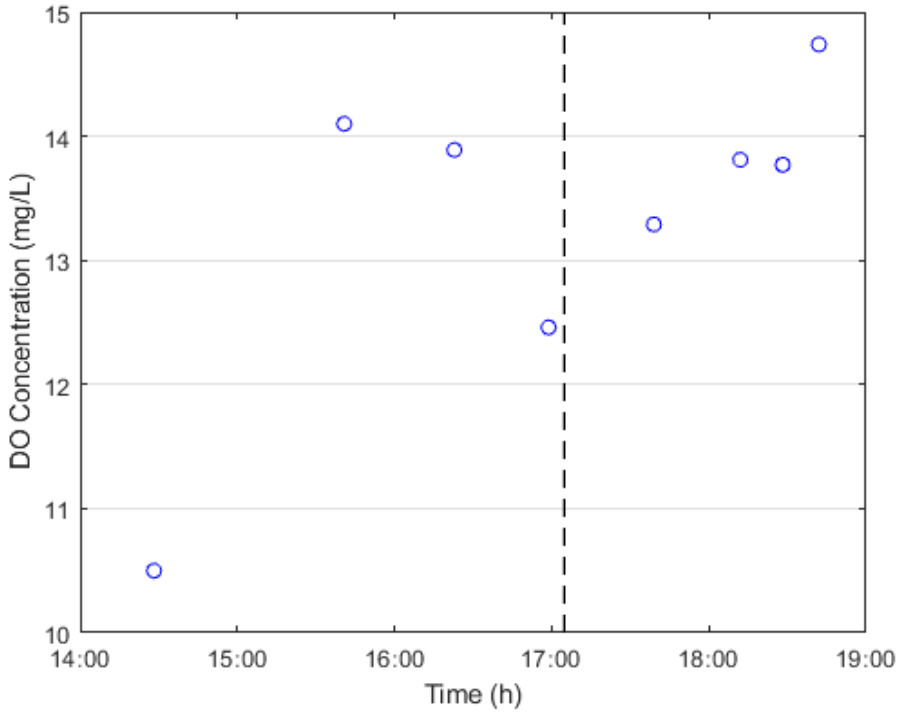

Figure 3.28 Dissolved oxygen data from WTW probe.

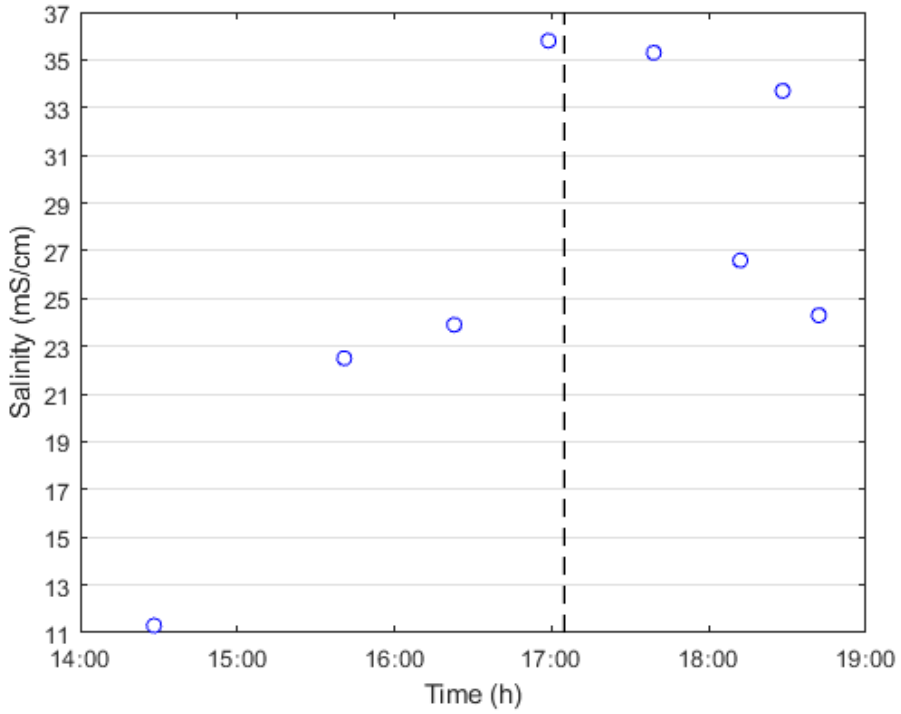

Figure 3.29 Salinity data from the WTW probe.

Nevertheless, nitrate concentrations trend shows a constant decrease, indicating a degradation inside the salt marsh. In this case, no increase is present during the ebb (as in Figure 3.11), but it is worth to notice that the final value is higher than every nitrate concentration value of May survey. This may indicate a maximum capacity of the salt marsh to process high nitrate inputs, which could also be connected to a decreasing temperature, which may have slowed down the biological processes.

In this case, it also possible to notice a great similarity in the concentrations trends in the creek and in the outside channel, highlighting the connection between these two different areas, as the second one is the input for the creek with rising tide, while this last one becomes an input to the outside channel during the ebb. This may be also connected to important stratification occurring in the outside channel. Indeed, this great correlation between marsh and channel concentrations trends could indicate that no mixing in the outside channel is happening and the samples on the surface are very similar to the marsh ones, due to the fact that freshwater is floating upon seawater and it takes all the output nitrogen from the surrounding salt marshes.

No complete probe results evaluation is possible, due to the presence of only one instrument during the campaign. From the few data, it is likely that no correlation is present between temperature and dissolved oxygen, since the first one decreases while the second one has the opposite trend. However, the sampling procedure directly inside the samples bottles may have given unreliable data. Salinity tends to have the same behavior, with increasing values with rising tide and decreasing ones during the ebb, due to mixing of fresh- and seawater. It possible to notice, though, the very low value at the beginning of the tide event, which indicated again a significative stratification in the channel, so that the high concentration value inside and outside the marsh are very likely due to nutrients input from the nearby Dese estuary.

3.2.5 Results of June 2017

The sampling campaign of June 2017 was carried out on 26/06/2017. It was characterized by an almost average tide event: it lasted 305 min with a peak of circa 25 cm (Figure 3.30) and no great rainfall event preceded the sampling campaign.

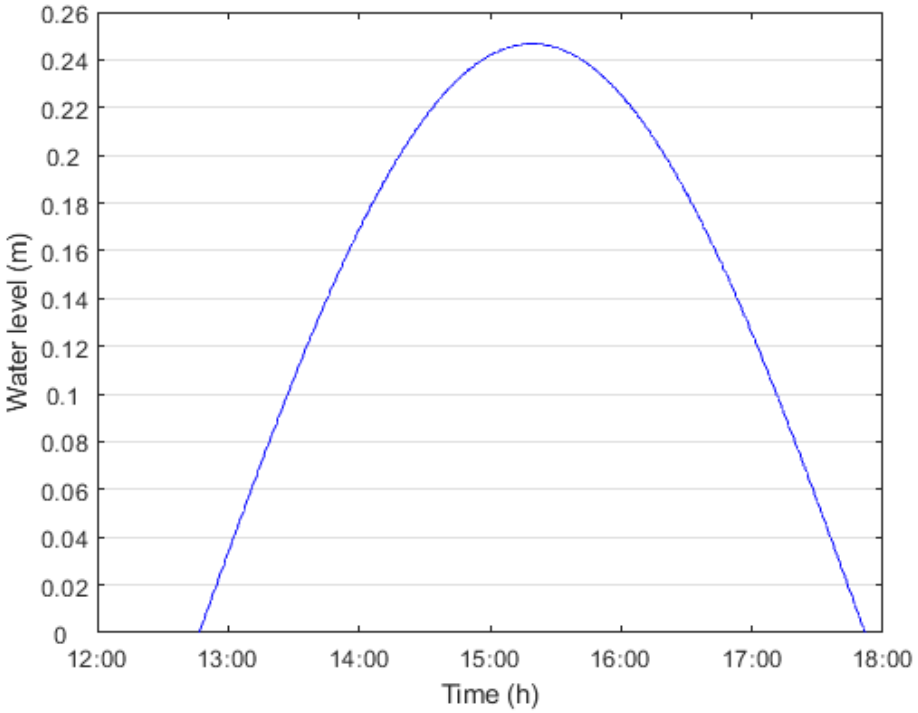

Figure 3.30 June 2017 tide event.

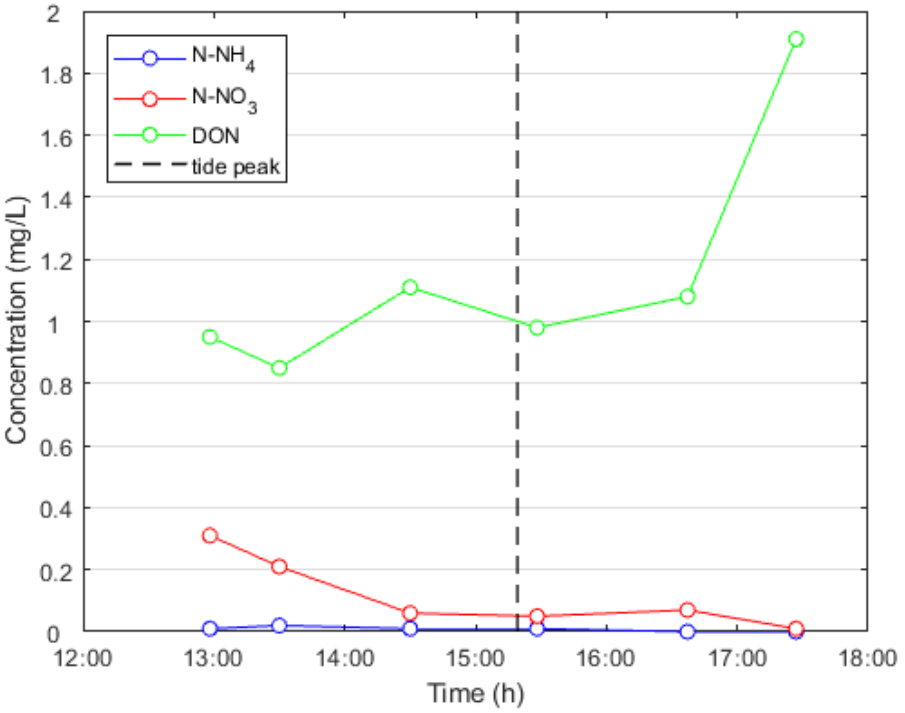

Figure 3.31 Concentration of nitrogen compounds inside the marsh creek.

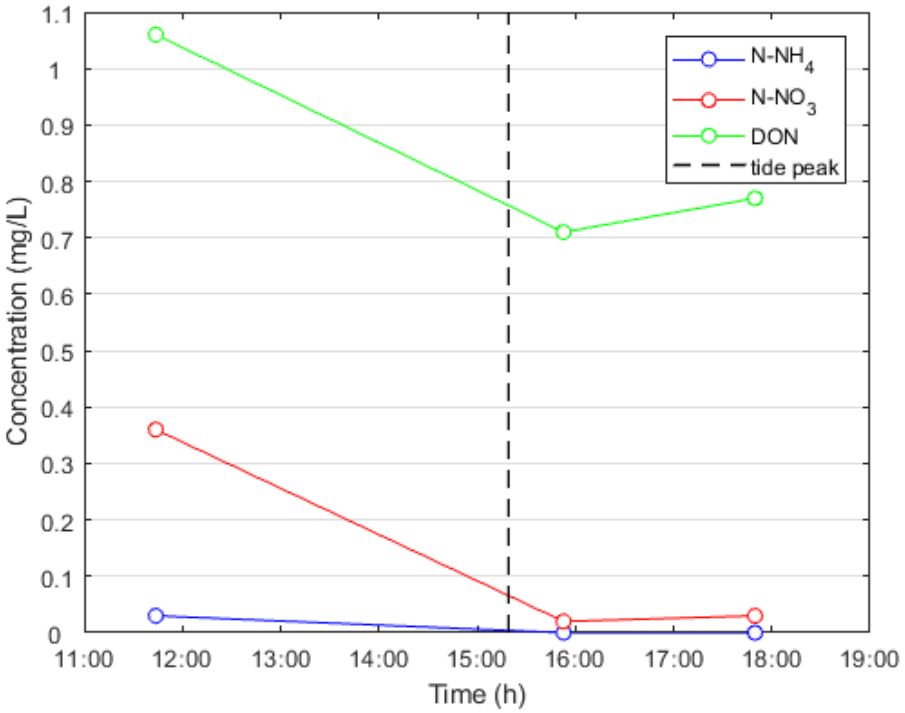

Figure 3.32 Concentration of samples taken at the surface of the channel outside the salt marsh.

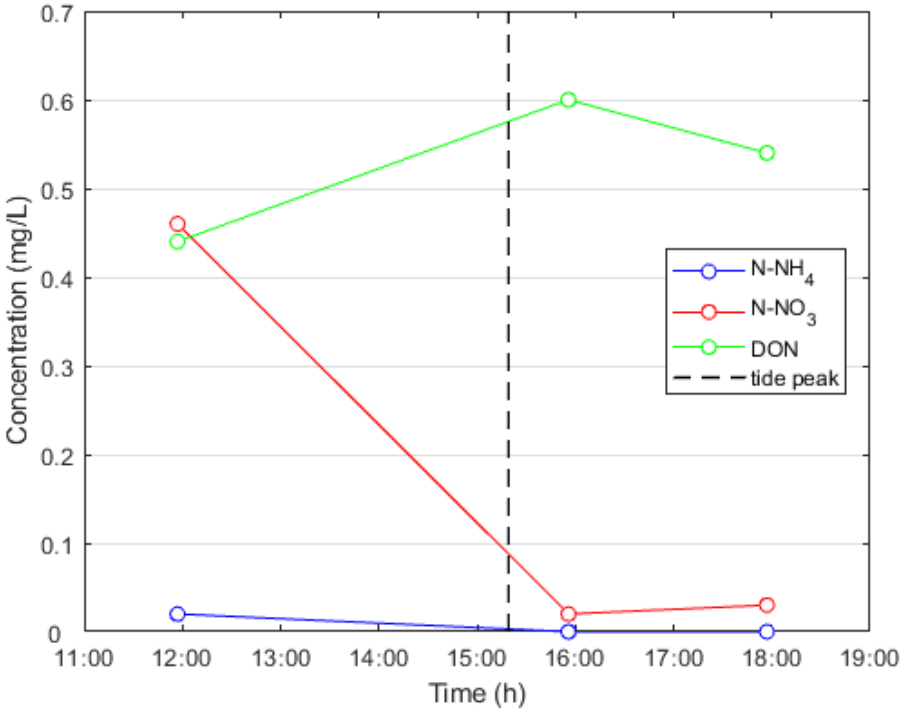

Figure 3.33 Concentration of samples taken at the bottom of the channel outside the salt marsh.

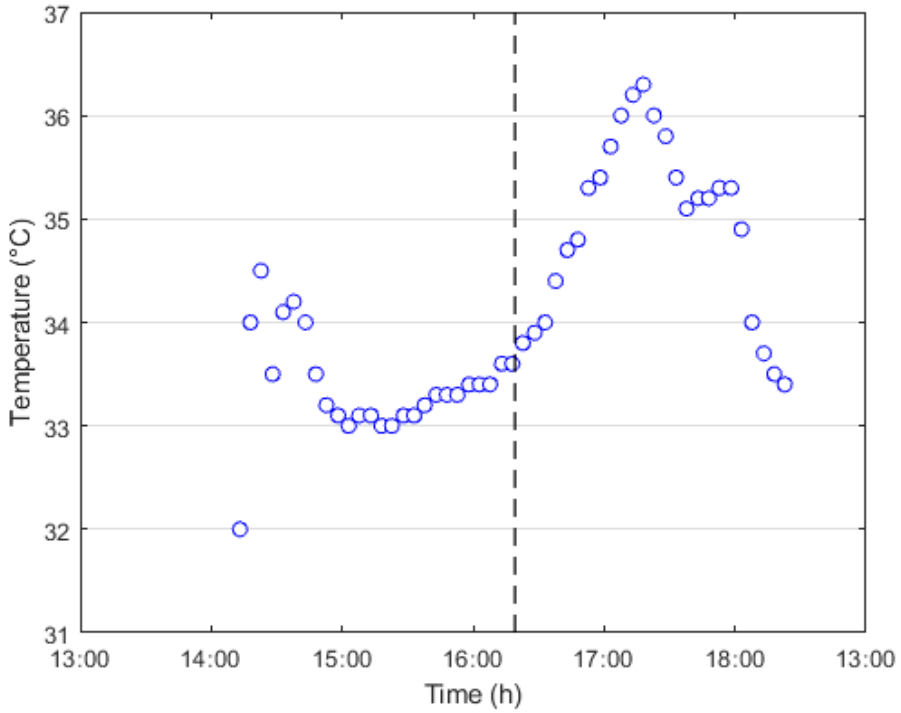

Figure 3.34 Concentration of samples taken at the bottom of the channel outside the salt marsh.

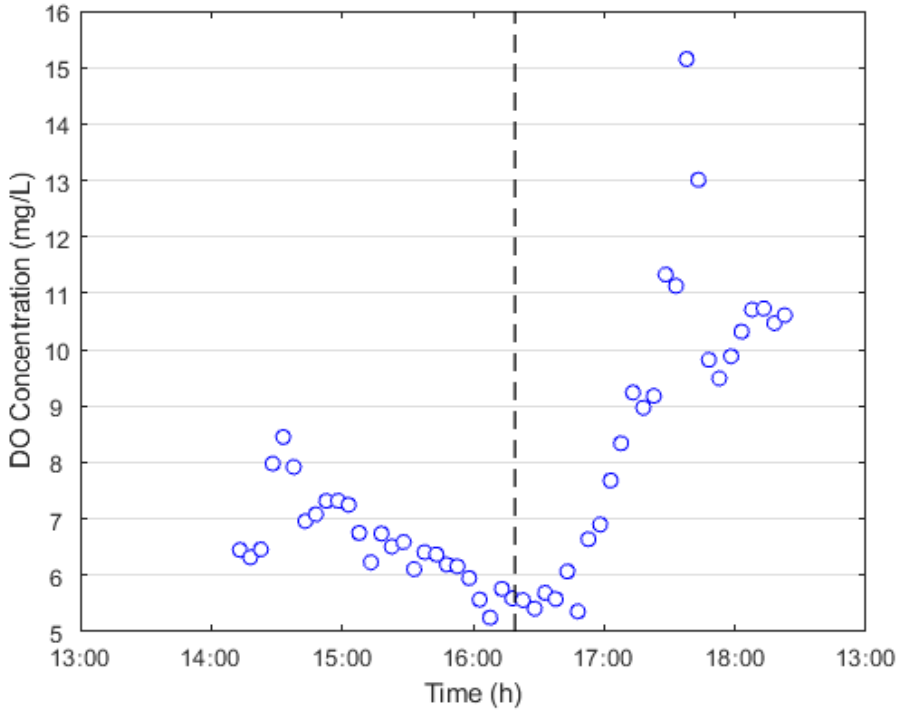

Figure 3.35 Dissolved oxygen data from WTW probe.

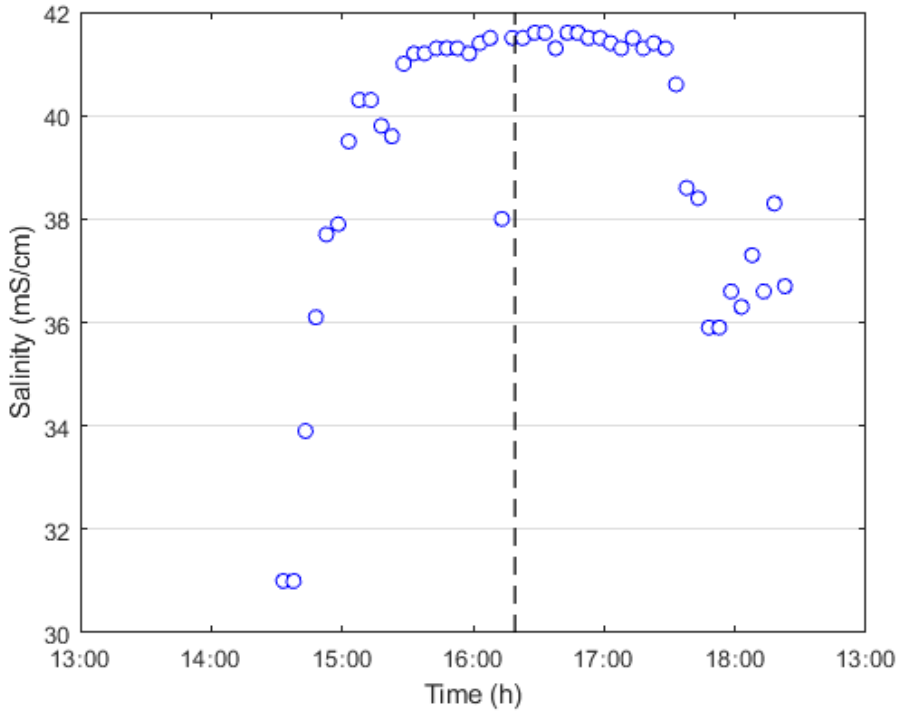

Figura 3.36 Salinity data from the WTW probe.

From the results of the samples in the creek (Figure 3.31), is it possible to notice a similar trend to the one observed in May: ammonim is constantly low, nitrate concentrations decrease and DON tends to increase. It is also important to point out that in this case nitrate tends to zero, which may be connected to the higher temperature that characterized that survey (Figure 3.34) and to the consequent higher biological activity. This assumption could be confirmed by the registered increasing DO concentration (Figure 3.35), connected again to the increase in water temperature.

Other interesting results come from the evaluation of the concentration in the channel outside the marsh (Figure 3.32; Figure 3.33). It is clear how ammonium and nitrate follow the same trend for the surface samples and for the bottom one, but DON values do not have similar values. This may indicate an important effect of exudation from phytoplankton, present in surface due to the higher light availability. From Venice Lagoon analysis in literature, it is possible to notice that phytoplankton bloom starts during June to reach the maximum in July and August (Solidoro et al., 2004), which may be consistent with these campaign results, since it was carried on at the end of June. The same could also happen inside the creek, explaining the increase in DON concentration during the tide event.

As far as salinity is concerned, it shows again the increasing trend for the increasing tide and decreasing values during the ebb, indicating a mixing occurring in the final part of the marsh creek

(Figure 3.36). However, in this case salinity values are higher than the previous analysis, which highlights a greater presence of seawater, respect to the freshwater coming from rivers.

3.2.6 Results of July 2017

The sampling campaigns in July (27/07/2017) was peculiar for different reasons. First, a high tide event was registered, with a peak of 42 cm and a duration of 425 min (Figure 3.37), which filled the marsh creek and nearly spilled out from its border at the sampling point. Secondly, the previous days were characterized by important rainfall events, which lead to think that great amount of nutrients were discharged in the lagoon. Moreover, the WTW probes were set with the wrong unit of measurement, using the percentage of DO respect to the saturation value instead of DO concentration and salinity values instead of conductibility (in mS/cm). Lastly, the temperatures were lower than the average summer values, even lower than the ones registered at the end of June.

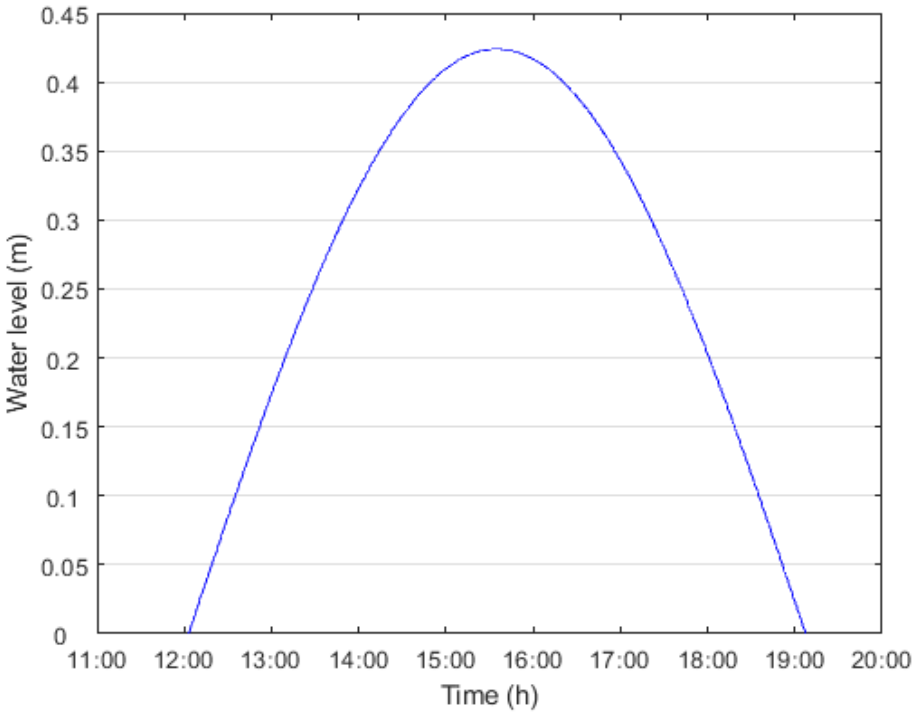

Figure 3.37 July tide event.

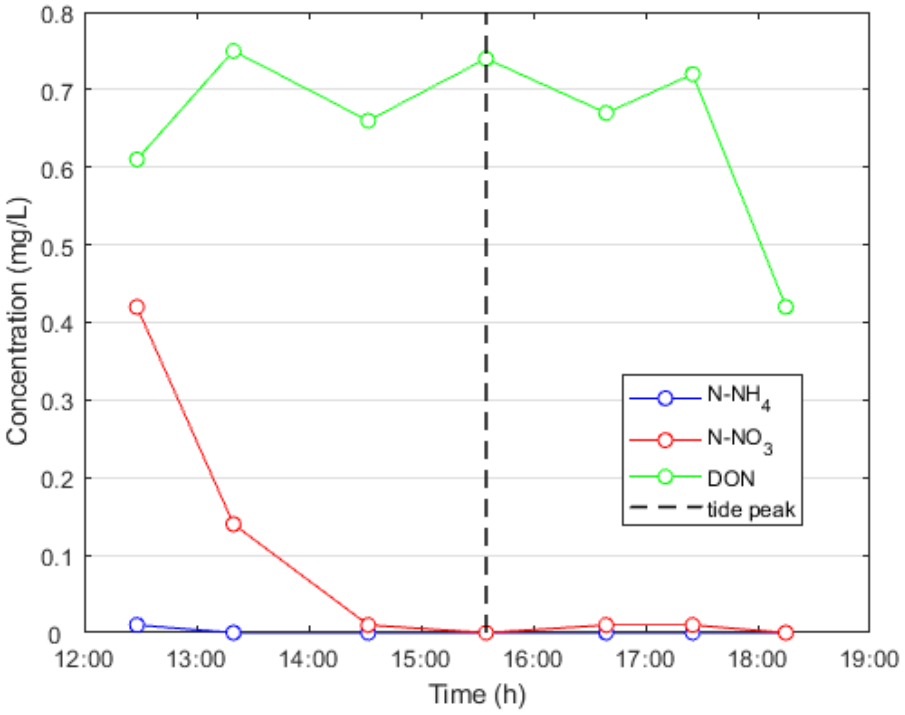

Figure 3.38 Concentration of nitrogen compounds inside the marsh creek.

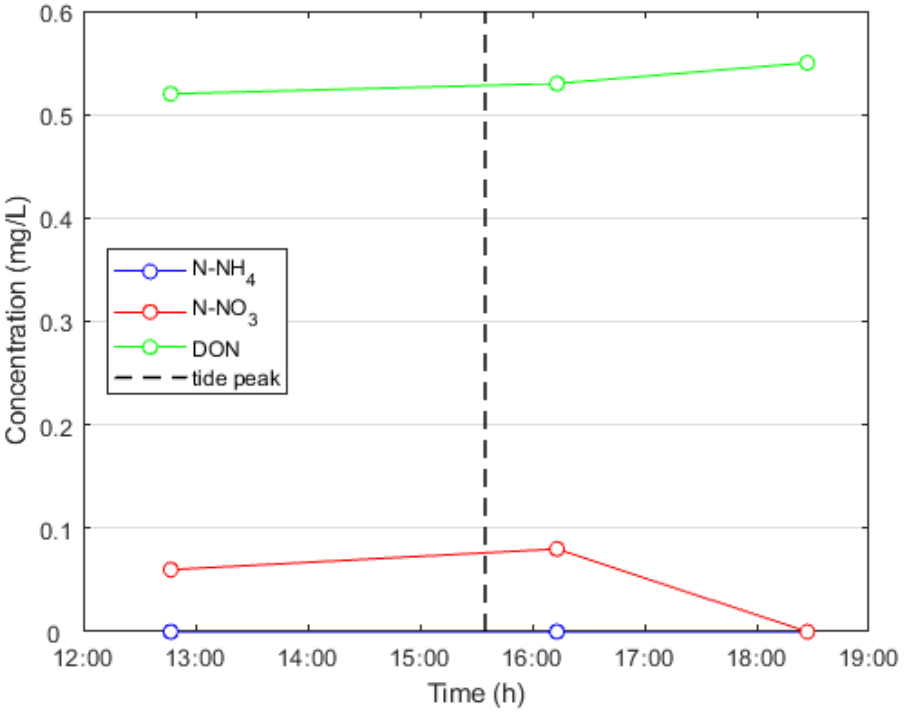

Figure 3.39 Concentration of samples taken at the surface of the channel outside the salt marsh.

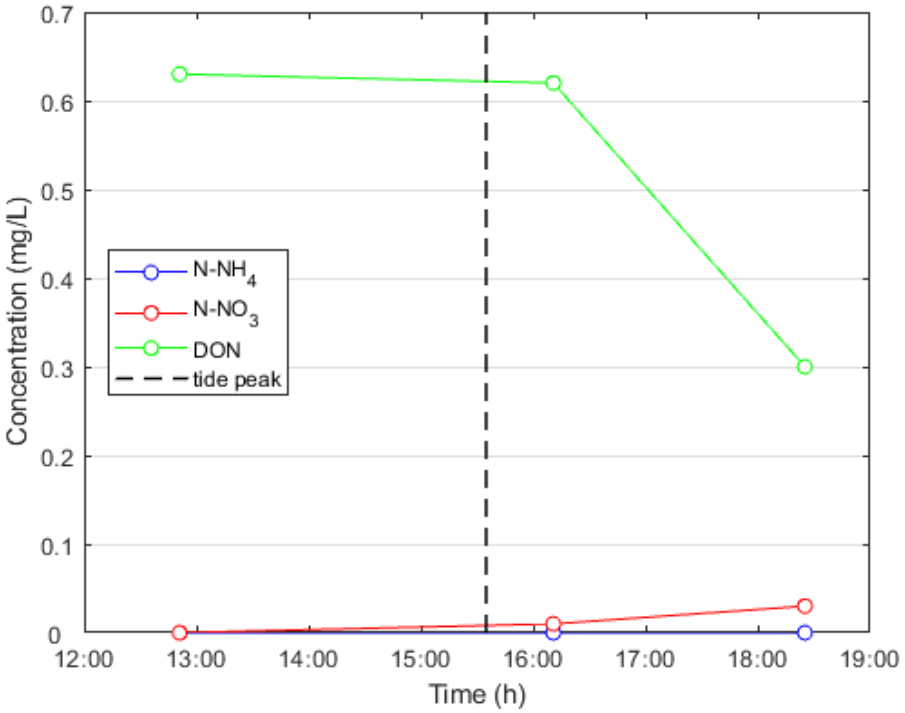

Figure 3.40 Concentration of samples taken at the bottom of the channel outside the salt marsh.

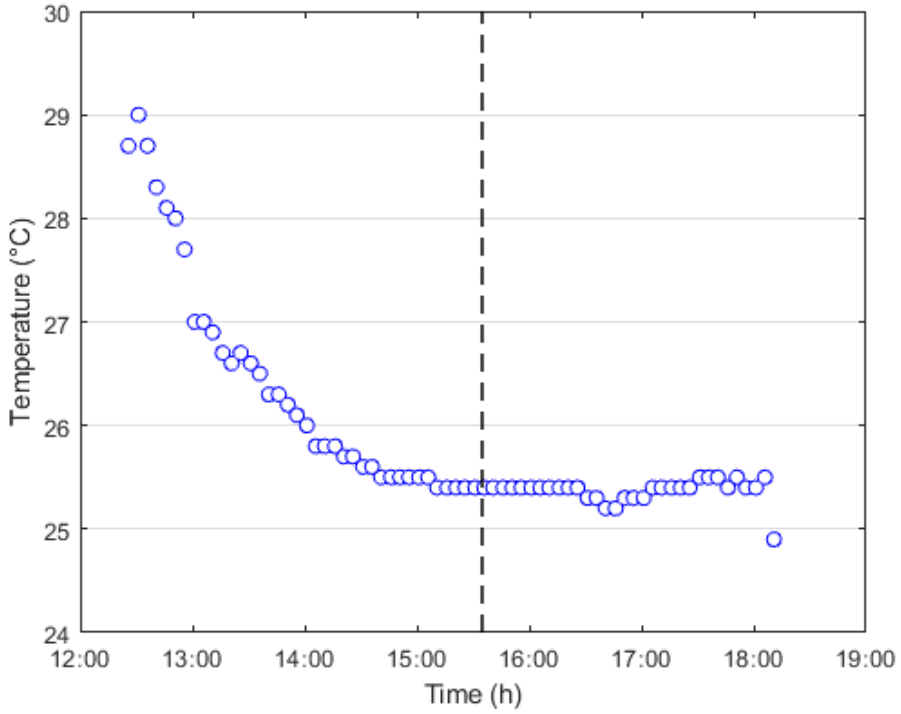

Figura 3.41 Temperature data from the WTW probe.

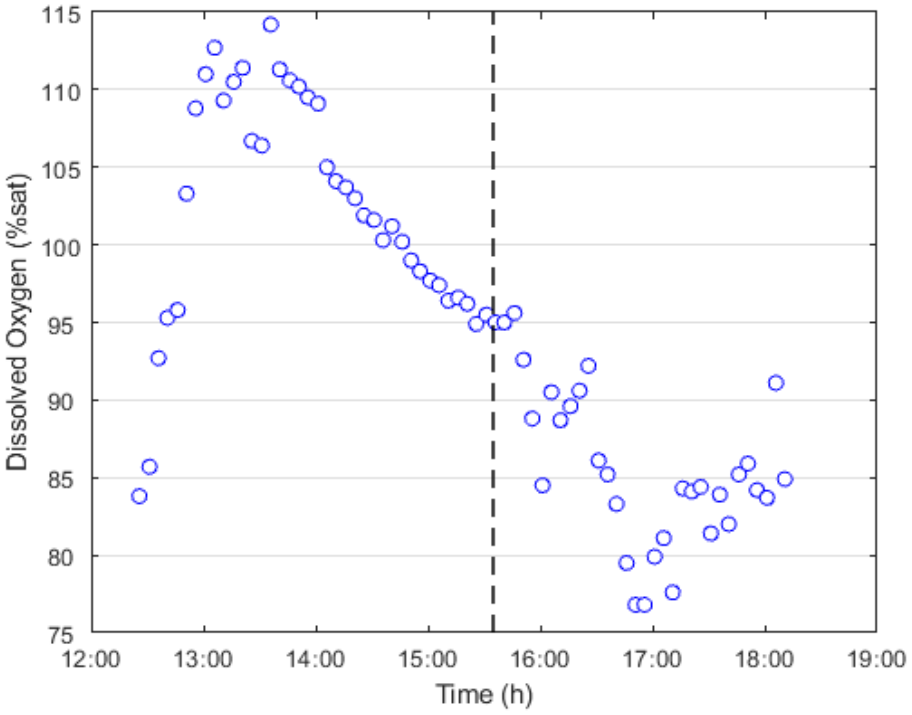

Figure 3.42 Dissolved oxygen data from WTW probe.

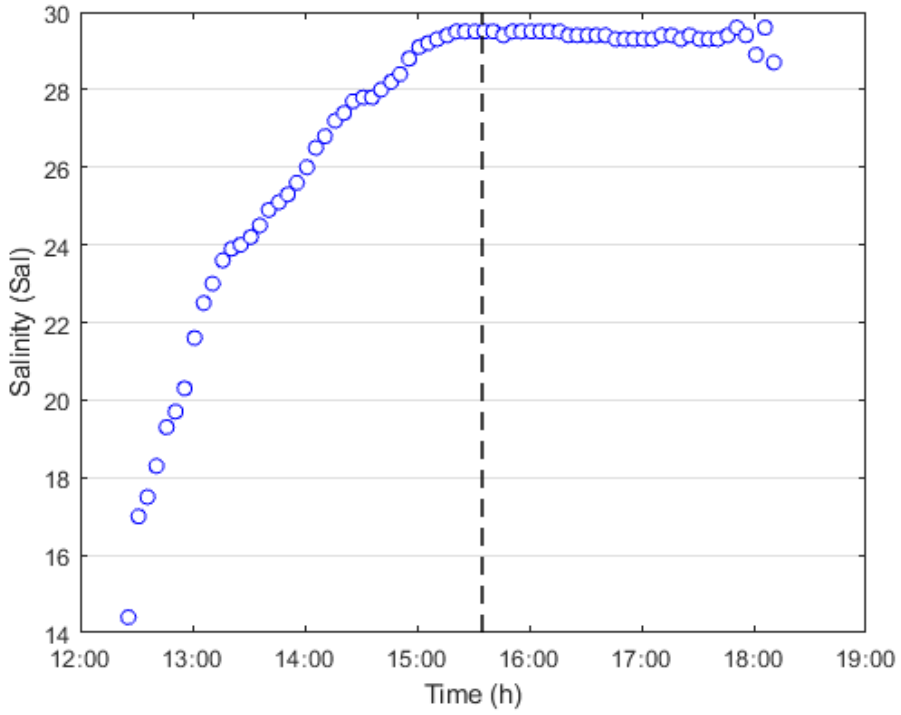

Figure 3.43 Salinity data from the WTW probe.

As it is possible to observe in Figure 3.39 and 3.40, despite the great amount of rainfall of the previous days, no great nutrients concentrations are detected in the channel outside the salt marsh. This may due to a degradation of the nitrogen compounds, occurred in the previous days, or maybe rivers did not discharged a great amount of nutrients in the lagoon due to the rainfall event.

Interesting is also the fact that nitrate concentrations tend to decrease to zero, maybe connected to the relative high temperatures (even if decreasing), and that, at the beginning of the tide event, concentration is higher inside the marsh creek than outside (Figure 3.38; Figure 3.39; Figure 3.40). The high initial nitrate concentrations are difficult to address, because many different processes can be the involved actors. It is unlikely that nitrification occurred, looking at the constant low values of ammonium. It is possible that a release from the sediment occurred during the first moments, maybe triggered by concentration gradient, but it did not last the entire tidal cycle, since, at the end, a net decrease in the concentration is registered. A probable explanation could be that in the previous days, due to rainfall events, nutrient were discharge in significative amount but the salt marsh could not process the entire discharged quantity, generating an entrapment in the salt marsh. Due to not favorable redox conditions in the sediments, though, they were immediately released (or consumed) during the next tidal cycles, when input from the outside channel were lower. However, more data are necessary to prove this interpretation and this particular case remains not completely clarified.

It is noteworthy how DON concentrations remains the major component of the TDN and that they tend to decrease during the entire tidal cycle, which seems to happen consequently, for some reasons, to previous important rainfall events. It follows an irregular trend, like in April and in June 2016 (both characterized by significative precipitations), and possible explanations do not completely clarify the values, since it can be a mix of dilution, exudation and sediment release. The final low value could be the result of hydrolysis occurring in the creek. Moreover, it is significant the difference in DON concentrations at the surface and the bottom of the channel at the end of the tidal cycle. This may be explained looking at the salinity trend (Figure 3.43): indeed, these values do not decrease like in the previous surveys, indicating that the exiting water has the same salinity of the seawater, which means also denser. During the low tide at the end of the ebb, freshwater begins to become predominant and, since it is lighter, is occupies the surface of the channel. This means that the salty water, exiting from the marsh with lower DON concentration, ends up at the bottom of the channel, which could explain the low analyzed value. The constant data at the surface may indicate the presence of phytoplankton (as in June 2017), contributing to DON concentration through exudation, but generating lower values than DON maybe due to temperature values.

However, it is important to better analyze the salinity results. As observed in the previous campaigns, there was always a mixing between fresh- and seawater, indicated by salinity decreasing trend. In this case this does not happen, but at the beginning it is clear how freshwater is entering. This could be explained in two ways: or the salt marsh releases salt, increasing the saltiness of the water, or evapotranspiration occurs, even if the temperature values decrease (Figure 3.41), maybe due to the effect of plants (likely at the end of July) and the low humidity, created by the rainfall events of the previous days. If this last assumption is true, it points out that it is very plausible that during the ebb, less water exited respect to the total amount that entered, which though does not created higher concentration values of nitrogen compound, due to accumulation of mass in a lower water volume.

Lately, analyzing DO and temperature trends (Figure 3.40; Figure 3.41), they show similar behavior also in this campaign, which means that as temperature decreases, also DO concentration decreases. This may indicate a lower biological activity, which does not coincide with the degradation highlighted by the concentrations trends inside the marsh creek.

3.2.7 Results of August 2015

This sampling campaign is the one used in the thesis of Baldan (2015), carried out on 13/08/2015. It is characterized by an important tide event (Figure 3.44), with a maximum of almost

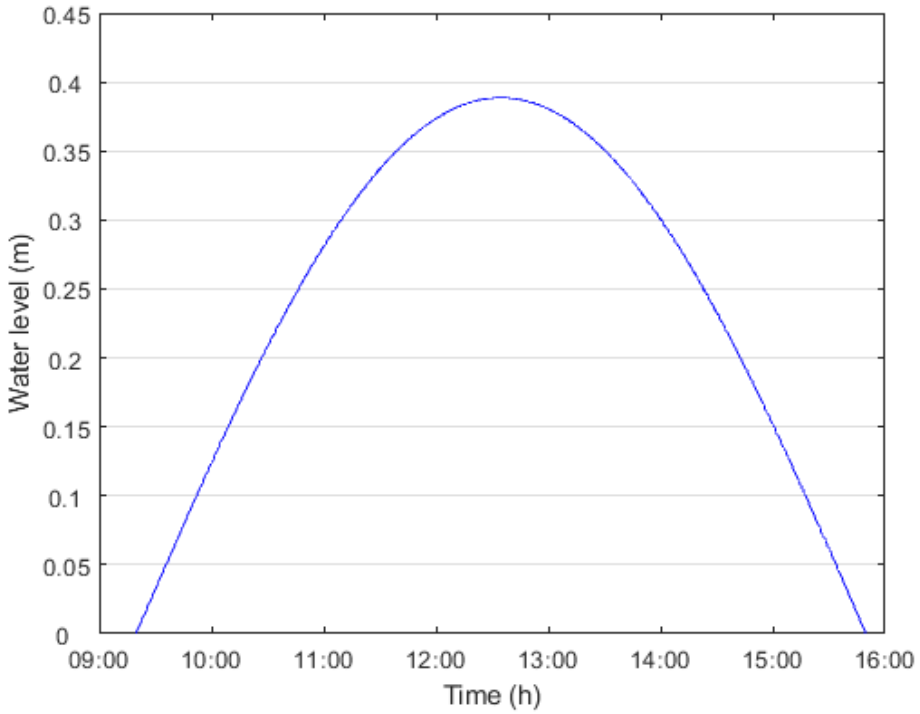

Figure 3.44 August tide event.

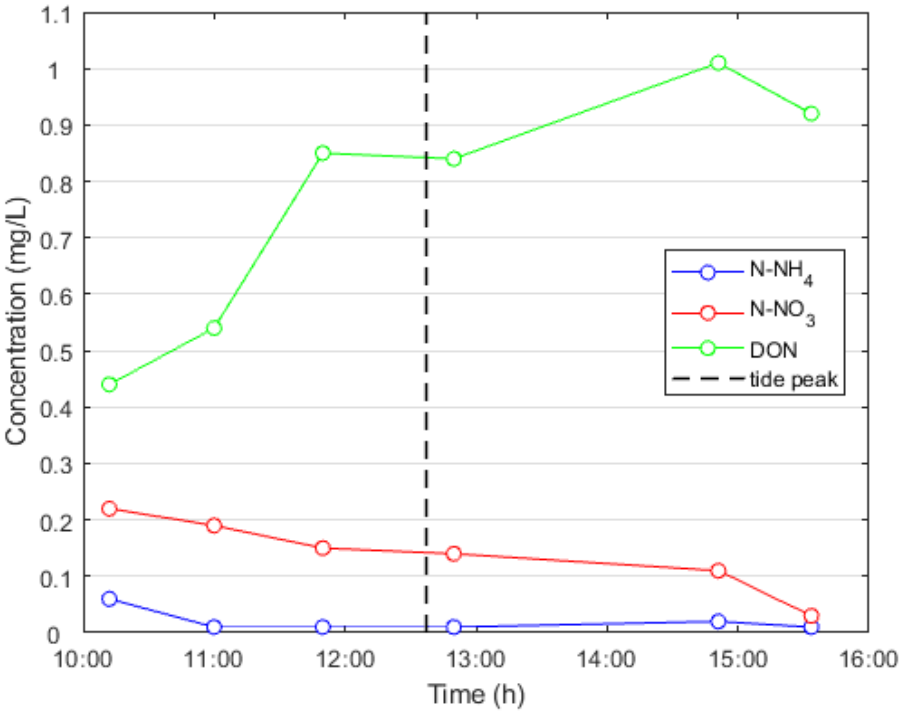

Figure 3.45 Concentration of nitrogen compounds inside the marsh creek.

39 cm and a duration of 390 min, and important temperature data (Figure 3.45), common for August period. No data were collected about the bottom concentration in the channel outside the salt marsh.

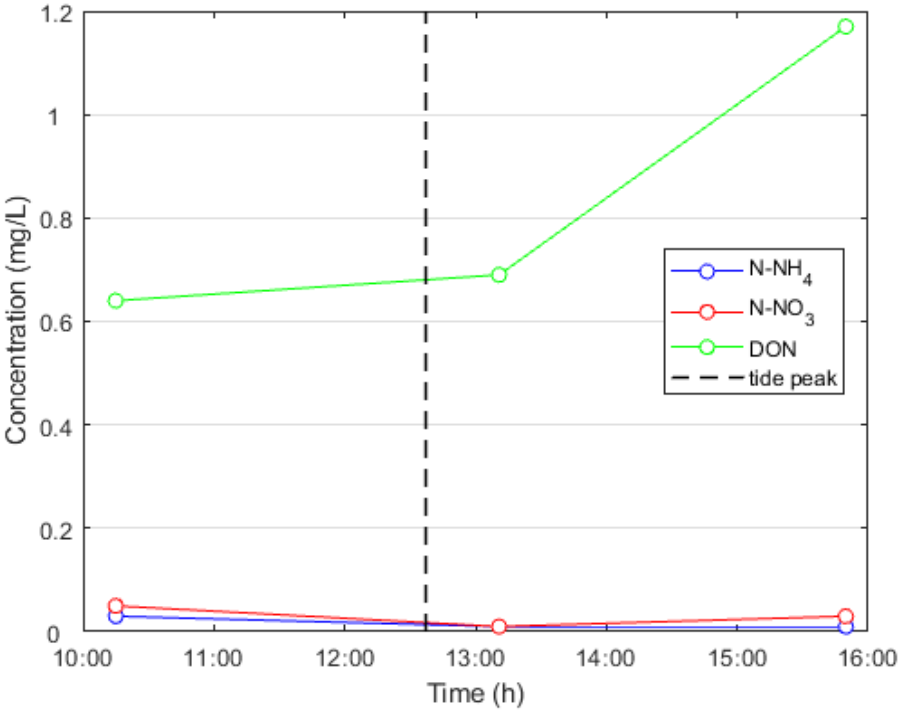

Figure 3.46 Concentration of samples taken at the surface of the channel outside the salt marsh.

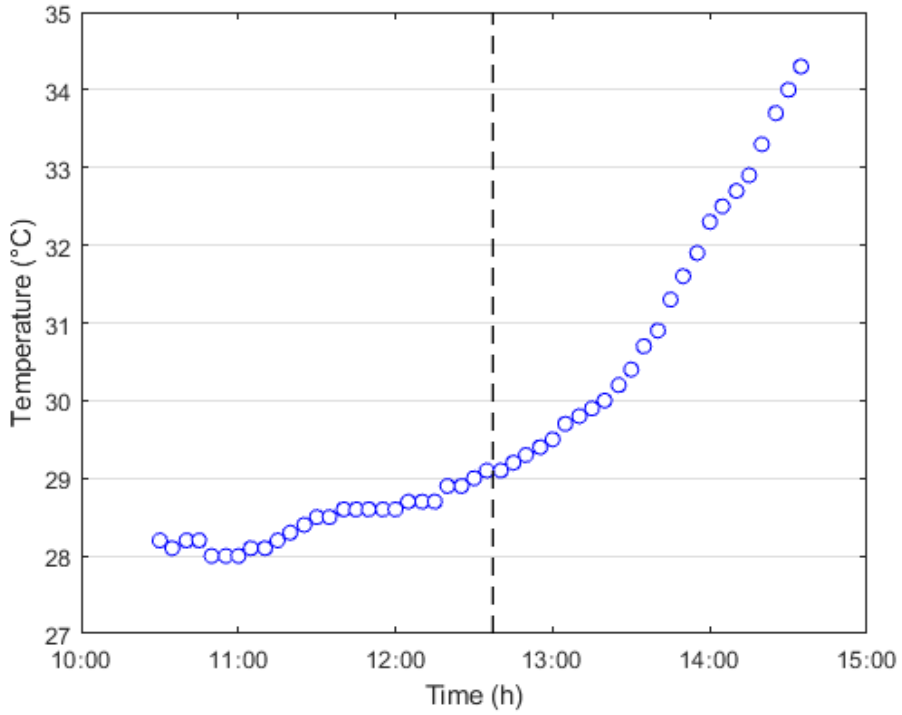

Figure 3.47 Temperature data from the WTW probe.

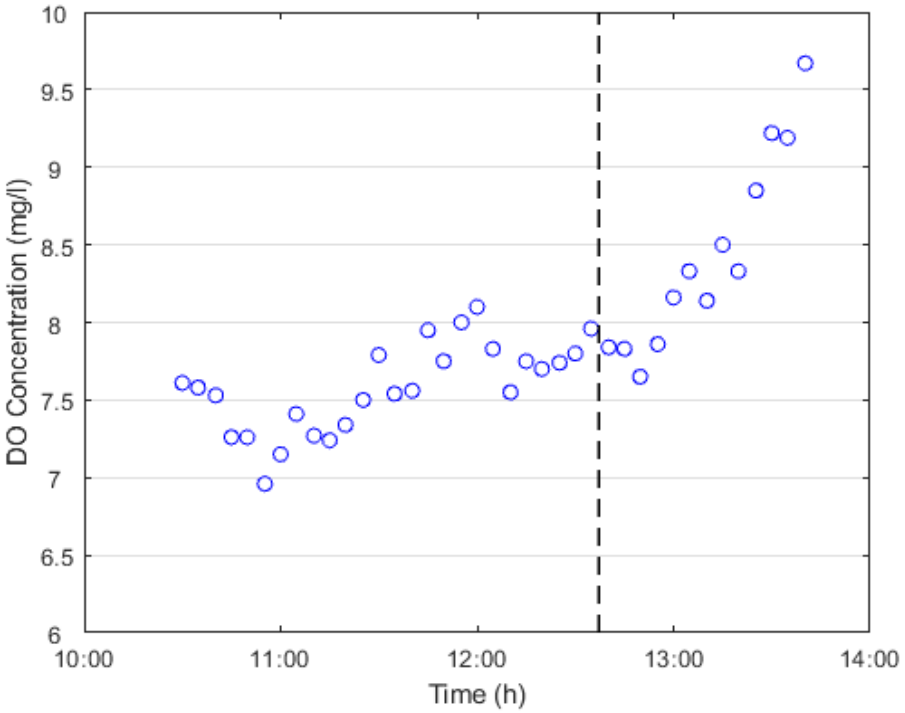

Figure 3.48 Dissolved oxygen data from WTW probe.

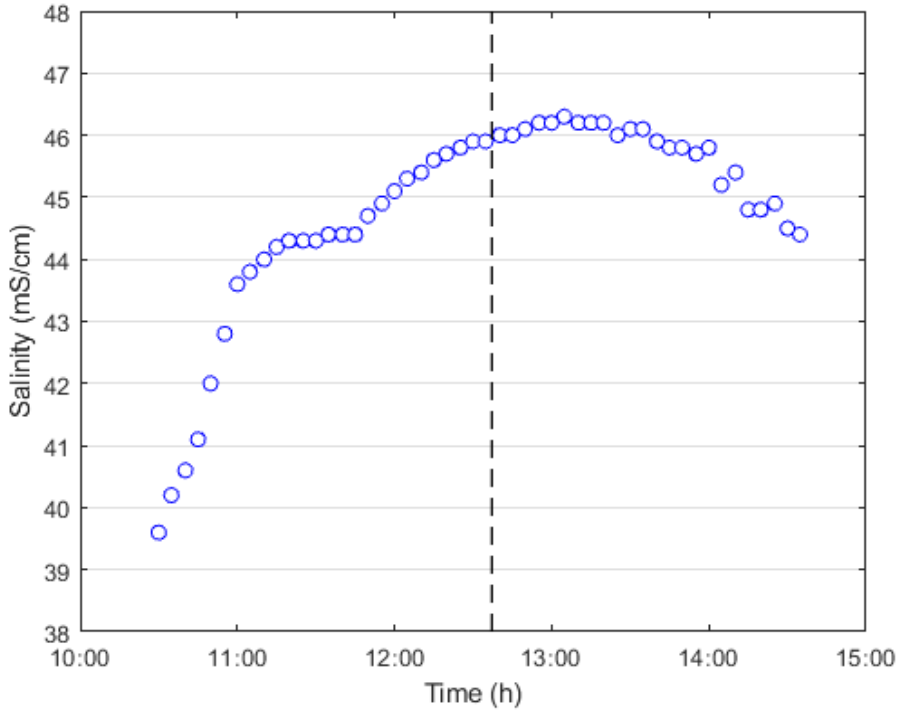

Figure 3.49 Salinity data from the WTW probe.

This campaign results present low concentration of ammonium, which is a constant behavior for the salt marsh and the lagoon water, and low concentration of nitrate (Figure 3.45). As it is possible to notice, though, there are differences in the concentration in the channel outside the marsh and the creek, which are higher for nitrate (Figure 3.45; Figure 3.46). On the contrary, DON values for the creek are lower than the one of the channel.

This may indicate that, for the first moment of the tide event, some transformations could happen in the first part of the creek, between its beginning and the sampling point, that may generate lower values of DON (hydrolysis) and higher values of nitrate (nitrification or sediments release). Despite this, for the final values during the tidal cycle, there is concordance between the output values from the creek and the samples in the outside water surface.

Moreover, the DON trend follows the same behavior of the other campaigns not characterized important rainfall eventin the previous days, and tends to increase during the tidal cycle. This could be connected to the increasing values of DO concentration, as well as an increase in temperature (Figure 3.47; Figure 3.48). As well as confirming another time the strict relationship between these two parameters, these results indicates a likely increase in biological activity, which likely resulted in DON release by phytoplankton or vegetation through exudation. It is important to notice that DO concentrations are lower respect to the other data from the previous sampling campaigns, which may point out a general low biological activity for that day, despite its increase after the tidal peak.

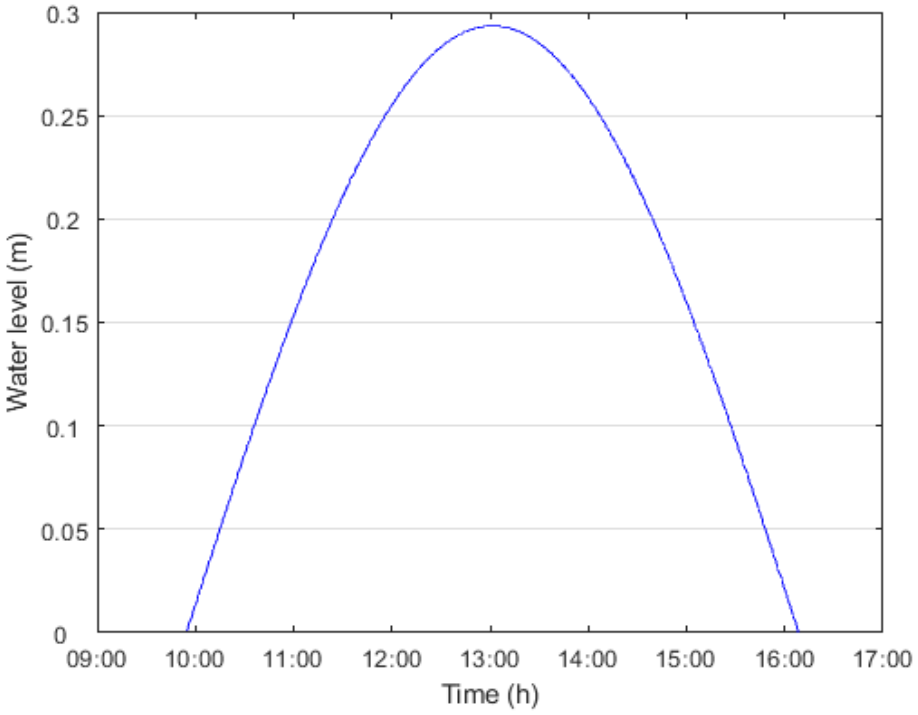

Figure 3.50 September tidal event.

As far as salinity data are concerned, they show similar trends to the previous surveys, with lower values during the increasing tide and decreasing values during the ebb. However, these results show higher salinity values during the ebb, which means that more seawater was present, respect to freshwater. Mixing occurred at the end of the creek but the final values is not equal to the mean of the values before the peak, indicating a not perfect mix, evapotranspiration (possible due to plant effect during hot days of August) or release of salt by the marsh.

3.2.8 Results of September 2017

This field survey was carried on during the first days of September, more precisely on the 04/09/2017. An average tide event occurred (Figure 3.50), with a duration of 374 min a mith a maximum of 29 cm, no particularly high precipitation characterized the previous days and there was already a significant change in water temperature, respect to August, for example.

It is interesting to notice how no great difference is present between the concentration in the surface and bottom of the main external channel, which indicates that no stratification happened or, at least, no difference is present between fresh- and seawater. (Figure 3.52; Figure 3.53). Moreover, no meaningful difference is occurring between the initial concentration inside and outside the marshes, with the creek concentrations comparable to the channel ones.

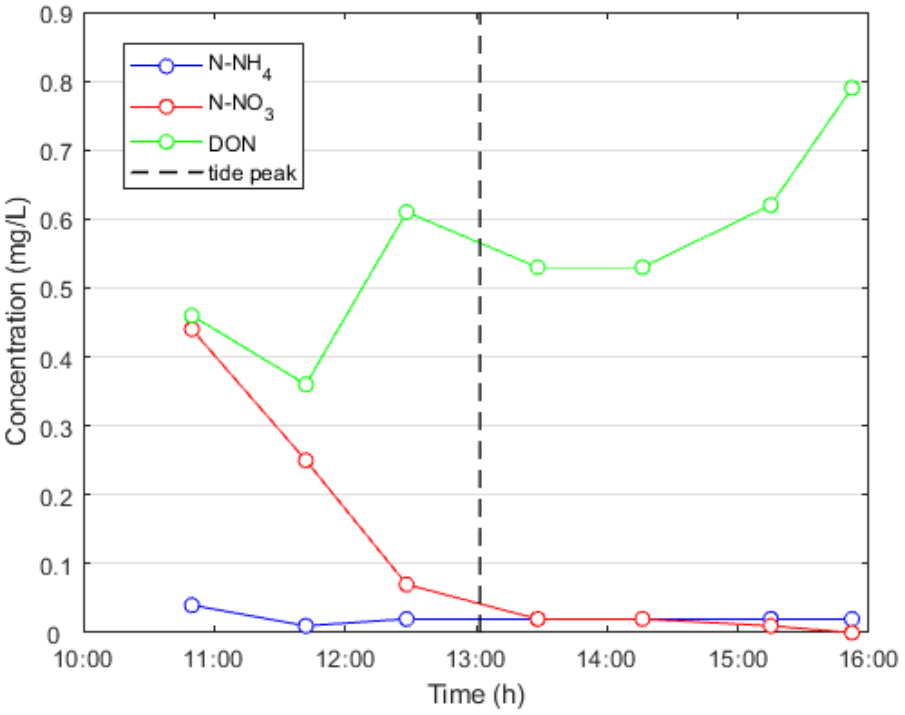

Figure 3.51 Concentration of nitrogen compounds inside the marsh creek.

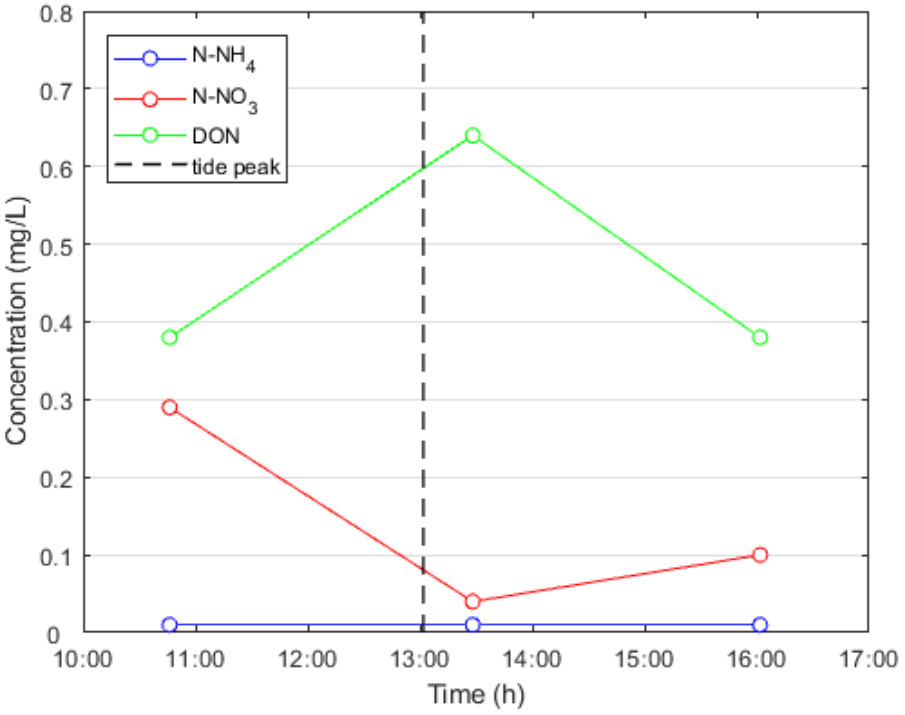

Figure 3.52 Concentration of samples taken at the surface of the channel outside the salt marsh.

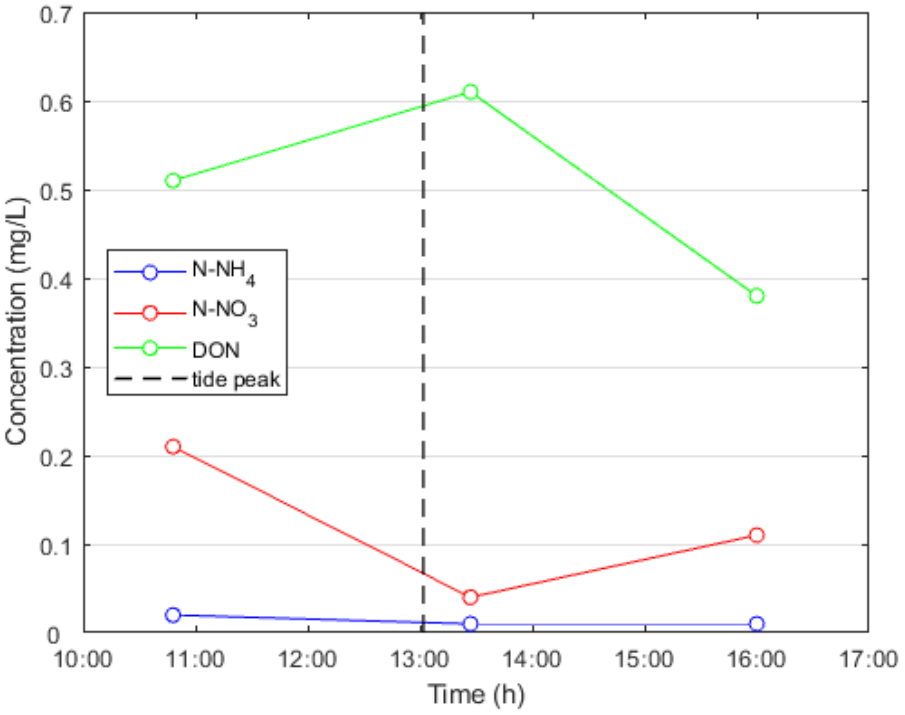

Figure 3.53 Concentration of samples taken at the bottom of the channel outside the salt marsh.

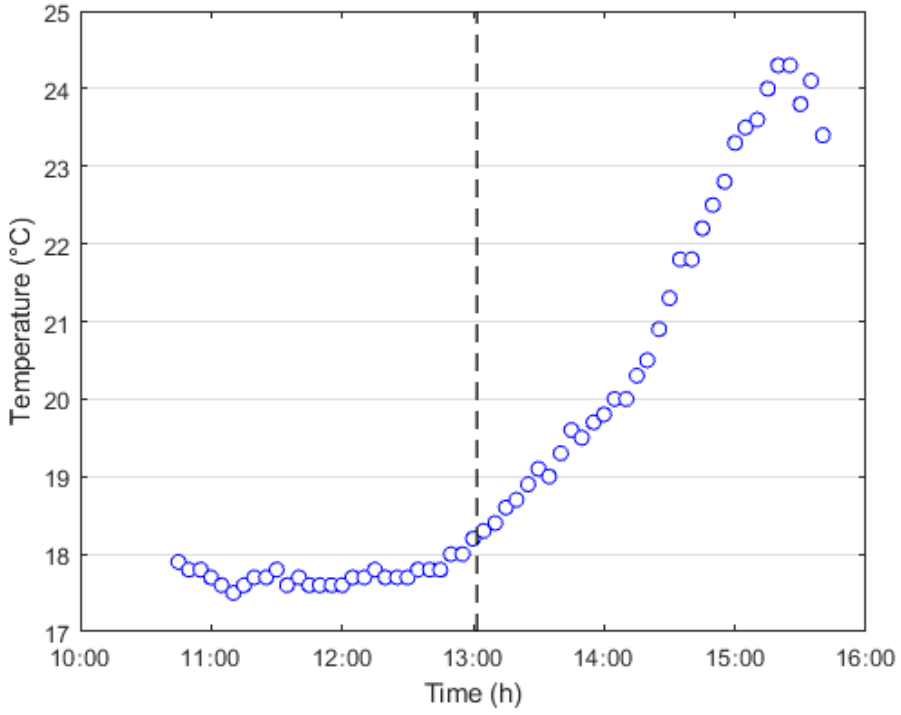

Figure 3.54 Temperature data from the WTW probe.

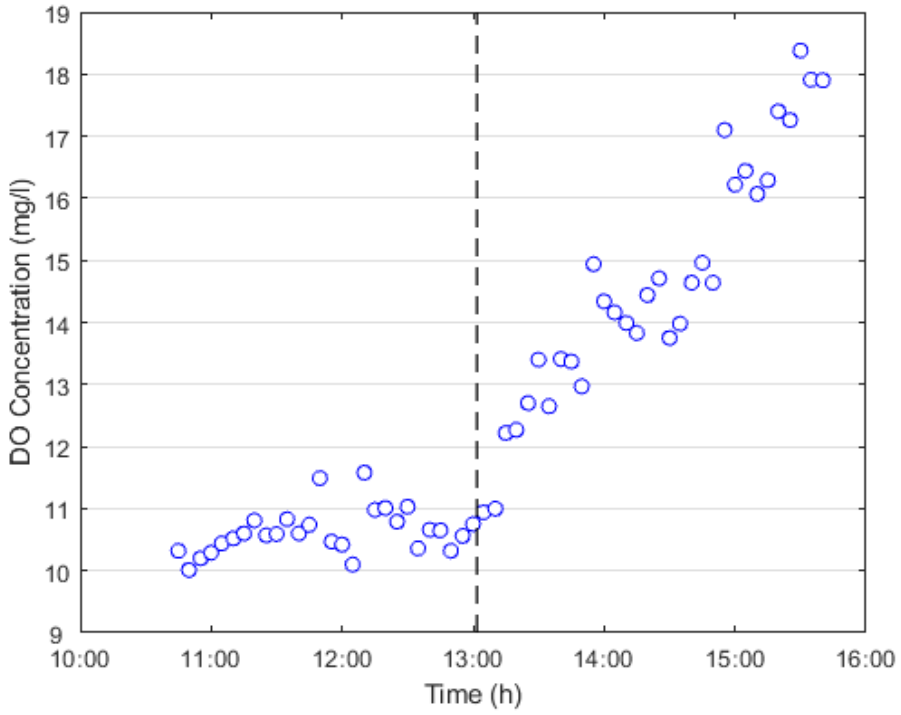

Figure 3.55 Dissolved oxygen data from WTW probe.

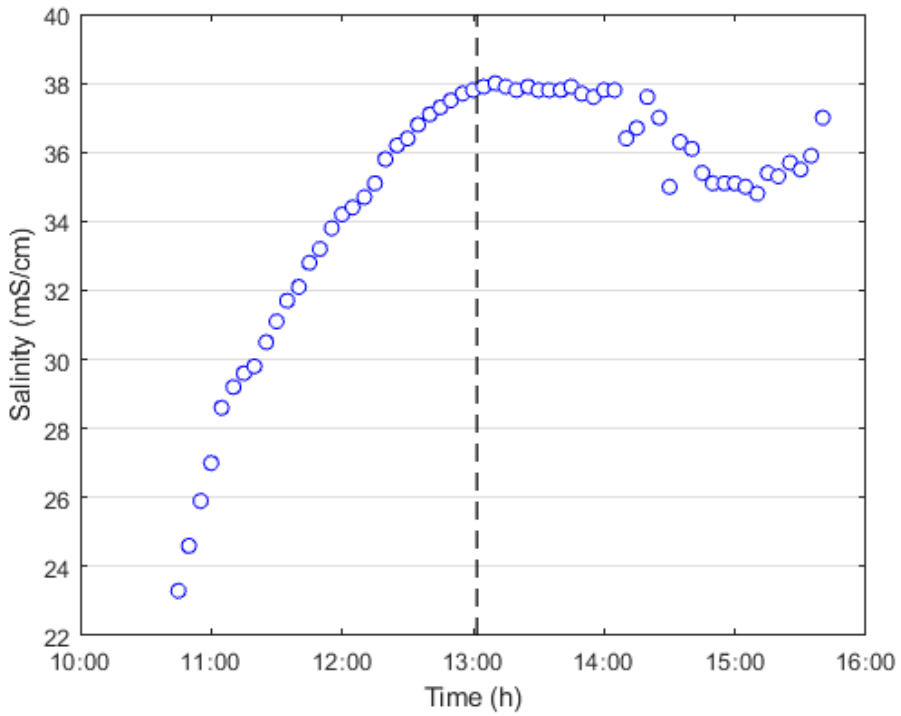

Figure 3.56 Salinity data from the WTW probe.

Despite the fact that the initial data are comparable, it is not possible to state the same for the final ones. Indeed, DON concentrations increase inside the salt marsh but decrease in the channel: such a significative difference is detected for the first time. It may be due to dilution in the channel, or some sort of degradative process occurring in the water column. Moreover, the same opposite trend is observed for the nitrate concentrations, but in this case, they increase outside the salt marsh, while decreasing inside. Anyway, the increase in the channel is very low, circa 0.5 mg/l, which may be the result of many processes, scarcely comprehensible, but the decrease of nitrate in the creek is more significant.

This nitrate degradation could be related to the increase of DO concentration and temperature, which still display the same trend during the tidal cycle. The biological activity may have increased, along with the tide, generating exudation of DON from the phytoplankton and nitrate consumption by bacterial activity or plant and phytoplankton uptake. Moreover, ammonium concentrations continue to remain very low, like in all the other field surveys.

Lastly, evaluating salinity data, they display again a tendency to increase, indicating an initial input of freshwater to the salt marsh, which is substituted with seawater during the tidal cycle. In this case, the final values of salinity show an average value higher than the one before the tidal peak (they display also a final increasing trend), which can be explained with the possibility of salt release from the marsh or a more likely evapotranspiration process (which may indicate another time a lower quantity of water in output respect to the input).

3.2.9 Results of October 2017

This was the last sampling campaign for this thesis. It was carried out on the 03/10/2017 and was characterized by an average tide event, which had a peak of 27 cm and a duration of 327 min (Figure 3.57), like the previous survey. A more significative decrease in water temperature is registered, indicating a net change in the external conditions from the summer period.

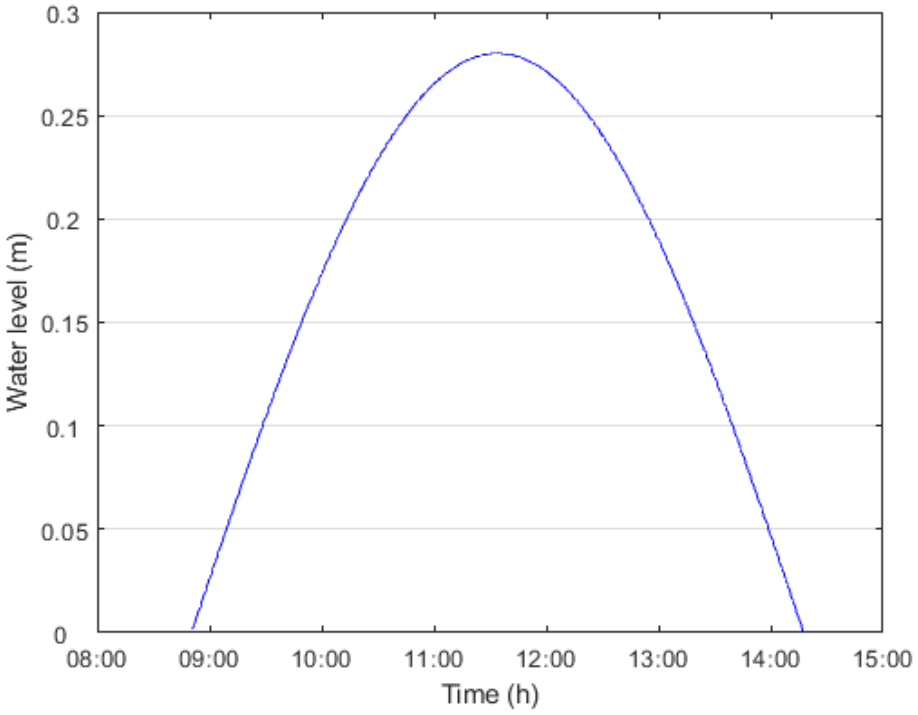

Figure 3.57 October tide event.

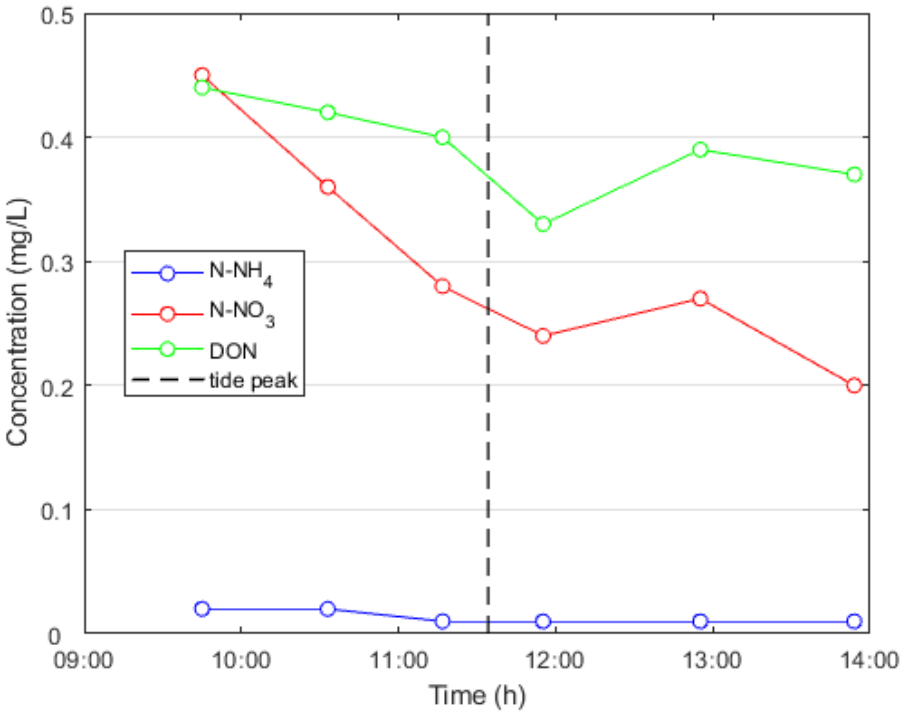

Figure 3.58 Concentration of nitrogen compounds inside the marsh creek.

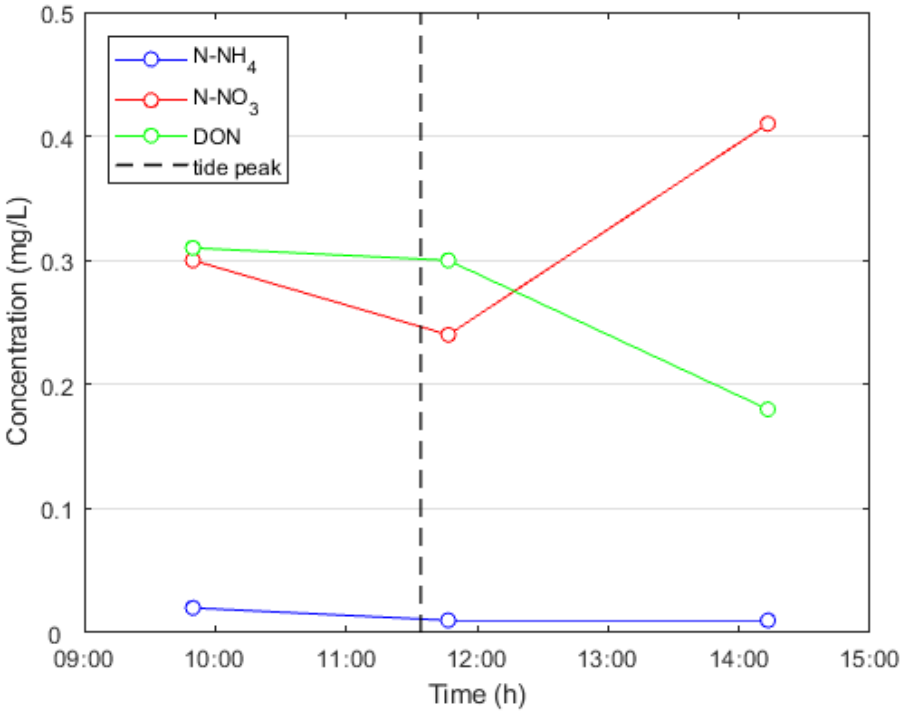

Figure 3.59 Concentration of samples taken at the surface of the channel outside the salt marsh.

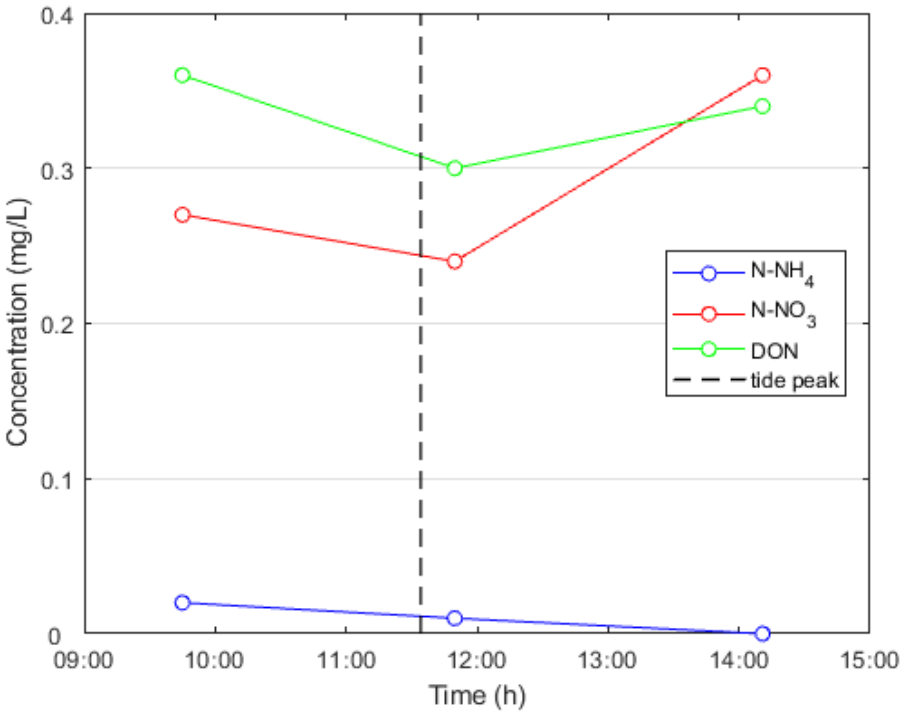

Figure 3.60 Concentration of samples taken at the bottom of the channel outside the salt marsh.

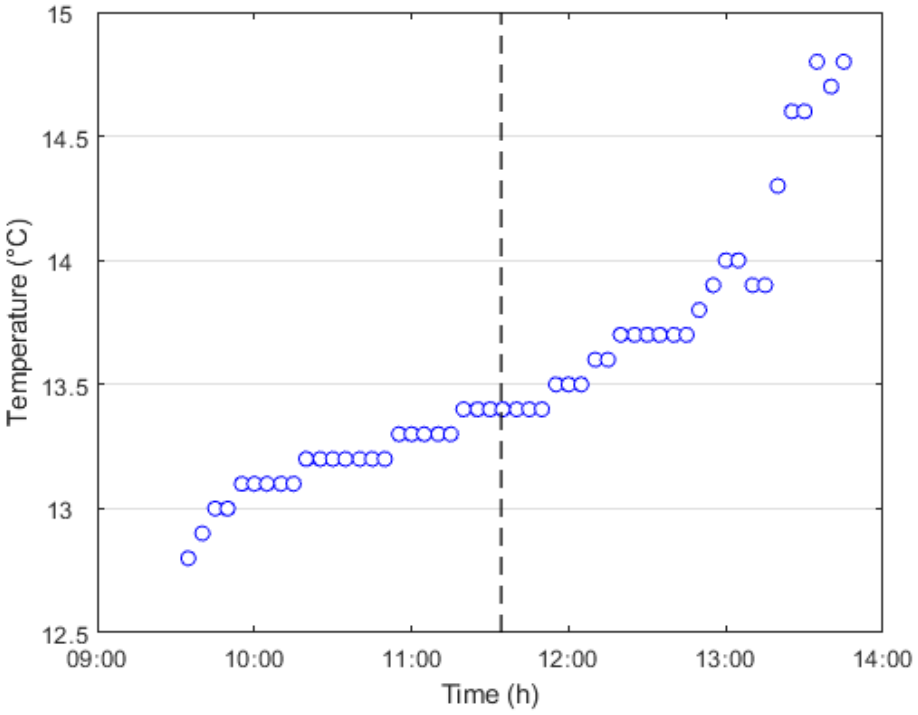

Figure 3.61 Temperature data from the WTW probe.

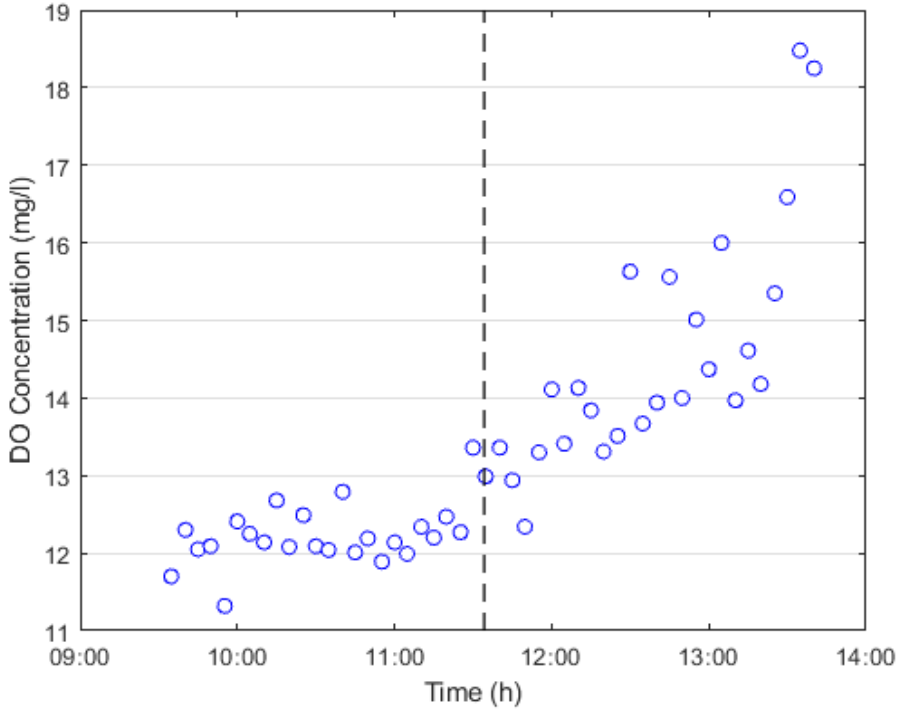

Figure 3.62 Dissolved oxygen data from WTW probe.

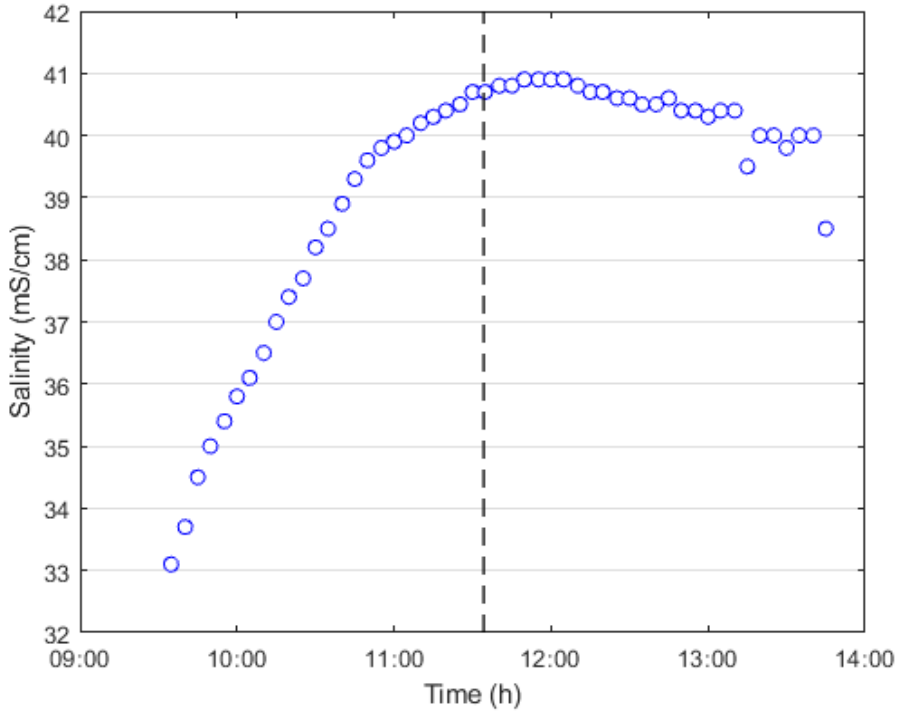

Figure 3.63 Salinity data from the WTW probe.

Evaluating the creek and channel concentrations, it is possible to notice the differences in the initial and final values for both the DON and the nitrate (Figure 3.58; Figure 3.59; Figure 3.60). For the DON, the values inside the marsh tend to decrease, starting from a value higher than the one outside the marsh, indicating a possible release from the sediment (exudation may be not concordant with the low DO concentration trend before the tidal peak). Moreover, it is the first time that the DON decreases during the tidal cycle without important rainfall events in the previous days.

Its decreasing trend in the salt marsh is not well correlated with the increasing trend on the surface of the channel, but may explain the decrease in the bottom concentration value. It could be likely that the same process supposed in July, occurred even in this case: the salinity at the end of the tidal cycle is high (Figure 3.63), so salty water exits from the marsh with low concentration of DON and, being denser, ends up at the bottom of the channel.

However, this does not explain the nitrate trend, whose values increase both for the surface and bottom samples outside of the marsh. This can be explained by a release from the sediment or by the hypothesis that, at the end of the tide event, the freshwater dominates the water column with a greater amount of nitrate respect to the seawater. Nevertheless, this is an explanation based on strong assumptions and more precise analysis and data should have been collected in the field to explain these trends.

Finally, DO concentration and temperature follow another time the same trend (Figure 3.61; Figure 3.62). The increase in DO concentration may also be connected to increase in biological

activity, which resulted in decrease of nitrate concentration by degradation but not in a DON release by phytoplankton and vegetation, which may be decreased in quantity or limited in their activity, respectively due to the end of the bloom and due to the average low temperatures. Moreover, salinity shows again a slight decrease in values during the ebb, which can be explained, as in July and September, by two possible phenomena, which are the release of salt by the marsh or the evapotranspiration. This last one can be less probable in this period, due to the likely decrease activity by the plants. However, if this analysis were correct, this would indicate a lower water volume in output respect to the input.

3.2.10 Discussion of sampling campaigns results

From the previous paragraphs, it is clear that it is very difficult to define a general behavior of the salt marsh with respect to nitrogen processing capacity. From campaign to campaign, the concentrations trends are heterogeneous and peculiar for that precise day, even if it is possible to notice some common behaviors. The relationship between the salt marsh and the outside channel, in terms of nitrogen concentration, is not so clear and it is not always possible to identify a clear connection. It is likely that, at the beginning of the tide event, the first part of the creek (between its initial point and the sampling one) has an important effect on the concentrations at the point where samples were collected (Figure 2.3), which may explain the differences between the channel and the creek values. Therefore, better investigation should be carried on in order to address this issue.

As far as the concentrations at the end of the ebb are concerned, the contrasts may be due to the lack of knowledge of the hydraulic and the flow behavior in the main channel, or also due to the effect of the other salt marshes surrounding the studied one, which may have some unpredictable effects on the concentrations in the channel.

However, despite the difficulties in obtaining a generalization about the marsh behavior during the seasons, there are some aspects in commons in all the analysis.

First, the relationship between the DO concentration and the temperature shows the same trends in all the campaigns, even if the involved average values can change, depending on the particular external conditions. This result is very interesting, since the DO concentration is likely related to photosynthesis by phytoplankton and vegetation or to other biological activities, which are triggered or limited by temperature (so energy) tendency. Only during the June 2016 campaign, this trend is not so confirmed, but few data are available (due to the presence of only one WTW probe), which were taken directly from the samples bottles. For this reason, these data could be not reliable.

Secondly, the salinity trend is interesting and may raise doubts about the quantity of water that exits from the marsh respect to the input one. In the majority of cases, the values tend to increase during the tidal cycle, indicating that always there is freshwater that enters in the salt marsh at the beginning of the tide. This freshwater can be less "fresh" from survey to survey, since the initial data changes, and for this reasons is reasonable to suppose different contributions of Dese River discharge to the salt marsh during the year. However, it is possible to notice how, in the campaign preceded by important rainfall events (April, June 2016 and July), the initial salinity data are very small, which means that important stratification was occurring in the outside channel and then the initial input to the salt marsh were probably mainly river freshwater. Nevertheless, also in May and September, the initial salinity values were very low: for the first case, a very low tide event occurred that day, allowing assuming a less important presence of seawater in the water input to the marsh creek. Instead, September was characterized by a small rainfall events in the previous days (not comparable, though, to the April, June 2016 and July ones), so it is possible that stratification due to precipitations was occurring that day.

Besides the indication of stratification, salinity results from probes also indicate the mixing of freshwater and seawater occurring inside the salt marsh, but also may point out the possibility that less water is exiting respect to the total entering volume. If perfect mixing is occurring, the final salinity values must be almost equal to the average values during the rising tide, but this is not always happening. Indeed, in September, in October and, above all, in July, the final data display higher values than the average of the first part of the graph (Figure 3.43; Figure 3.56; Figure 3.63). This trend may be explained by two possible factors: the release of salt by the salt marsh or the evapotranspiration. The last factor may be the more likely, because between July and October, the blooming of two of the main vegetation species present in the marsh (*Salicornia veneta* and *Limonium narbonense*) is occurring (Anoè et al., 1984), which are plants that grow mainly along the marsh creek (and along higher marsh borders). However, in August this trend is not present, which means that more in-depth analysis are necessary in order to prove this assumption.

As far as the ammonium dynamics are concerned, they show a constant low value and a decreasing trend (to appreciate this, see numerical values of concentrations in the Appendix 7.12). This is concordant with seasonal ammonium trends studied by (Solidoro et al., 2004), which indicates a maximum concentration value of 0.2 mg/l in April, mainly due to nutrients discharge by river freshwater. Only the Porto Marghera area is characterized by the maximum concentrations in different moments of the year, but for the other parts of the lagoon this does not happen. From these results, it is also possible to understand that ammonium represents the smaller contribute to the salt marsh mass balance.

Figure 3.64 Remains of anoxic sediments attached to the pole used to sustain the WTW probe.

Nitrate trends, are decreasing for every campaigns results, showing a consumption or uptake of nitrate. As well as DON, nitrate often shows important differences with the outside channel concentrations, highlighting the possible presence of release from sediments or another not considered processes in the first part of the salt marsh. However, it is clear how less nitrate exits from the salt marsh, respect to the input. Denitrification seems to be the prevalent process in nitrate consumption, followed by biomass and phytoplankton uptake. Denitrification is recognized to be limited by nitrate supplies (Poulin et al., 2007), but this does not seem true for our salt marsh. Moreover, the DO concentration in the channel may lead to think that denitrification cannot occur, since it is an anaerobic process. It is necessary to remember that marsh sediment is anoxic (notice its black color in Figure 3.64) and it is likely that it is the place where denitrification occurs. Literature data, obtained by sediments samples in the Venice Lagoon, show the same trend, with higher denitrification rates for unvegetated creek respect to vegetated soil (Eriksson et al., 2003). Nevertheless, in some campaigns results, it appears that not all the nitrate mass is consumed (June 2016 and October), like it happens in other resulting trends. It could be explained by the fact that a limit may be present for the salt marsh in the consumable nitrate quantity or, during that day, the biochemical processes (mainly denitrification) were inhibited due to different causes. Other data and a more detailed analysis are needed in order to explain this trend.

Finally, DON concentrations show the most heterogeneous tendency and the greater concentration values in almost all the campaigns (only June 2016 represents an exception, since it is

very likely that a great nutrient discharge occurred by Dese River). In some cases, DON tends to decrease, while in others the opposite behavior is registered. It also frequent to observe that, despite a defined trend during the tidal cycle, DON shows an oscillating trend between two subsequent concentration values. This could mean that DON is characterized by a complex fate inside the salt marsh, and processes that concur to its production or degradation may not have constant contributes along a tide event. Important are the exudation from vegetation and phytoplankton (so connected with their biological activity), but also the release form the sediment, due to concentration gradients or degradation of dead organic mass. However, there is a sort of correlation between DON dynamics and rainfall events in the previous day: for April, June 2016 and July the global trend during the ebb is characterized by decreasing concentrations, while for the other campaigns the results show a release of DON from the salt marsh. Only in October it is not detectable a similar relationship, but it could be given by to some changes in biological and chemical dynamics in the marsh due to the autumn period and the lower temperatures. Nevertheless, this is another interesting result which need a specific focus, in order to explain the reasons for these trends and this apparent relationship "rain - no release of DON".

To sum up, it is very difficult to give a complete picture of what happens inside the salt marsh, in order to explain completely the nitrogen compounds behavior. To our knowledge, this is the first long-term monitoring analysis of nitrogen dynamics carried on inside a salt marsh of the Venice Lagoon. For this reason, it is difficult to give perfect explanations of the observed data, since it is the first time that such data are collected and analyzed. However, it is clear that salt marshes have an important role in nitrogen processing for the lagoon ecosystem, especially in nitrate concentration reduction, but dynamics are not fully clarified. Some hypothesis are made to obtain possible logical answers in this paragraph, but it would be interesting and necessary to carry on more focused sampling campaigns (with more sampling points, for example) to achieve a better understanding and consequent scientific knowledge of these important ecosystems.

3.2.11 Mass balances analysis

From the concentrations values and the discharges obtained with the hydraulic submodel, fluxes in input and output for every campaigns are carried out, using Eq. 28.

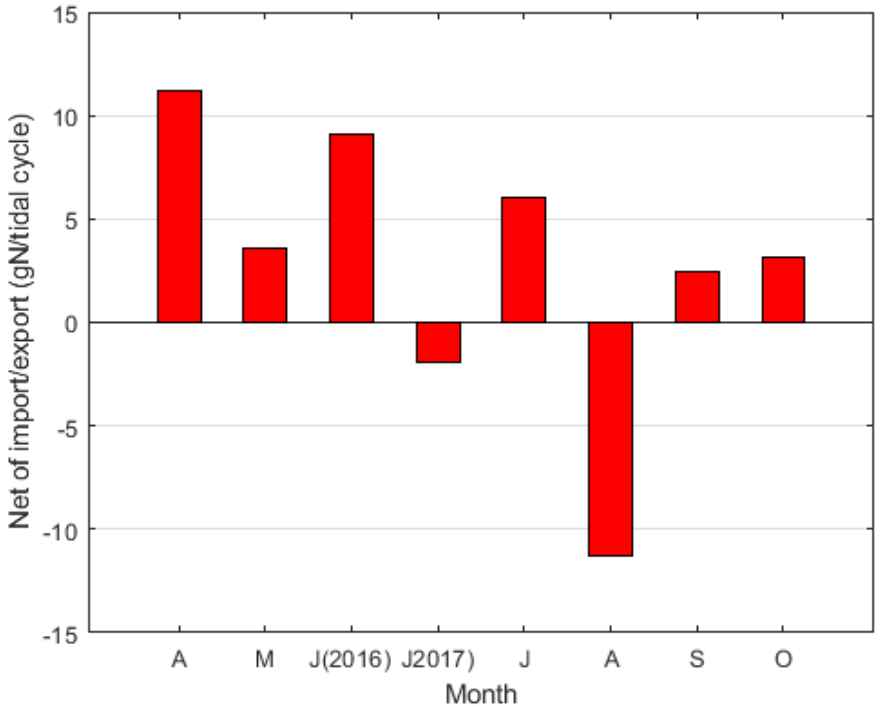

Figure 3.65 Results of mass balances during the entire tide event for each month.

Results are shown in Figure 3.65. There is not a define trend of net mass balance for the salt marsh along with the sampling campaigns. June 2016 and July show, at a first look, a different behavior respect to the previous and successive data. It is also significant see the differences in fluxes values for the two campaigns in June (2016 and 2017), which depict very different net fluxes values for the same month in the salt marsh.

In order to better understand these results, an analysis of the mm of rainfall in the two previous days for every field survey was carried on. Data are collected from ARPAV meteorological data (www.arpa.veneto.it), in particular meteorological stations n. 102 (Castelfranco Veneto), n. 122 (Trebaseleghe), n. 184 (Zero Branco) and n. 227 (Mogliano Veneto). These stations are placed along Dese River and were studied in order to suppose a hydrological response from the water body due to precipitations event along its course, since no data of discharge were available. Rainfall data are summed up in Table 3.11.

Table 3.11 Precipitation data in [mm] obtained from ARPAV meteorological stations. Values refer to the sum of the precipitation of previous two days of the single sampling campaigns.

	Meteorological station number				**SUM [mm]**
	102	122	184	227	
April	34.6	23	22.2	22.4	67.6
May	0	0	0	0	0
June 2016	28	33.2	70.8	30.8	134.8
June 2017	10.8	3.4	2.8	2.2	8.4
July	11.4	26.2	46	27	99.2
August	0	0	0	0	0
September	4.8	8.8	6.8	15.2	30.8
October	3.6	3.2	1.8	0	5

April, June 2016 and July presents the higher precipitation data and the more important rainfall event, as already stated in the previous paragraphs. These data and mass balances results are plotted together in Figure 3.66, in order to analyze better their possible relationship.

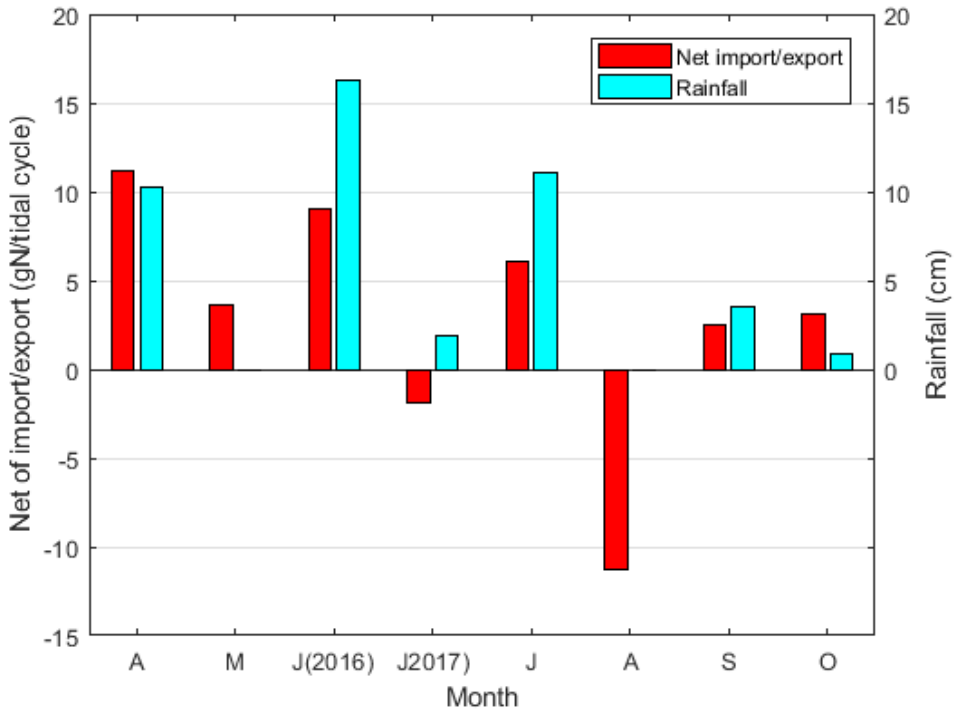

Figure 3.66 Mass balances results and precipitation data for the sampling campaigns.

From this graph, it is possible to better appreciate the fact that June 2016 and July mass balances show high value, as well as high values of rainfall in the two previous days. This is true also for April, and they coincide, as discussed in the previous paragraph, with the decreasing tendency of DON during the tidal cycle. Mass balances results are coherent with this trend, because if DON decrease, it means that there is less output than input, resulting in a positive import by the salt marsh; this, combined with the constant nitrate and ammonium decrease, explains well the net import. It could be very interesting to better analyze this DON trend when an important rainfall event is occurring, because it depicts quite clearly that the salt marsh imports a higher quantity of TDN when precipitations are high.

However, looking at the behavior of import/export in the other months, it seems that the salt marsh tendency is to decrease the import going towards the summer, and to increase again during late summer and autumn. This is concordant with the annual model results of Baldan (2015), showing that the simulation could be not so far from the real marsh behavior during the year. This annual trend could be explained by a likely higher biological activity by vegetation and biomass in this period, triggered by greater light availability and higher temperatures. This could generate a more important DON exudation rate by the biotic compartment and a greater organic mass degradation, resulting in a higher DON release. These processes then decrease in the late summer and autumn, when the external conditions are not so favorable.

Finally, an analysis of residence time (calculated as the ratio between the maximum volume and the maximum discharge) was carried out for every campaign, since it is an important aspect for wetlands (Kadlec and Knight, 2009). However, no significant relationship can be found between these data and mass balances results. Residence time data are presented in Table 3.12.

Table 3.12 Residence time values.

Month	**Residence time (min)**
April	84.22
May	53.69
June 2016	118.56
June 2017	89.99
July	86.94
August	90.33
September	106.41
October	94.08

To conclude, it is important to point out that this analysis was made using rainfall data and not the actual Dese River discharge values. This creates some uncertainties in the evaluation of the relationship between registered precipitations and mass balances results. A new analysis should be carried on, if discharge data are available, in order to confront them with meteorological data and to prove or contradict the results presented in Figure 3.66.

3.2.12 Phosphorus results analysis

For the 2017 sampling campaigns, samples were analyzed to obtain orthophosphate (PO_4^{3-}) concentrations, as described in Paragraph 2.4. Results are shown from Figure 3.67 to Figure 3.72.

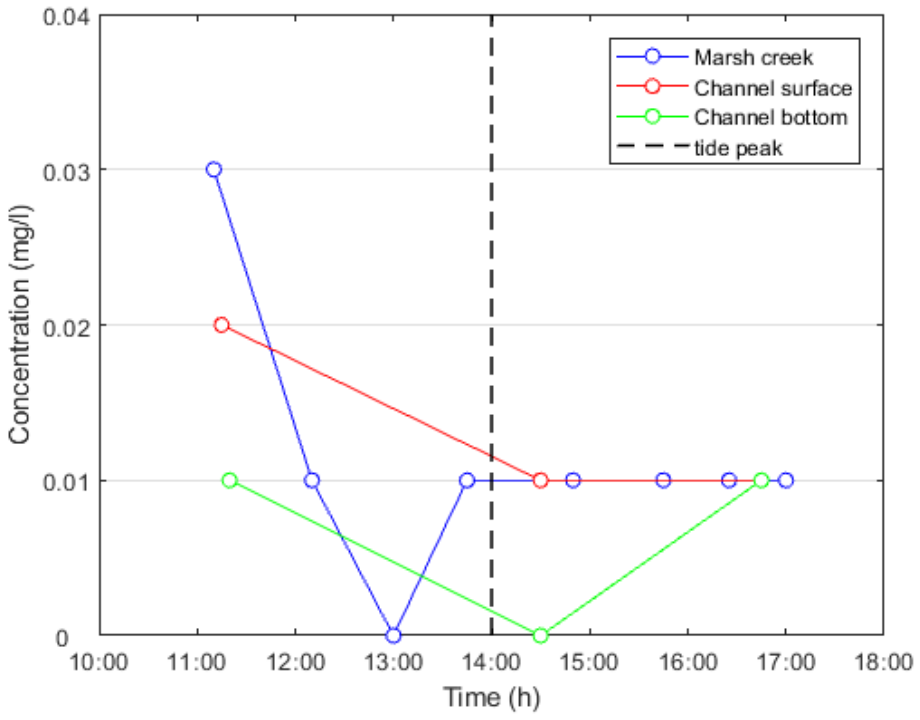

Figure 3.67 Phosphorus concentrations dynamics in April.

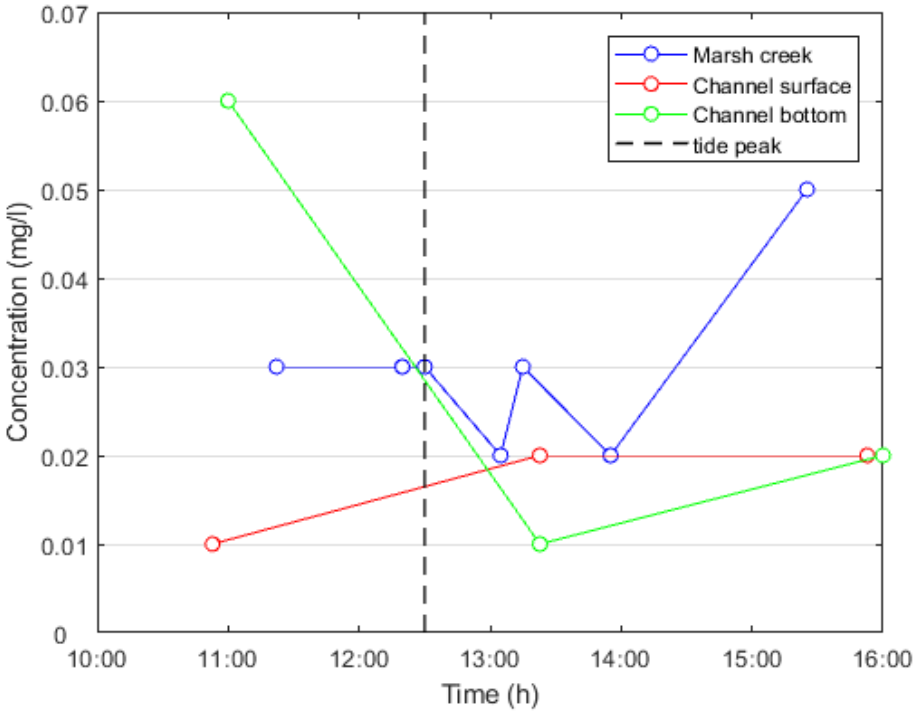

Figure 3.68 Phosphorus concentrations dynamics in May.

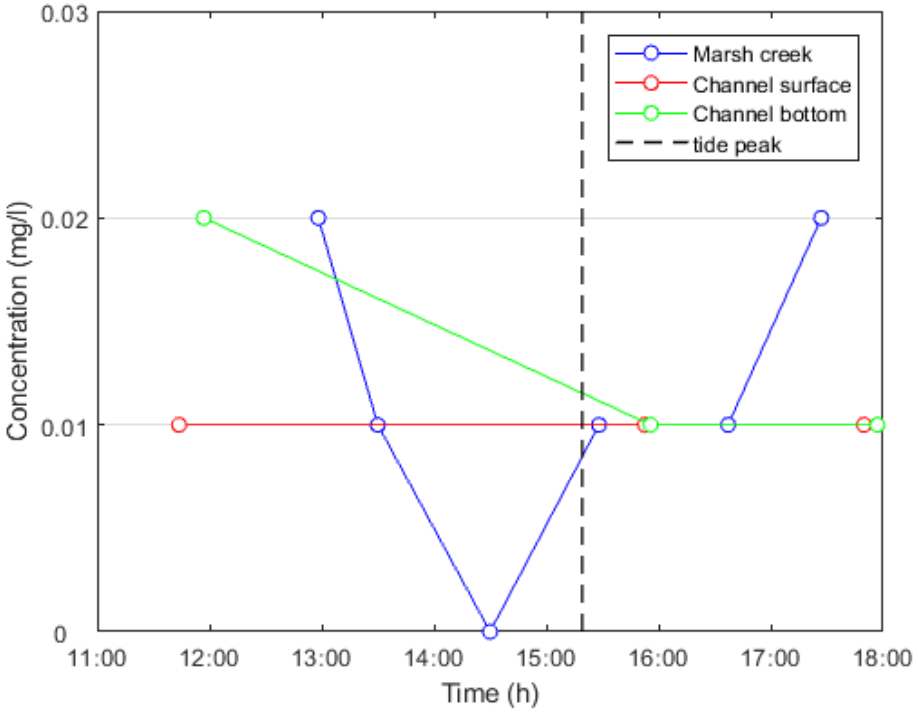

Figure 3.69 Phosphorus concentrations dynamics in June 2017.

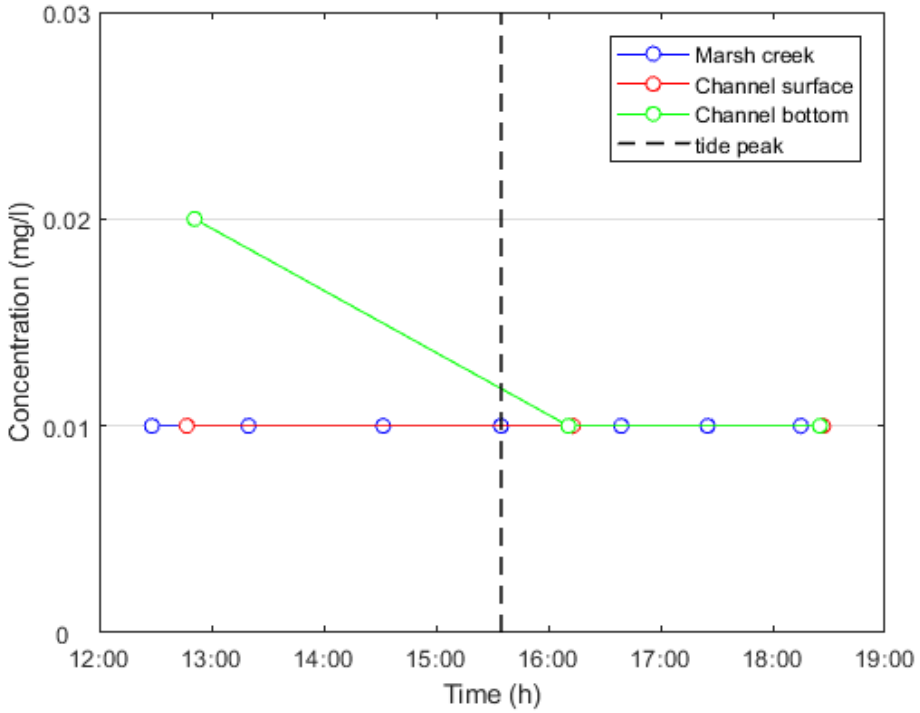

Figure 3.70 Phosphorus concentrations dynamics in July.

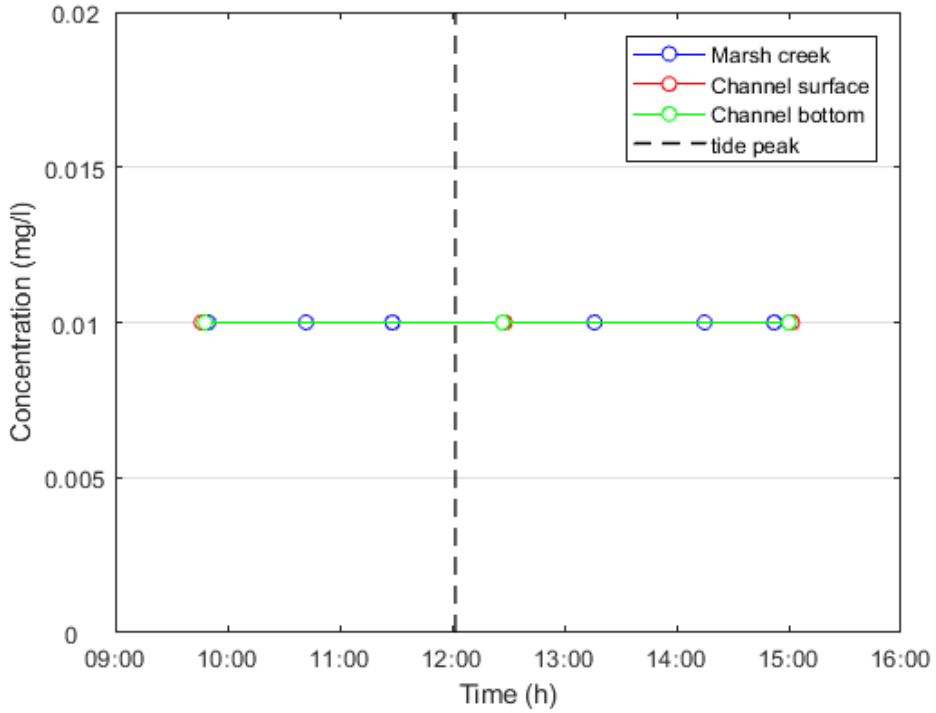

Figure 3.71 Phosphorus concentrations dynamics in September.

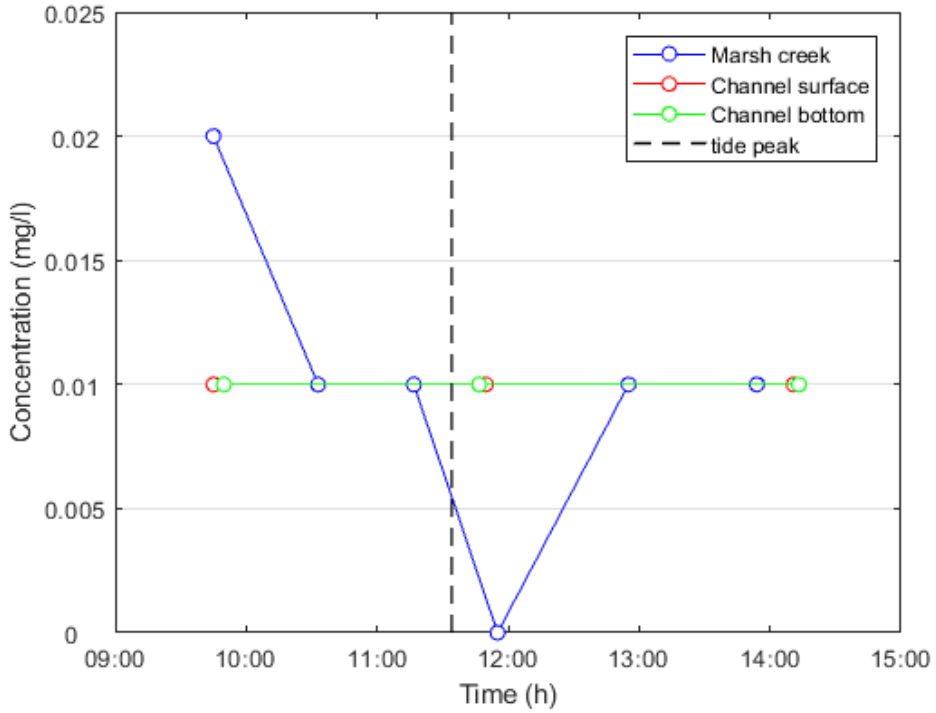

Figure 3.72 Phosphorus concentrations dynamics in October.

Orthophosphate shows always very low values for every sampling campaigns. These results are coherent with the ones of (Solidoro et al., 2004), which found a maximum orthophosphate concentration in the lagoon of 0.05 mg/l. In this thesis, a maximum of 0.06 mg/l was detected. No particular trends are present, showing a complex behavior, difficult to analyze considering the low observed concentrations.

However, it is possible to norice that:

- Phosphorus is higher in the bottom of the channel, indicating a likely interaction with the lagoon sediments;
- The fact that phosphorus shows such low values may also indicate that our laboratory technique may be not so correct and the implementation of another procedure, more sensitive to low concentration, should be considered;
- No analysis for TDP has been carried on and, for this reason, there is no indication of the quantity of reactive phosphorus respect to the total.

The low concentrations are due to policy of phosphorus reduction in detergent applied in 1980s (Pastres et al., 2004). This explains how low is the reactive phosphate in the lagoon, which is an important aspect, since both nitrogen and phosphorus are essential elements for the biotic compartment. From these result, it is likely to assume that phosphorus is the limiting element in the lagoon, as observed by (Pastres et al., 2005; Solidoro et al., 2010), and not the nitrogen, as stated,

regarding costal ecosystems, in other papers (Simas and Ferreira, 2007; Langis et al., 1991; Valiela and Cole, 2002).

3.3 Calibration and model selection

3.3.1 Calibration results

After the evaluation and discussion of possible general salt marsh behavior from the sampling campaigns results, the modeling step is carried out. Firstly, the short model along the tidal scale was reconstructed and tested. After successful and logic results from the script, the short model was later calibrated, using all the data available from the sampling campaigns.

Respect to Baldan (2015), the model was slightly improved, because no fixed data for temperature and initial concentration were used, but interpolation of WTW probe data (for the temperature) and of the channel concentrations were developed to obtain input data for the model equations (Eq. 10; Eq. 11; Eq. 12). Moreover, in this thesis, no sediment concentrations variation is assumed, since the value of nitrogen trapped in the sediment is kept constant during a tidal cycle. This led to the elimination of one of the four equations in Baldan (2015) and three out of 15 parameters, the ones connected with the sediment dynamics.

As far as the calibration procedure is concerned, the aim was to obtain a unique set of kinetic parameters that creates the best fit between the model results and all the observed data from the field surveys. In order to achieve this, the calibration was carried out using the data of a single campaign, and then repeating the procedure for every dataset. This allows obtaining a best set of initial values and parameters ranges, which gives the best possible fitting efficiencies for every set of observed data. Using these best initial values and ranges, a global calibration was carried on fitting all the dataset at the same time. In this way, a single set of parameters is obtained that fits in the best possible way all the observed values.

For the first step of this calibration procedure, many attempts were made with different initial parameters and ranges, but eventually it was possible to define a single best set of data for every campaign results. The choice of the calibrated parameters follows the results of the sensitivity analysis described in Baldan (2015).The only exception is the addition of the parameter for DON release by the sediment (k_{RN}), since a definitive improvement in efficiencies occurred when it was added to the calibrated values. The non-calibrated parameters have fixed values during the procedure:

- k_{AUP}=0.01 $m^2\ g^{-1}\ min^{-1}$;
- k_{NUP}=0.001 $m^2\ g^{-1}\ min^{-1}$;
- k_{DEXP}=10^{-6} min^{-1};
- k_{RA}=10^{-7} min^{-1};
- k_{RN}=10^{-7} min^{-1}.

The best initial values and the resulting efficiencies are summed up in Table 3.13 and Table 3.14.

Table 3.13 Best initial and range values obtained with the calibration on the single campaigns.

KINETIC PARAMETERS	INITIAL VALUES	RANGE VALUES		UNIT OF MEASUREMENT
		MIN	MAX	
k_{AU}	0.002	0.0001	0.009	$m^2\ g^{-1}\ min^{-1}$
k_{NU}	$5.00 \cdot 10^{-6}$	0.000001	0.000009	$m^2\ g^{-1}\ min^{-1}$
k_{DEXB}	$4.50 \cdot 10^{-6}$	0.000001	0.00009	min^{-1}
k_{nitr}	0.0024	0.001	0.5	min^{-1}
k_{hydrD}	0.0034	0.0001	0.09	min^{-1}
k_{denitr}	0.0027	0.0001	0.09	min^{-1}
k_{RN}	$1.00 \cdot 10^{-7}$	10^-8	10^-7	min^{-1}

Table 3.14 Efficiencies and best parameters results from calibration on single survey. First two parameters are in $m^2\ g^{-1}\ min^{-1}$, while the others are in min^{-1}. A stands for ammonium, N for nitrate. Values in italics are the one that differs largely from the others.

	EFFICIENCIES RESULTS							
	April	May	June 2016	June 2017	July	August	September	October
A	0.3635	1.0000	0.1601	-0.8668	-0.0576	0.0860	0.5099	0.4629
DON	0.4225	0.6848	0.3578	0.8670	-0.2091	0.7587	0.3992	0.6430
N	0.9272	0.9093	0.3732	0.6065	0.9006	0.3165	0.8244	0.8126
	BEST PARAMETERS VALUES							
$\mathbf{k_{AU}}$	0.009	*0.0001*	0.0001	0.009	0.0075	0.0065	0.003	*0.0003*
$\mathbf{k_{NU}}$	$4.99\cdot10^{-6}$	$4.27\cdot10^{-6}$	$1.00\cdot10^{-6}$	$7.09\cdot10^{-6}$	$1.80\cdot10^{-6}$	$4.77\cdot10^{-6}$	$4.99\cdot10^{-6}$	$4.99\cdot10^{-6}$
$\mathbf{k_{DEXB}}$	$3.20\cdot10^{-5}$	$2.42\cdot10^{-5}$	$1.00\cdot10^{-6}$	$3.96\cdot10^{-5}$	$1.06\cdot10^{-6}$	$1.92\cdot10^{-5}$	$6.01\cdot10^{-6}$	$1.71\cdot10^{-5}$
$\mathbf{k_{nitr}}$	0.005	0.11	0.0076	*0.5*	0.0321	0.0011	0.001	0.1322
$\mathbf{k_{hydrD}}$	0.0049	0.0146	0.0019	0.0017	*0.0001*	0.0011	*0.0007*	0.0041
$\mathbf{k_{denitr}}$	0.0123	0.0244	*0.0004*	0.0829	0.0397	*0.0005*	0.0123	0.0087
$\mathbf{k_{RN}}$	$1.18\cdot10^{-8}$	$9.92\cdot10^{-8}$	$1.00\cdot10^{-8}$	$3.38\cdot10^{-8}$	$1.00\cdot10^{-8}$	$1.96\cdot10^{-8}$	$1.02\cdot10^{-8}$	$1.03\cdot10^{-8}$

As it is possible to notice, not every values of efficiencies is positive, which indicates a not perfect fit. However, the two negative results for ammonium in June 2017 and July are due to the fact that final ammonium results are equal to zero, and the model has some difficulties reproducing those values. In addition, the efficiency for DON in July is negative, but it is a common result for every attempt. Indeed, as it is possible to observe in Figure 3.38, the DON concentrations have an irregular trend, with a final value lower than the other ones. This behavior is not so easy to replicate by the model, which fits sufficiently good the first values, but not the last one. Moreover, the DON values remain almost constant (Figure 3.38): because Nash-Sutcliffe efficiency is calculated based on a ratio between the fitting capacity of the model and the "fitting capacity" of the mean of the field data (Eq. 40), the mean could have a good fit with the observed data (since they are almost constant) and therefore, the final efficiency value may be negative, even if the model has good general fit.

An analysis was made on this best parameters, in order to find some seasonality or some correlation with external condition (rainfall events) or internal one (residence time) but no significant results are obtained. This may be explained by the fact that parameters are lumped all

over the marsh area, but biochemical processes are likely to occur at the different rates in different zone, as stated in Paragraph 2.5.1. For example, denitrification is higher in unvegetated creek than in salt marsh soil (Eriksson et al., 2003). These could indicate some limits in the model and in the CSTR approach.

After this step, the global calibration was applied, which finds the best parameters and calculate the efficiencies using all the dataset at the same time, starting from values in Table 3.13. Results are shown in Table 3.15 and in Table 3.16.

Table 3.15 Results of the global calibration efficiencies.

	EFFICIENCIES OF FIRST ATTEMPT OF GLOBAL CALIBRATION
Ammonium	-3.1969
DON	-0.8149
Nitrate	0.6361

Table 3.16 Best parameters of global calibration.

PARAMETERS	**BEST PARAMETERS VALUES**	**UNIT OF MEASUREMENT**
$\mathbf{k_{AU}}$	0.0118	$m^2\ g^{-1}\ min^{-1}$
$\mathbf{k_{NU}}$	4.82E-06	$m^2\ g^{-1}\ min^{-1}$
$\mathbf{k_{DEXB}}$	2.55E-05	min^{-1}
$\mathbf{k_{nitr}}$	0.0025	min^{-1}
$\mathbf{k_{hydrD}}$	0.0074	min^{-1}
$\mathbf{k_{denitr}}$	0.0154	min^{-1}
$\mathbf{k_{RN}}$	3.59E-07	min^{-1}

It is necessary to highlight that not every dataset was used in the global calibration. In the very first attempts, they were all considered but it was clear, going on with the simulations, that two set of data were misleading the calibration. Dataset 2 (May) and dataset 3 (June 2016) were not used. The first one has been discarded because that day was characterized by a low tide event and few samples were taken. In Figure 3.18, many data are present, but it is due to the fact that in some moments two data were taken with two different sampling methods, in order to evaluate possible differences. So only one of them is considered for the calibration. Moreover, the last two values were not used, since the last one was collected beyond the end of the tide event , while the second

last one is very close to the end of the tide cycle and the short model results are fixed to zero at those time values. This could be a problem for the calculation of the efficiency and so they were discarded. Dataset 3 was not used because temperature data were not as numerous as in the other campaigns (as explained in Paragraph 3.2.4) and they could be not so reliable for the interpolation.

Anyway, as it is possible to observe, efficiencies are negative and not good, except for nitrate. This may due to different reasons, mainly connected to the different trends that DON displays in the sampling campaigns results and the low value of ammonium, which are difficult to reproduce by the model. The efficiencies values are improved with the selection of the best model (see Paragraph 3.3.2).

3.3.2 Best model selection

The selection of the best model was done implementing different times the iteration procedure, neglecting some parameters, in order to evaluate the model that gives the best efficiencies and Akaike's Information Criterion (AIC) values, while trying to reduce the complexity (by reducing the number of parameters).

Three models where evaluated:

- Model M1, which is the same starting model, without neglecting parameters (Figure 3.73);
- Model M2, where the ammonium (k_{RA}) and nitrate release from the sediment (k_{RN}) were neglected (Figure 3.74). This choice is based upon the assumption that very low concentrations of ammonium are present in the lagoon and, for this reason, it is likely that also in the sediment ammonium values in very low and negligible. For nitrate, it is assumed that in the sediment only reduced compounds can be present (due to anoxic condition): therefore, no nitrate are hypothesized to be present. This can also be supported by the hypothesis that denitrification occurs in the sediment and so it is probable that no significant nitrate concentration are present throughout the year;
- Model M3, where, from model M2, also all the parameters concerning the phytoplankton are neglected, which means ammonium uptake k_{AUP}, nitrate uptake k_{NUP} and DON exudation k_{DEXP} (Figure 3.75). This decision is taken considering that phytoplankton may be present only in specific time of the year (summer in particular), subsequent to their bloom (Solidoro et al., 2004). For this reason, it may be wrong to calibrate the kinetic parameters associated with their biological activity, if their presence is not constant during the year.

Model M1 has 12 parameters, model M2 has 10 parameters, while model M3 7. Calibration procedure was carried on with all three models, in order to determine the best one based on the Nash-Sutcliffe efficiency and AIC value. Results are summed up in Table 3.17, Table 3.18 and Table 3.19.

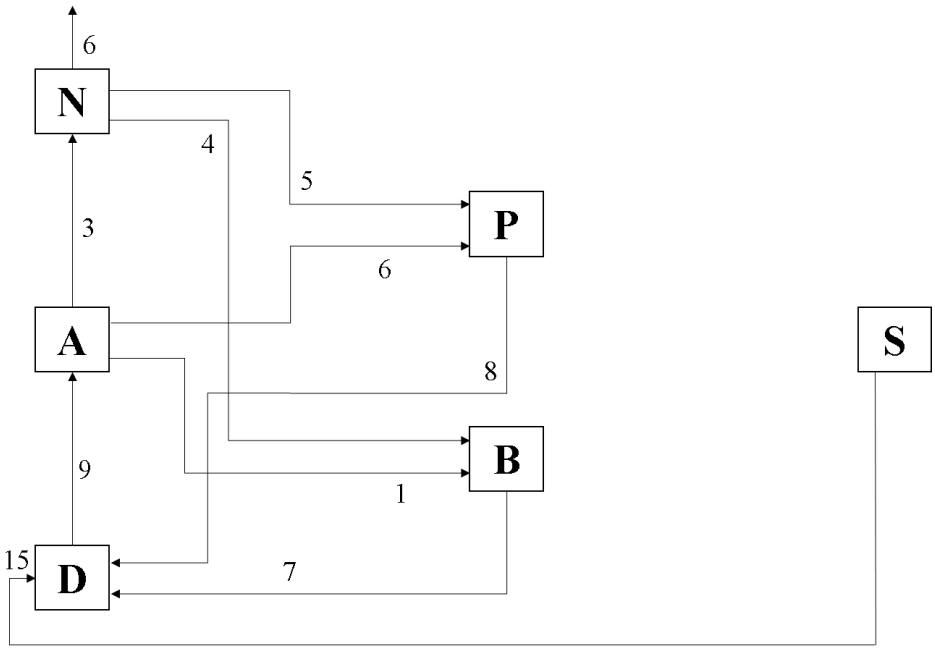

Figure 3.73 Graphical representation of model M1. It differs from Figure 2.9, because that figure was just a full representation of the nitrogen cycle in the salt marsh. See Fig. 2.12 for legend.

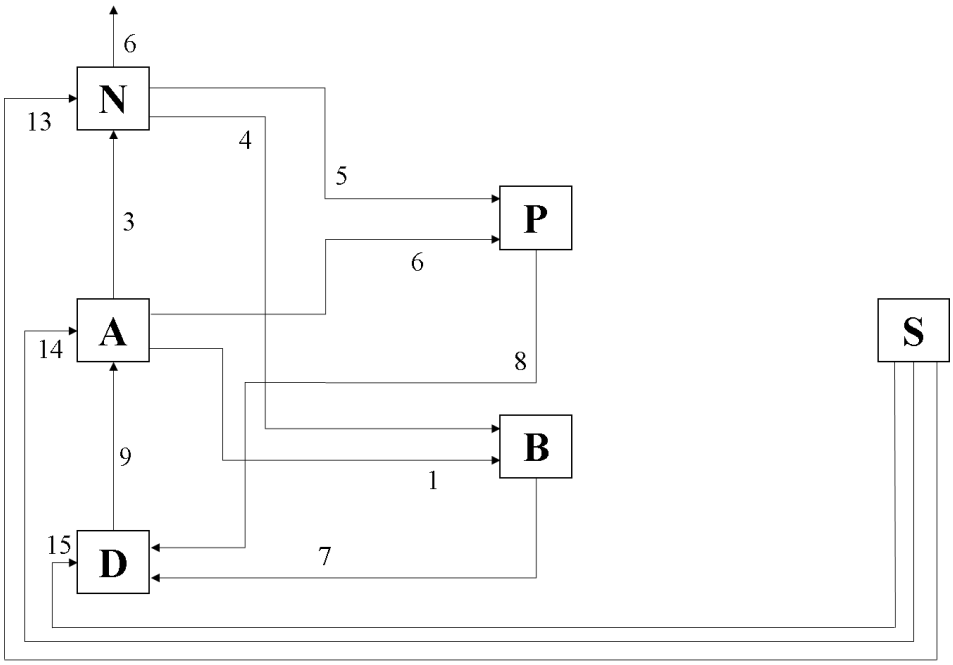

Figure 3.74 Graphical representation of model M2. See Fig. 2.12 for legend.

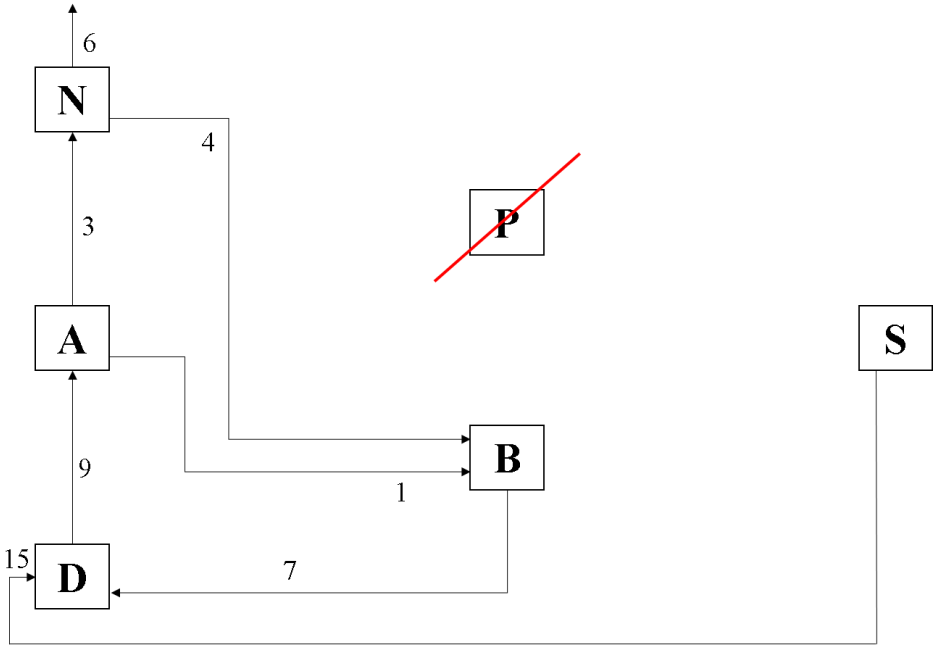

Figure 3.75 Graphical representation of model M3. See Fig. 2.12 for legend.

Table 3.17 Results of the calibration with the three tested models. In italic, the non-calibrated parameters. Results of model M1 coincide obviously with results in Table 3.16.

KINETIC PARAMETERS	MODEL M1	MODEL M2	MODEL M3	UNIT OF MEASUREMENT
k_{AU}	0.0118	1.02E-4	0.0198	$m^2\ g^{-1}\ min^{-1}$
k_{AUP}	0.01	0.1	/	$m^2\ g^{-1}\ min^{-1}$
k_{NU}	$4.82\cdot 10^{-6}$	$1.25\cdot 10^{-6}$	$5.09\cdot 10^{-6}$	$m^2\ g^{-1}\ min^{-1}$
k_{NUP}	0.001	0.001	/	$m^2\ g^{-1}\ min^{-1}$
k_{DEXB}	$2.55\cdot 10^{-5}$	$2.10\cdot 10^{-6}$	$5.10\cdot 10^{-6}$	min^{-1}
k_{DEXP}	10^{-6}	10^{-6}	/	min^{-1}
k_{nitr}	0.0025	0.0069	0.0037	min^{-1}
k_{hydrD}	0.0074	$1.01\cdot 10^{-4}$	0.0013	min^{-1}
k_{denitr}	0.0154	0.0148	0.0106	min^{-1}
k_{RA}	10^{-7}	/	/	min^{-1}
k_{RN}	10^{-7}	/	/	min^{-1}
k_{RD}	$3.59\cdot 10^{-7}$	$1.19\cdot 10^{-7}$	$2.00\cdot 10^{-7}$	min^{-1}

Table 3.18 Efficiencies results for the calibration of the three models.

	MODEL M1	MODEL M2	MODEL M3
Ammonium	-3.1969	0.5211	-1.5308
DON	-0.8149	-0.0813	-0.2156
Nitrate	0.6361	0.6265	0.6761

Table 3.19 AICc values for the three models.

	AICc VALUES
MODEL M1	-272.24
MODEL M2	-288.36
MODEL M3	-292.89

Results for model M2 are the best, since they considerably improve the global efficiencies respect to model M1 and the have a lower value of AICc. However, model M3 has the lowest AICc number, but the difference respect to model M2 is very low (close to 2, the smallest variation in AICc that makes sense to consider), and do not justify the choice of this simpler model due to its worse efficiencies.

For these reasons, model M2 is selected as best model, since it has good efficiencies and a lower AICc number respect to the starting model (M1), and it is then used to solve the long scale mass balance for the salt marsh. The negative efficiency for DON is accepted, since graphical validation of this set of parameters with the field data shows that DON trends are well represented; moreover, it is valid the problem with NS efficiency explained in Paragraph 3.3.1. The fact that this model gives the best results, may confirm the hypotheses at its base. More analysis should be carried on to better understand the dynamics and quantity of ammonium and nitrate in the sediments of this salt marsh. Moreover, since model M3 gives no good results, it may indicate that the presence of phytoplankton activity is not negligible during the year. To address this issue, evaluation of chlorophyll *a* should be done during the year in the salt marsh creek.

3.4 Long term model results

The long scale model was implemented, as described in Paragraph 2.5.4, using the best model kinetic parameters and using different forcing functions (nitrogen compounds concentration in entering waters, monthly average temperature values and the average tide event). In addition, biomass and phytoplankton forcing values are used, but they are the same implemented also in the short scale model, since they are supposed to vary only from month to month and not during a tidal cycle.

The model solves the mass balance one time for each month, using the specific forcing function values. From the results, the fluxes are calculated (Eq. 28), which are successively multiplied by 2, since there are two tide events that affect the salt marsh during a day, and then by 30, in order to obtain a monthly value. The biomass and sediments fluxes are also evaluated. The results are then summed to the input given by atmospheric deposition and sediment accretion (which includes also nitrogen bacterial fixation; see Paragraph 2.5.4).

Monthly input and output fluxes of ammonium, nitrate, DON, total TDN (total dissolved nitrogen) and net fluxes are shown in Figure 3.76, Figure 3.77, Figure 3.78, Figure 3.79 and Figure 3.80.

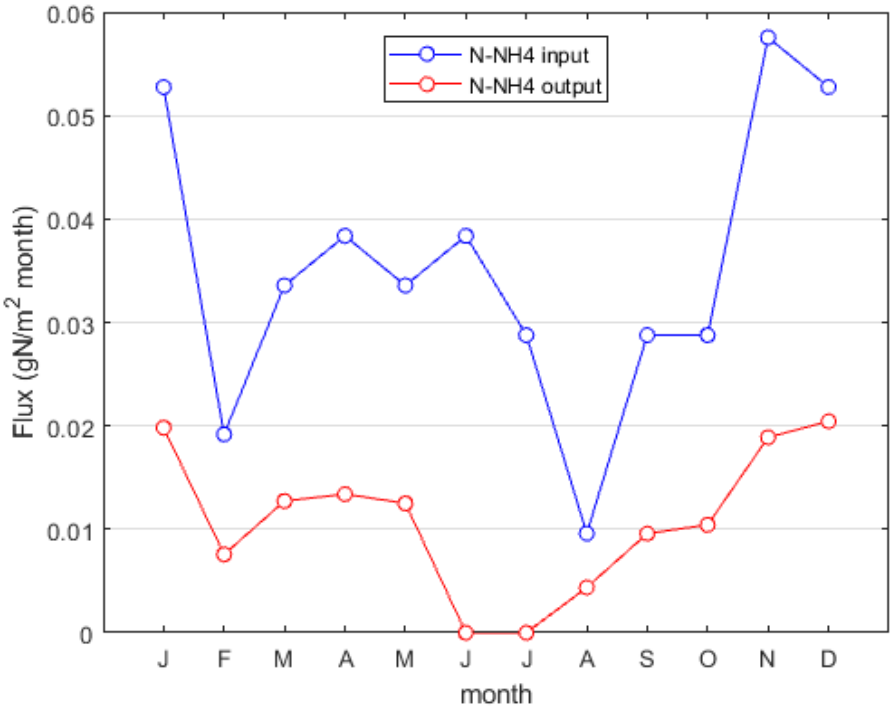

Figure 3.76 Total monthly ammonium fluxes in input and output to the salt marsh.

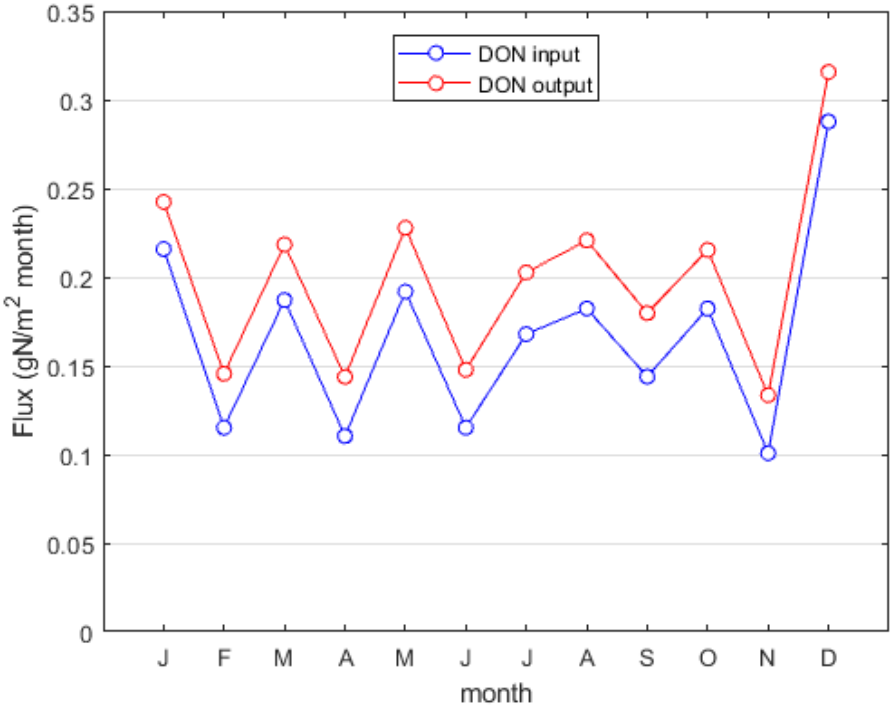

Figure 3.77 Total monthly DON fluxed in input and output to the salt marsh.

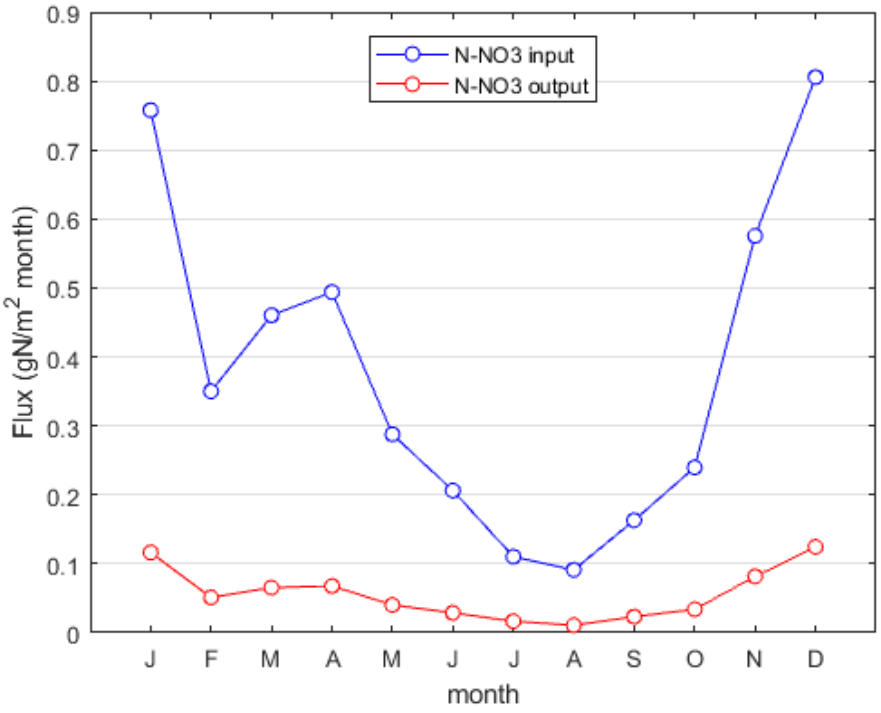

Figure 3.78 Total monthly nitrate fluxed in input and output to the salt marsh.

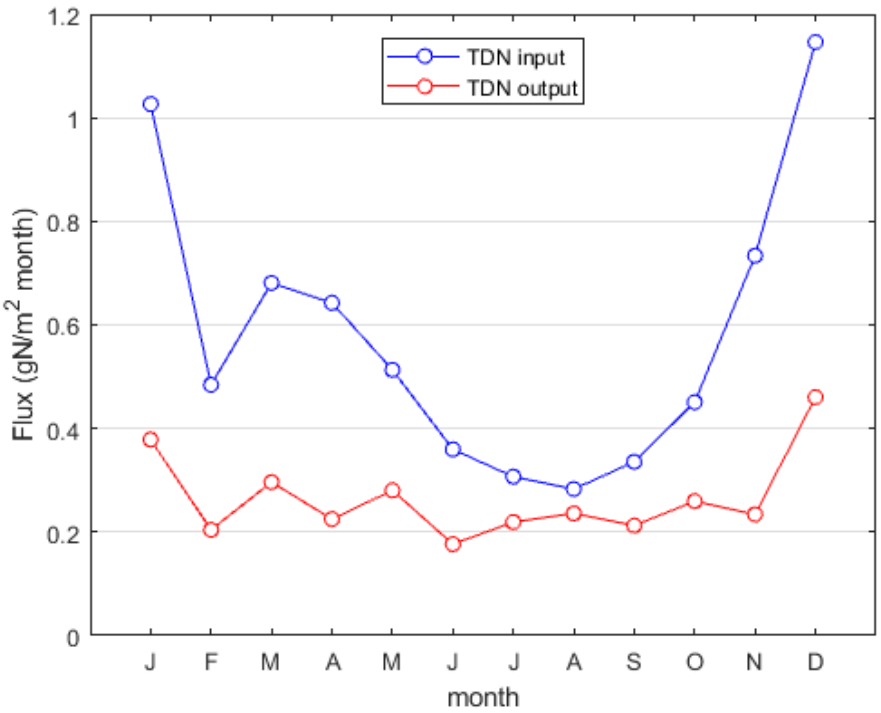

Figure 3.79 Total monthly TDN fluxes in input and output to the salt marsh.

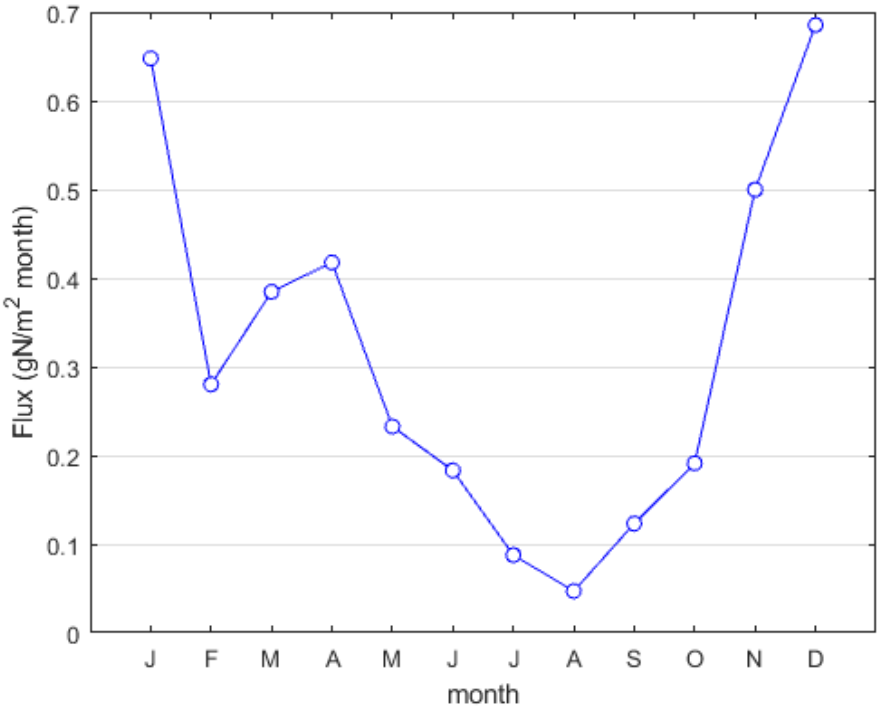

Figure 3.80 Net monthly fluxes of DIN in the salt marsh.

Ammonium contributes to the net DIN fluxes of the salt marsh with a lower extent: this is in agreement with the results from the field sampling. The fact that the concentration is higher for the winter period may indicate lower ammonium consumption, due to reduced biological activity inhibited by low temperatures.

Nitrate and DON modeled fluxes differ from the modeled data, since nitrate presents higher fluxes than the DON (the only exception is in summer). This is due to higher N-NO_3^- concentrations in input with respect to the DON values (Figure 2.17). In the studied marsh creek and in the outside channel, however, the DON concentrations are rarely lower than the nitrate concentrations, which raise a problem on the validity for those forcing functions, which come from a long analysis (2003-2008) of water quality in the Venice Lagoon (Rapporto tecnico I anno (MELa2); Rapporto tecnico II anno (MELa2); Rapporto tecnico finale sulle attività di monitoraggio della qualità delle acque Volume 1. Rapporto di sintesi (MELa3)). This issue is difficult to address and to solve without other data, but it is a concept that should be solved.

However, is possible to notice that, analyzing the annual trends, low quantity of nitrate exits from the salt marsh, which is confirmed by the field survey results. This highlights a high nitrate consumption inside the salt marsh, which is mainly due to denitrification, and this reflects the analysis made in Paragraph 3.2.10 and obtained from sediments studies in the Venice lagoon (Eriksson et al., 2003). Moreover, DON outputs are higher than DON inputs during the year and the

same result is obtained from most of the creek samples analyses. Only the campaigns characterized by important rainfall events displayed a different trends (with decreasing DON), but the reasons are not so clear and, if this relationship is always present, it could be related only to few moments of the year, and could be negligible in the yearlong nitrogen mass balance for the salt marsh. Moreover, it is possible to observe how DON does not show a net seasonality, as ammonium and nitrate, and this is related to DON concentrations used as forcing functions, since they display the same annual trend, or to incapacity of the model to simulate DON trend (despite the graphical validation of best parameters with observed data).

As far as the total TDN trend and net monthly fluxes are concerned, the inputs to the salt marsh are always higher than the outputs, resulting a positive flux (import) of nitrogen. Interesting is that no dependence on the temperature can be detected (confronting with Figure 2.14), which should increase the uptake and transformation rates. Respect to Baldan (2015), no export are simulated by the model for the summer period. Indeed, comparing the mass balances obtained with the nitrogen concentration in the creek (Figure 3.65) with the net fluxes (not monthly values, but the results on a single tidal cycle) obtained with the model, interesting results can be obtained (Figure 3.81).

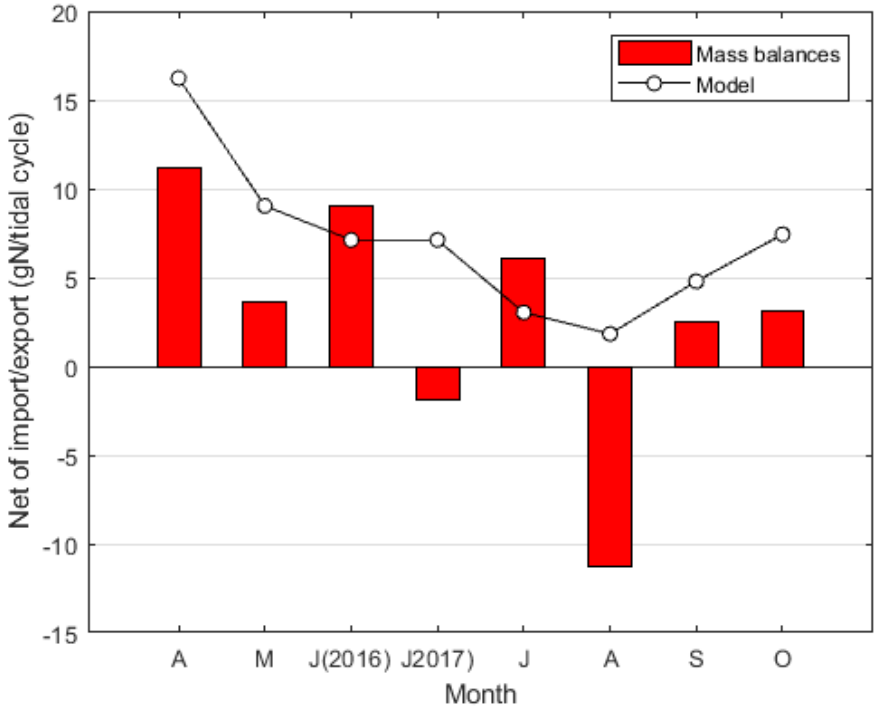

Figure 3.81 Comparison between fluxes computed with the concentrations results of the field surveys and the model output.

It was not expected that the model and observed fluxes were equal, because the first ones are obtained using nitrogen concentrations averaged upon a period of 5 years (2003-2008) and using an average tidal event, which was not comparable with some tidal cycles of the sampling campaigns. However, considering the model results as a hypothetical indicator of the average behavior of the salt marsh, it is possible to notice that almost every sampling campaign shows some peculiarities and differences from the mean. For example, June 2016 and July (characterized by important rainfall events; Table 3.11), are the ones that show higher imports than the model, but a high tide peak was registered during those days. Other significative examples are May and June 2017, which show very different values respect to the model: the first one was characterized by a short tide event and was not used for the calibration procedure due to the low number of useful data, while the second one was characterized by a high export of DON (circa 1 mg/l), which determined a negative flux and a net export from the salt marsh. Moreover, also August is not very well represented by the model, which is something complex to address without additional data or information. All these considerations may suggest some limits in the model ability to simulate the seasonal trend of the salt marsh net fluxes. They may also indicate that there are important fluctuations in the marsh behavior during a month (as suggested by the differences between June 2016 and 2017), which makes the comparison between a single net flux for a single campaign and the average modelled result not meaningful. More campaigns during a single month should be done in order to address this interesting issue.

To the results in Figure 3.79 and 3.80, the other nitrogen input to the salt marsh are summed, which means atmospheric deposition and accretion. Results are shown in Figure 3.82 and 3.83.

Total import fluxes are significantly increased and the net monthly ones, as a consequence. This indicates that nitrogen input by sedimentation or accretion (which has higher monthly values than atmospheric deposition) is more important than the TDN fluxes imported by the salt marsh.

The annual mass balances is then computed, taking into account also the sediment and vegetation biomass stock variation (Figure 3.84; Figure 3.85). Results are shown in Table 3.20.

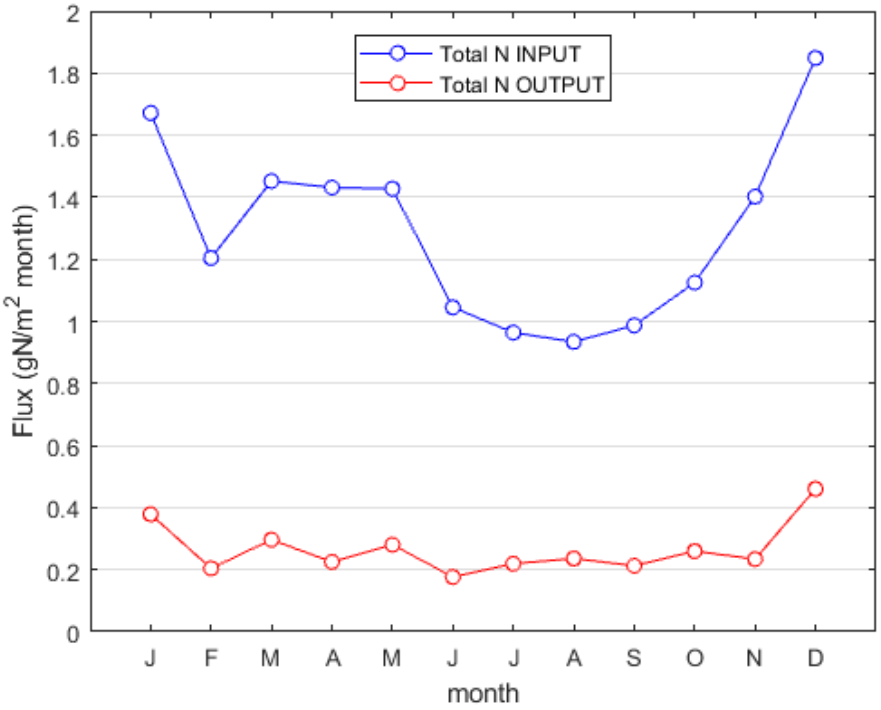

Figure 3.82 Input and output monthly fluxes from the salt marsh, including atmospheric deposition and accretion.

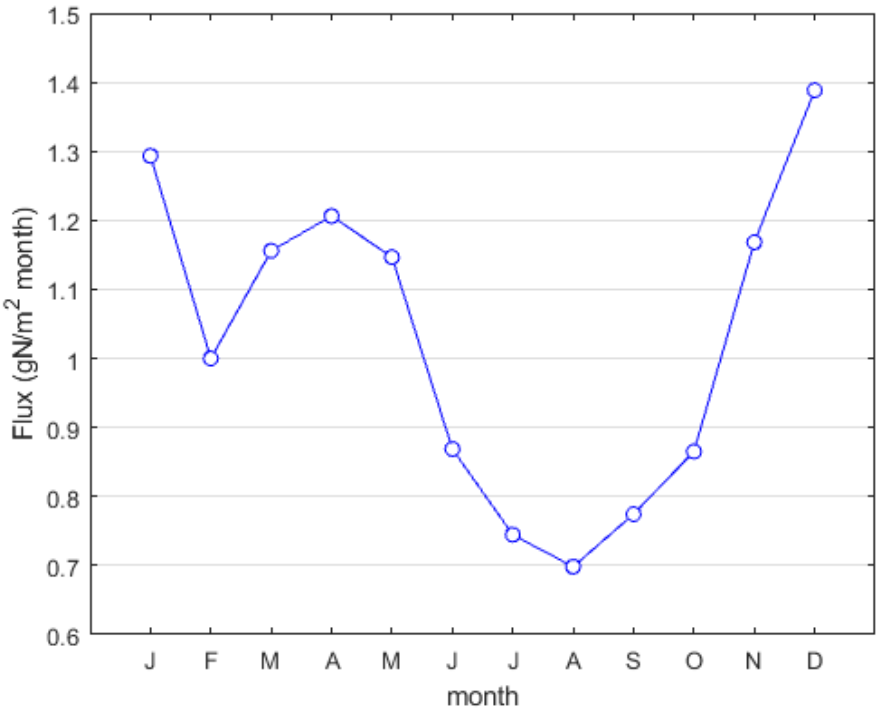

Figure 3.83 Net monthly fluxes from the salt marsh, including atmospheric deposition and accretion.

Table 3.20 Total yearly import and export fluxes from the salt marsh.

FLUXES	**IMPORT (gN m^{-2} y^{-1})**	**EXPORT (gN m^{-2} y^{-1})**
Ammonium	0.42	0.13
Nitrate	4.54	0.66
DON	2.00	2.39
Sediments stock change	62.38	62.38
Plant biomass stock change	5.22	5.22
Accretion	7.09	/
Atmospheric deposition	1.5	/
Denitrification	/	4.15
TOTAL	83.15	74.93

As it is possible to notice, the salt marsh has a positive yearly mass balance, with a net import of nitrogen. Nitrate are the nitrogen compound with the greatest reduction and denitrification is the most important output flux, highlighting another time the importance of this process in the salt marsh, while ammonium is confirmed to be the compound with contributes less to the total mass balance. Moreover, sediments and vegetation biomass stock fluxes have equal values for import and export, which means that important internal recycling of nitrogen occurs in the salt marsh. This last result is very important, since it is a characteristic connected to mature ecosystems (Odum, 1969).

Eventually, neglecting the export flux due to denitrification, because it release nitrogen in the gaseous and not bioavailable form (N_2), it is possible to obtain that the salt marsh processes 12.37 gN m^{-2} y^{-1}. This estimation is lower respect the one calculated in Baldan (2015). This is due to the fact that, improving the A(h) curve, lower values for wetted area, volume and discharge have been evaluated, resulting in lower fluxes over a tidal cycle. However, it is confirmed that the salt marsh has a positive import and it is an important nitrogen processor and sink for the Venice Lagoon.

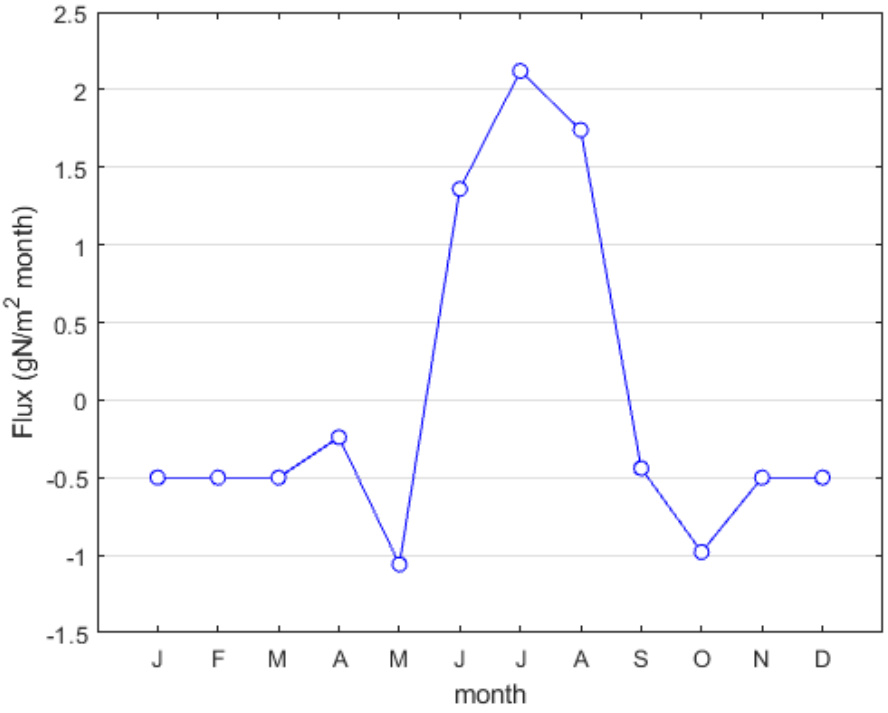

Figure 3.84 Vegetation biomass nitrogen stock variation.

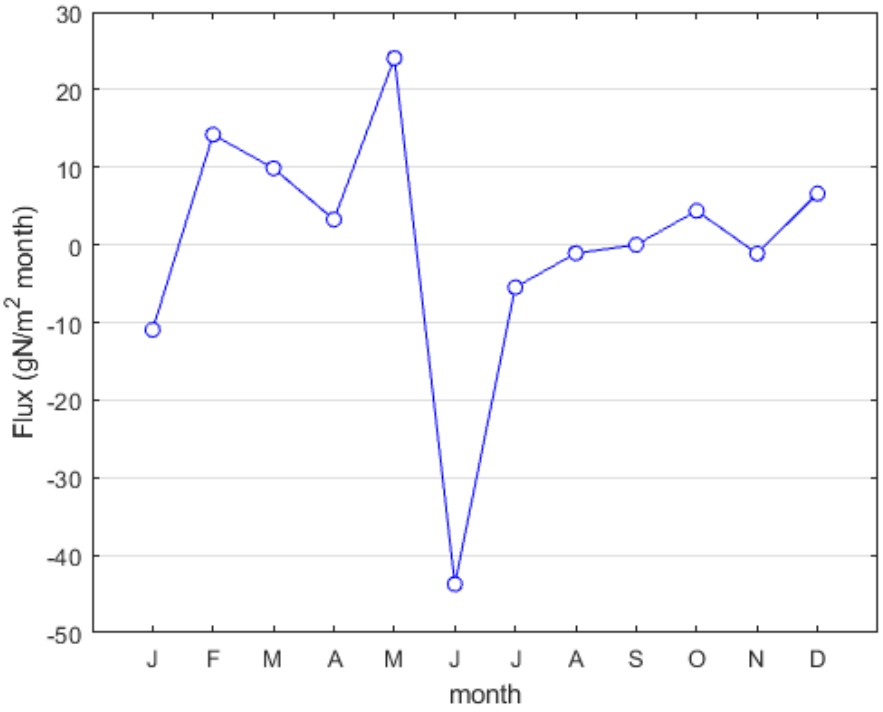

Figure 3.85 Sediment nitrogen stock variation.

3.5 Ecosystem service evaluation

Salt marshes provide many ecosystem services (ES), which are described in Paragraph 1.3. Only one of them is evaluated in this thesis, which is the nitrogen loads reduction, connected to the nitrogen cycle regulation service. The ecosystem service is calculated in terms of replacement costs (Heal, 2000), which is the amount of money that the society would spend if the concerned service would not be provided by nature.

Other two ES are related to the nitrogen cycle regulation service, which are impacts on trophic networks in terms of quality of TDN composition and impact on trophic networks in terms of quantity of TDN adsorbed or released during a year (lamination effect). However, to evaluate them, in addition to the mass balance calculation, a trophic network modeling is required and this is not carried on in this thesis.

As far as the ES evaluation is concerned, it could be possible to evaluate the economic efforts made by Regione Veneto in order to achieve the Venice Lagoon quality standards fixed in the law "Piano Direttore per la Laguna di Venezia" (Regione Veneto, 2000). The Regione Veneto allocated 1 900 million € in order to reach the standards, and the planned interventions included reduction of diffused civil loads, improvement of the wastewater treatment plants (WWTPs) serving the lagoon area, interventions on factories in the industrial area of Porto Marghera and Fusina and many others. Unfortunately, it is not possible to understand how much of the total allocated money was used to decrease nitrogen loads. Therefore, a case-specific evaluation is not feasible.

For this reason, an analysis of cost for nitrogen reduction in WWTPs in carried on, as in Baldan (2015). The results in cost per unit of nitrogen removed, needed to obtain a 90% reduction of input nitrogen concentration, are presented in Table 3.21 (Hautakangas et al., 2014), which are dependent on the size of the plants, expressed in population equivalent (PE).

Table 3.21 Nitrogen treatment cost for different WWT plants sizes.

Plant dimension (PE)	**Cost (€ kgN^{-1})**
< 80 000	12
80 000 – 200 000	8
200 000 – 500 000	7.50
> 500 000	6

From (ARPAV, 2009), the number and the size of the WWTPs serving the Venice Lagoon has been evaluated and data are shown in Table 3.22.

Table 3.22 WWTPs serving the Venice Lagoon.

Plant dimension	Number of plants	Served PE
Very small (< 10 000)	8	66 700
Small (< 80 000)	21	247 380
Medium (80 000 – 200 000)	1	110 000
Big (200 000 – 500 000)	1	330 000
TOTAL	31	754 080

The majority of the existing WWTPs are small size plants, serving less than 80 000 PE; only two (one medium size and one big size) bigger plants are present.

For the cost evaluation, it is assumed that the 8 very small plants do not have nitrogen treatment lines or processes, since commonly plants with those sizes are very simple, with only organic matter removal techniques. The average nitrogen treatment cost has been evaluated as the average of removal cost weighted on the numbers of PE served for each size class, and the result is 9.44 € kgN^{-1}.

Using this value, it is possible to calculate the ES of nitrogen loads reduction provided by the salt marsh. Since the salt marsh can process 12.37 gN m^{-2} y^{-1}, the economic value is equal to 0.117 € m^{-2} y^{-1} or 1170 € ha^{-1} y^{-1}. The total surface covered by salt marshes in the lagoon in 47 km^2, so the total benefit provided by them is 5 488 322 € y^{-1}. This value is very significative and it must be taken into account that this is the evaluation of only one of the many ecosystem services related to salt marshes, which means that their total economic value could be much higher.

As far as the salt marshes of the LIFE VIMINE Project are concerned (Paragraph 1.4), they cover a total area of 15.28 ha and for this reason, their benefit is 17 878 € y^{-1}. The marginal benefit is also evaluated. It is calculated as the difference between the actual condition with the LIFE VIMINE Project interventions (which are assumed to stop completely the salt marsh erosion) and the business as usual (BaU) scenario, without any interventions. The erosion rate has been evaluated in (Grechi, 2015) and it predicts a total salt marsh surface of 10.4 ha in 2050. From 2017 until 2050, in the LIFE VIMINE scenario, the salt marshes provide a benefit equal to 589 961 €, while in BaU scenario it is equal to 401 544 €, with a total marginal cost of 188 417 € (not actualized value). On

33 years, the marginal cost, in a scenario without erosion preventing techniques, is equal to 5383 € y^{-1} (not actualized value).

4. Conclusion

In this thesis, a long-term set of field surveys has been carried on in order to assess the behavior of a salt marsh in the Venice Lagoon, with a focus on the nitrogen dynamics. The collected data are then used to calibrate a model, which solves the nitrogen mass balance for the salt marsh for the short time scale (lower than the tidal cycle) and for the long time scale. Baldan (2015) developed the model in a previous work and here was improved under different aspects (type of input data, number of equations) and calibrated with a greater set of observed data. A lack of studies about nitrogen dynamics in the salt marshes in the Venice Lagoon is found in literature and, in our knowledge, this is the first study that analyzed nitrogen fate in this ecosystem on the long term

The model includes a set of three ordinary differential equations that solves the mass balances for ammonium (NH_4^+), nitrate (NO_3^-) and dissolved organic nitrogen (DON) and different chemical-physical processes are considered, such as ammonification, nitrification, denitrification, release from the sediment and plant and phytoplankton activities (related to uptake or exudation). The global calibration of the model, taking into consideration all the observed data at the same time, allowed obtaining good efficiencies and the selection of the best model highlighted the some processes could be neglected, which are the ammonia and nitrate release by the sediment. Annual mass balance is then carried on and shows how the salt marsh is able to process 12.37 gN m^{-2} y^{-1}, which is an important data since it is greater, for example, than the denitrification rate observed in literature (2 gN m^{-2} y^{-1}; Eriksson et al., 2003).

The result that emerges from the monitoring and modeling approaches is that salt marsh behavior changes considerably along the year and confirms the role of the salt marsh as nitrogen processor. Literature studies address this ecosystem as nitrogen buffer area rather than nitrogen abatement zone, releasing nitrogen during the winter and retaining it during the summer. It is only possible to confirm partially this paradigm from this thesis. The model results show that a higher import is occurring during the winter, due to higher nitrate concentration, while decreases during the summer. From field data analysis, a total export is register in June (2017) and August, confirming the tendency to release nitrogen during the summer (mainly as DON).

However, other results suggest how the salt marsh is highly dependent on external condition, mainly on rainfall events, which tend to generate high imports by the marsh (as observed from June 2016 and July data). Moreover, the annual mass balance points out how sedimentation represents an important nitrogen input to the salt marsh and that vegetation biomass and sediment are correlated to internal nitrogen recycling, indicating a mature ecosystem (Odum, 1969).

The modeling approach, combined with long-term field data, allows to obtain a realistic picture of what happens inside the salt marsh for both the short and long time scale, without huge effort. The limitation of the model are known and should be addressed, but the final results allow to support conservation operations for this ecosystem, which is increasingly threatened by erosion. Ecosystem service (ES) regarding nitrogen loads reduction is evaluated to be equal to 1170 € ha^{-1} y^{-1}, contributing in this way to the social well-being by supporting a fully functional ecosystem with a huge buffer capacity

This thesis gave a first indication of the differences in nitrogen dynamics occurring along the seasons, but more focused analyses are needed to assess the high heterogeneity detected during the field campaigns, since it is possible to give only potential answers from the collected data. It is necessary to understand, for example, the importance of plants and phytoplankton role and to confirm or to confute the calibration results regarding ammonium and nitrogen sediment release. Another important aspect would be deeper examination of salt marsh hydraulic, since salinity results may indicate that, during summer, less water exits from the marsh respect to the input one, due to evapotranspiration. Finally, CSTR approach is limited and a PFR conceptualization should be implemented. Moreover, the relationship between nitrogen fate in salt marshes and important rainfall events should be better studied and demonstrate with future studies.

Despite this the ecosystem service value computed can be used in the future management of the lagoon, fir instance by allocating more economic resources to salt marshes conservation.

5. References

Anderson, D.R., 2008. *Model based inference in the life sciences*. Springer.

Anderson, I. C., McGlathery, K. J., Tyler, A. C., 2003. *Microbial mediation of 'reactive' nitrogen transformations in a temperate lagoon*. Marine Ecology Progress Series 246, 73 – 84.

Anoè, N., Calzavara, D., Salviato, L., 1984. *Flora e vegetazione delle barene. Note e schede*. Società Veneziana di Scienze Naturali, Lavori, Vol. 9.

ARPAV, 2009. *Bacino Scolante nella laguna di Venezia. Rapporto sullo stato ambientale dei corpi idrici*. Anni 2005-2007.

ARPAV, 2012. *Progetto per l'integrazione delle conoscenze sui carichi inquinanti immessi nella laguna di Venezia dai bacini a scolo meccanico della gronda lagunare*.

APAT, IRSA-CNR, 2003. *Metodi analitici per le acque*.

Baldan, D., 2015. *Mass balance of nitrogen on a salt marsh in the northern Venice Lagoon*. Master thesis in Environmental Engineering, University of Padua.

Barausse, A., Grechi, L., Martinello, N., Musner, T., Smania, D., Zangaglia, A., Palmeri, L., 2015. *An integrated approach to prevent the erosion of salt marshes in the Lagoon of Venice*. Environmental Quality 18, 43 – 54.

Bendoricchio, G., De Boni, G., 2005. *A water-quality model for the Lagoon of Venice, Italy*. Ecological Modelling 184, 69 – 81.

Bendoricchio, G., Palmeri, L., 2005. *Quo vadis ecosystem?*. Ecological Modelling 84, 5 – 17.

Bonometto, L., 2003. *Ecologia applicata e ripristino ambientale nella laguna di Venezia: analisi e classificazione funzionale delle barene e delle tipologie di intervento sulle barene*. CPM, Comune di Venezia.

Bowden, W. B., 1986. *Nitrification, Nitrate Reduction, and Nitrogen Immobilization in a Tidal Freshwater Marsh Sediment*. Ecology 67, 88 – 99.

Bradley, P. M., Morris, J. T., 1990. *Influence of Oxygen and Sulfide Concentration on Nitrogen Uptake Kinetics in Spartina Alterniflora*. Ecology 71, 282 – 287.

Chen, W., Ge, Z. M., Fei, B. L., Zhang, C., Liu, Q. X., Zhang, Q. L., 2017. *Soil carbon and nitrogen storage in recently restored and mature native* Scirpus *marshes in the Yangtze Estuary, China: Implications for restoration*. Ecological Engineering 104, 150 – 157.

Clarkson, B. R., Ausseil, A. E. G., Gerbeaux, P., 2013. *Wetland Ecosystem Services*. Ecosystem services in New Zealand: conditions and trends, 192 – 202.

Costanza, R., d'Arge, R., de Groot, R., Farber, S., Grasso, M., Hannon, B., Limburg, K., Naeem, S., O'Neill, R. V., Paruelo, J., Raskin, R. G., Sutton, P., van den Belt, M., 1997. *The value of the world's ecosystem services and natural capital*. Nature 387, 253 – 260.

Costanza, R., d'Arge, R., de Groot, R., Farber, S., Grasso, M., Hannon, B., Limburg, K., Naeem, S., O'Neill, R. V., Paruelo, J., Raskin, R. G., Sutton, P., van den Belt, M., 1998. *The value of ecosystem services: putting the issues in perspective*. Ecological Economics 25, 67 – 72.

D'Alpaos, L., 2010. *Fatti e misfatti di idraulica lagunare.* Memorie. Classe di scienze fisiche, matematiche e naturali. Istituto veneto di Scienze, lettere ed arti.

D'Alpaos, A., Lanzoni, S., Mudd, S. M., Fagherazzi, S., 2006. *Modeling the influence of hydroperiod and vegetation on the cross-sectional formation of tidal channels*. Estuarine, Coastal and Shelf Science 69, 311 – 324.

D'Alpaos, A., Marani, M., 2015. *Reading the signatures of biologic–geomorphic feedbacks in salt-marsh landscapes*. Advances in Water Resources 93, 265 – 275.

Davy, A. J., Bishop, G. F., Costa, C. S. B., 2001. Salicornia *L. (*Salicornia pusilla *J. Woods,* S. ramosissima *J. Woods,* S. europaea *L.,* S. obscura *P.W. Ball & Tutin,* S. nitens *P.W. Ball & Tutin,* S. fragilis *P.W. Ball & Tutin and* S. dolichostachya *Moss)*. Journal of Ecology 89, 681 – 707.

Dollhopf, S. L., Hyun, J. H., Smith, A. C., Adams, H. J., O'Brien, S., Kostka, J. E., 2005. *Quantification of Ammonia-Oxidizing Bacteria and Factors Controlling Nitrification in Salt Marsh Sediments*. Applied and Environmental Microbiology 71, 240–246.

Eriksson, P. G., Svensson, J. M., Carrer, G. M., 2003. *Temporal changes and spatial variation of soil oxygen consumption, nitrification and denitrification rates in a tidal salt marsh of the Lagoon of Venice, Italy*. Estuarine, Coastal and Shelf Science 58, 861 – 871.

Etheridge, J. R., Burchell II, M. R., Birgand, F., 2017. *Can created tidal marshes reduce nitrate export to downstream estuaries?*. Ecological Engineering 105, 314 – 324.

Fagherazzi, S., Wiberg, P. L., Temmerman, S., Struyf, E., Zhao, Y., Raymond, P. A., 2013. *Fluxes of water, sediments, and biogeochemical compounds in salt marshes*. Ecological Processes 2, 1 – 16.

Google Earth, 2017.

Grasshoff, K., Ehrhardt, M., Kremling, K., 1983. *Methods of Seawater Analysis (Second, Revised and Extended Edition)*. Verlag Chemie.

Grechi, L., 2015. *LIFE VIMINE ES evaluation – Carbon sequestration*. Internal report.

Greenberg, A. E., Clesceri, L. S., Eaton, A. E., 1992. *Standard Methods For the Examination of Water and Wastewater*. American Public Health Association, American Water Works Association, Water Environment Federation.

Hautakangas, S., Ollikainen, M., Aarnos, K., Rantanen, P., 2014. *Nutrient Abatement Potential and Abatement Costs of Waste Water Treatment Plants in the Baltic Sea Region*. Ambio 43, 352 – 360.

Heal, G., 2000. *Valuing Ecosystem Services*. Ecosystem 3, 24 – 30.

Hobbs, N.T., Hilborn, R., 2006. *Alternatives to statistical hypothesis testing in ecology: a guide to self teaching*. Ecological Applications 16, 5 – 19.

Hopkinson, C. S., Giblin, A. E., 2008. *Nitrogen Dynamics of Coastal Salt Marshes*. Nitrogen in the Marine Environment (2nd Edition), 991 – 1036.

Hopkinson, C. S., Schubauer, J. P., 1984. *Static and Dynamic Aspects of Nitrogen Cycling in the Salt Marsh Graminoid Spartina Alterniflora*. Ecology 65, 961 – 969.

https://www.autodesk.it/products/autocad/overview

https://it.mathworks.com/products/matlab.html

Jones, K., 1974. *Nitrogen Fixation in a Salt Marsh*. Ecology 62, 553 – 565.

Jørgensen, S. E., 1979. *Handbook of Environmental Data and Ecological parameters*. International Society for Ecological Modelling.

Jørgensen, S. E., Bendoricchio, G., 2001. *Fundamentals of ecological modelling*. Elsevier.

Kadlek, R. H., Wallace, S. D., 2009. *Treatment wetlands, 2nd Edition*. CRC Press, Boca Raton, FL.

Langis, R., Zalejko, M., Zedler, J. B., 1991. *Nitrogen Assessments in a Constructed and a Natural Salt Marsh of San Diego Bay*. Ecological Applications 1, 40 – 51.

McCuen, R. H., Knight, Z., Cutter, A. G., 2006. *Evaluation of the Nash - Sutcliffe Efficiency index*. Journal of Hydrologic Engineering 11, 597 – 602.

Ministero delle Infrastrutture e dei Trasporti – Provveditorato Interregionale alle OO. PP del Veneto – Trentino Alto Adige – Friuli Venezia Giulia tramite il suo concessionario Consorzio Venezia Nuova, 2003. *Rapporto tecnico I anno, ESECUTIVO DEL 2° STRALCIO TRIENNALE (2002-2005) MELa2*.

Ministero delle Infrastrutture e dei Trasporti – Provveditorato Interregionale alle OO. PP del Veneto – Trentino Alto Adige – Friuli Venezia Giulia tramite il suo concessionario Consorzio Venezia Nuova, 2003. *Rapporto tecnico II anno, ESECUTIVO DEL 2° STRALCIO TRIENNALE (2002-2005) MELa2*.

Ministero delle Infrastrutture e dei Trasporti – Provveditorato Interregionale alle OO. PP del Veneto – Trentino Alto Adige – Friuli Venezia Giulia tramite il suo concessionario Consorzio

Venezia Nuova, 2003. *Rapporto tecnico finale sulle attività di monitoraggio della qualità delle acque Volume 1. Rapporto di sintesi; 3^ FASE (2003 – 2005) MELa 3 – OP/285*.

Morris, J. T., 1990. *The Nitrogen Uptake Kinetics of Spartina Alterniflora in Culture*. Ecology 61, 1114 – 1121.

Odum, E. P., 1969. *The Strategy of Ecosystem Development*. Science 164, 262 – 270.

Pastres, R., Ciavatta, S., Cossarini, G., Solisoro, C., 2005. *The seasonal distribution of dissolved inorganic nitrogen and phosphorus in the lagoon of Venice: A numerical analysis*. Environment International 31, 1031 – 1039.

Pastres, R., Solidoro, C., Ciavatta, S., Petrizzo, A., Cossarini, G., 2004. *Long-term changes of inorganic nutrients in the Lagoon of Venice (Italy)*. Journal of Marine Systems 51, 179 – 189.

Pomeroy, L. R., Wiegart, R. G. (Eds.), 2012. *The cycles of Nitrogen and Phosphorus, in: The Ecology of Salt Marshes*. Springer.

Poulin, P., Pelletier, E., Saint-Louis, R., 2007. *Seasonal variability of denitrification efficiency in northern salt marshes: An example from the St. Lawrence Estuary*. Marine Environmental Research 63, 490 – 505.

Regione Veneto, 2000. *Piano per la prevenzione dell'inquinamento e il risanamento delle acque del bacino idrografico immediatamente sversante nella laguna di Venezia*.

Rossini, P., Guerzoni, S., Molinaroli, E., Rampazzo, G., De Lazzari, A., Zancanaro, A., 2005. *Atmospheric bulk deposition to the lagoon of Venice Part I. Fluxes of metals, nutrients and organic contaminants*. Environmental International 31, 959 – 974.

Scarton, F., 2006. *Produttività primaria epigea di sette alofite in laguna di Venezia*. Bollettino del Museo civico di Storia Naturale di Venezia 57, 53 – 71.

Silvestri, S., Defina, A., Marani, M., 2005. *Tidal regime, salinity and salt marsh plant zonation*. Estuarine, Coastal and Shelf Science 62, 119 – 130.

Simas, T. C., Ferreira, J. G., 2007. *Nutrient enrichment and the role of salt marshes in the Tagus estuary (Portugal)*. Estuarine, Coastal and Shelf Science 75, 393 – 407.

Solidoro, C., Bandel, V., Aubry Bernardi, F., Camatti, E., Ciavatta, S., Cossarini, G., Facca, C., Franzoi, P., Libralato, S., Melaku Canu, D., Pastres, R., Pranovi, F., Raicevich, S., Socal, G., Sfriso, A., Sigovini, M., Tagliapietra, D., Torricelli, P., 2010. *Response of the Venice Lagoon Ecosystem to Natural and Anthropogenic Pressures over the Last 50 Years*. Coastal Lagoons: Systems of Natural and Anthropogenic Change, 483 – 511.

Solidoro, C., Pastres, R., Cossarini, G., Ciavatta, S., 2004. *Seasonal and spatial variability of water quality parameters in the lagoon of Venice*. Journal of Marine Systems 51, 7 – 18.

Solidoro, C., Pastres, R., Cossarini, G., 2005. *Nitrogen and plankton dynamics in the lagoon of Venice*. Ecological Modelling 184, 103 – 123.

Spohn, M., Giani, L., 2012. *Carbohydrates, carbon and nitrogen in soils of a marine and a brackish marsh as influenced by inundation frequency*. Estuarine, Coastal and Shelf Science 107, 89 – 96.

Teal, J. M., 1962. *Energy flow in the salt marsh ecosystem of Georgia*. Ecology 43, 614 – 624.

Valiela, I., Cole, M. L., 2002. *Comparative Evidence that Salt Marshes and Mangroves May Protect Seagrass Meadows from Land-derived Nitrogen Loads*. Ecosystems 5, 92 – 102.

Valiela, I., Teal, J. M., 1979. *The nitrogen budget of a salt marsh ecosystem*. Nature 280, 652 – 657.

van Wijnen, H. J., Bakker, J. P., 2000. *Annual nitrogen budget of a temperate coastal barrier salt-marsh system along a productivity gradient at low and high marsh elevation*. Perspectives in Plant Ecology, Evolution and Systematics 3, 128 – 141.

www.arpa.veneto.it

www.lifevimine.eu

6. Acknowledgements

Per me è davvero difficile tentare di ringraziare tutte le persone che hanno contribuito, in una maniera o in un'altra, a questo mio percorso universitario e di tesi finale. Sono stati 5 anni (e qualcosa in più) che sono letteralmente volati, senza davvero rendersene conto si era ormai arrivati alle ultime battute. Cercherò quindi di essere breve e conciso, andando senza un particolare ordine, sperando davvero di non dimenticare nessuno.

Le prime persone che mi viene da ringraziare sono i miei genitori, perché senza di voi non sarei mai arrivato fin qui, un po' perché siete stati voi materialmente a permettermi di raggiungere questo traguardo, ma anche per tutte le volte in cui, nelle mie sfuriate, nervoso perché "tanto questo esame non lo passo", mi avete sempre spronato a dare il meglio o, nel caso peggiore, a farlo per la volta successiva. Ovviamente a questi ringraziamenti si aggiunge anche Andrea, mio fratello, perché qualsiasi cosa succeda, che possa essere lontananza o periodacci, come diciamo sempre, ci siamo sempre l'uno per l'altro. Anche se non siamo molto bravi a dimostrarlo esplicitamente. Come dice sempre la mamma, "voi due siete proprio orsi!".

Un grazie enorme e speciale va ovviamente ad Elena, per tutti questi anni ed ogni singola cosa. Non basterebbe la lunghezza di questa tesi per descrivere tutti i motivi per cui ti dovrò sempre un enorme grazie. Dalle prime chiacchierate quando neppure stavamo assieme (e quando io facevo fatica ad accorgermi dell'ovvio), alla pazienza che hai avuto con me in questi anni, perché mi hai sempre supportato e sopportato, fino ad arrivare all'aiuto che mi hai dato ad organizzare questa laurea, con i tuoi consigli e tutto il resto.

Vorrei poi ringraziare i miei nonni, nonna Nella, nonna Wally, nonno Basilio, per tutto ciò che mi avete sempre dato in questi anni, dall'infinito affetto al continuo interesse e preoccupazione per come mi andassero gli studi. Vi voglio bene!

Un ringraziamento va anche a tutti i miei zii, ai miei cugini, e a tutte le altre persone che, per parentele o semplice amicizia, fanno parte della famiglia, con cui è sempre un piacere rivedersi, incontrarsi, scambiare quattro chiacchiere e parlare del più e del meno.

Ovviamente vorrei ringraziare anche tutta la marmaglia di amici che mi ritrovo, Perol, Roby, Sgoge, Davide, Max, Duri, Edo, Diego, Longo, Del Francia, coi quali siamo ancora qui dopo tanti anni, con qualche pezzo in più e con qualche pezzo in meno, con i quali si continua a sentirci e a vederci. Un grazie anche a voi, perché spesso tornare a casa e uscire la sera è stato anche un modo per rilassarmi dagli impegni universitari e ridere e scherzare assieme, anche se il "non posso, devo studiare" è stato spesso una costante. Ed ora qualche universitario tra voi mi capisce bene!

Lo stesso discorso del continuare a sentirci negli anni non mi fa che ringraziare Giada e Jessica, con le quali è sempre bellissimo uscire e ritrovarci, dopo tutti questi anni dal liceo. I discorsi negli anni sono cambiati, dalle lamentele sui professori alle lamentele sull'università, ma ciò che non è cambiato mai è questo legame che spero davvero si possa portare avanti ancora "a lunghissimo".

Vorrei ovviamente ringraziare anche tutti gli amici dell'università, Gianluca, Alessandro, Gianmarco, Alessia e tutti gli altri che ho incontrato lungo questo cammino e con cui ho condiviso gioie e dolori dell'università. Per non dimenticare anche delle nostre camminate nei dintorni di Vipiteno, delle nostre serate qui a Padova e di tutto ciò che c'è stato in questi anni e che ha permesso di creare la nostra amicizia. E collegandomi ad amicizie di lunga data e università, non posso che ringraziare Erica, perché è sempre un piacere trovarsi (in università o per andare a teatro), scambiare quattro chiacchiere e magari anche qualcuna di più, come facevamo sulla corriera per il liceo.

Passando da amicizie di lunga data ad altre più nuove, vorrei naturalmente ringraziare anche Giulio e Federico, per tutte le serate assieme, per le gite a Capodanno, per le chiacchierate fino a tarda notte e per aver predetto il futuro tra me e Elena anni fa! Davvero, grazie mille per questa amicizia che si è creata!

Infine, vorrei ringraziare tutte le persone che hanno ruotato attorno a questo lavoro di tesi, in maniera diretta o indiretta. Un grazie va innanzitutto al Prof. Palmeri, per aver fatto nascere in me l'interesse per la modellistica ambientale con i suoi corsi; ad Alberto Barausse, per la pazienza dedicatami nell'interpretazione dei risultati o per qualsiasi dubbio io avessi; ai ragazzi di Osmotech, Alberto, Francesco e Alice, per aver sopportato per mesi l'orrendo rumore della ventola del mio pc; a Karim, per tutti i passaggi in auto verso e di ritorno dal cantiere nautico; a tutte le altre persone del LASA, come Marco e Marco, Laura, Andrea e tutti gli altri.

Un ringraziamento speciale va però a due persone che sono state fondamentali per questa tesi e a cui vorrei dedicare un ringraziamento a parte: la prima persona è Dario, per la sua passione per la laguna che trasmette a chiunque, per tutto ciò che mi ha insegnato e raccontato su di essa e non, per tutta la pazienza che ha avuto nell'organizzare le uscite e portarci in barca in barena, per le discussioni tra un campionamento e l'altro, insomma tutte cose che hanno reso ogni uscita in barena e questa mia tesi speciale e per me indimenticabile. La seconda persona invece, a cui davvero va tutto il mio ringraziamento e riconoscimento, è Damiano, per avermi sempre aiutato in qualsiasi momento avessi un problema o un dubbio con la tesi (anche e soprattutto adesso dall'Austria), per tutta la pazienza che ha avuto nello spiegarmi tutto ciò che c'è da sapere sulle barene di uscita in uscita o per seguirmi nella programmazione con Matlab e nel risolvere tutti i vari problemi che ci

sono stati, per ogni singola cosa che ha fatto per me e per questo lavoro da marzo fino all'ultimo momento: davvero, davvero, grazie infinite ad entrambi!

7. Appendix

7.1 Model for tide event recreation

```
clear all
close all
clc

Altez_marea = fopen ( 'Hobs.txt' , 'r');
Hobs = fscanf ( Altez_marea , '%g %g' , [2 inf] );
fclose ( Altez_marea );
Hobs=Hobs';


a = 20;
b = 0.01;
c = 0.1;

tspan=[0:1:249];

for i=1:length(tspan);
   h(i)= a*sin(b*tspan(i)+c);
end


a_range = [1 50];
b_range = [0.0001 0.1];
c_range = [0.005 0.8];

lb = [a_range(1) b_range(1) c_range(1)];
ub = [a_range(2) b_range(2) c_range(2)];

param = [a b c];

options = psoptimset('MaxFunEvals',10000,'MaxIter',5000,'Display','iter');

[param_fitted, resnorm] =
patternsearch(@residuals_sinu,param,[],[],[],[],lb,ub,[],options);

a_fit = param_fitted (1);
b_fit = param_fitted (2);
c_fit = param_fitted (3);

for i=1:length(tspan);
   h(i)= a_fit*sin(b_fit*tspan(i)+c_fit);
end;

figure;
plot (tspan,h,'-k', Hobs (:,1), Hobs (:,2), 'ro');

'fitted parameters are'
a_fit
b_fit
c_fit
```

7.2 Residues function for the sinusoid

```
function RSS=residuals_sinu(param)

Altez_marea = fopen ( 'Hobs.txt' , 'r');
Hobs = fscanf ( Altez_marea , '%g %g' , [2 inf] );
fclose ( Altez_marea );
Hobs=Hobs';

a = param (1);
b = param (2);
c = param (3);

tspan=[0:1:249];

for i=1:length(tspan);
   h(i)= a*sin(b*tspan(i)+c);
end;

differences = 0;
for ii=1:size(Hobs,1);
    differences = [differences; (Hobs(ii,2) - interp1(tspan,h,Hobs(ii,1)) )];
end
differences(1)=[];
RSS = sum(differences.^2);
```

7.3 Hydraulic submodel

```
clear all
close all
clc


numfiles=8;


% Read A(h) curve
Discharge= fopen ( 'Serbatoi_new.txt' , 'r');
A = fscanf ( Discharge , '%g %g' , [2 inf] );
fclose ( Discharge );
A=A';

% Read water level data

for j=1:numfiles
   j;
   nomefile=['Altezze' sprintf('%g',j) '.txt'];
   fi=fopen(nomefile);

   h = fscanf ( fi , '%g %g' , [2 inf] );
   fclose ( fi );
   h=h';


%% Derivative computation
```

```
tspan=1:1:length(h);

dh=diff(h(:,2));
dt=diff(h(:,1));
dhdt=dh./dt; % m/min

tspan2=1:1:length(dhdt);

%% Model


 for t=1:length(tspan2)
    Q(t,1)=tspan2(t);

Q(t,2)=interp1(tspan2,dhdt,t,'spline')*interp1(A(:,1),A(:,2),h(t,2),'spline'); %
m3/min
 end;

 % Output file correction

 for i=1:20
    if Q(i,2)<0
    Q(i,2)=0; % m3/min
    else
    end
 end;

 for i=(length(Q)-20):length(Q)
    if Q(i,2)>0
    Q(i,2)=0; % m3/min
    else
    end
 end;

 if j==2;
     Q(1,2)=0;
 else
 end

%% Wetted area
for i=1:length(tspan);
    As(i,1)=tspan(i);
    As(i,2)=interp1(A(:,1),A(:,2),h(i,2),'spline');
end;

 % Output file correction

 for i=1:20
    if As(i,2)<0
    As(i,2)=0; % m3/min
    else
    end
 end;

 for i=(length(As)-20):length(As)
    if As(i,2)<0
    As(i,2)=0; % m3/min
    else
```

```
    end
 end;

 for i=length(As)
     As(i,2)=0;
 end

 if j==2;
     As(1,2)=0;
 else
 end


%% Inundated volume
dz=0.001;
for t=1:length(h(:,1));
     V(t,1)=h(t,1);
     hh=[0:dz:h(t,2)];
     AA=interp1(A(:,1),A(:,2),hh,'spline');
     V(t,2)=trapz(AA)*dz;
end;

 % Output file correction

 for i=1:30
    if V(i,2)<0
    V(i,2)=0; % m3/min
    else
    end
 end;

  for i=(length(V)-30):length(V)
    if V(i,2)<0
    V(i,2)=0; % m3/min
    else
    end
 end;

 for i=length(V)
     V(i,2)=0;
 end

 if j==2;
     V(1,2)=0;
 else
 end


%% SAVE FILE

%Print the results into files

namefile1=['Discharge'  sprintf('%g',j) '.txt'];

fileID1 = fopen(namefile1,'wt');
for i=1:size(Q,1)
  fprintf (fileID1,'%g\t', Q(i,:));
  fprintf (fileID1, '\n');
end
```

```
fclose (fileID1);

namefile2=['Volume'  sprintf('%g',j) '.txt'];

fileID2 = fopen(namefile2,'wt');
for i=1:size(V,1)
  fprintf (fileID2,'%g\t', V(i,:));
  fprintf (fileID2, '\n');
end
fclose (fileID2);

namefile3=['SubArea'  sprintf('%g',j) '.txt'];

fileID3 = fopen(namefile3,'wt');
for i=1:size(As,1)
  fprintf (fileID3,'%g\t', As(i,:));
  fprintf (fileID3, '\n');
end
fclose (fileID3);

clearvars Q As V

end
%% plots

% Discharge= fopen ( 'Discharge1.txt' , 'r');
% Q= fscanf ( Discharge , '%g %g' , [2 inf] );
% fclose ( Discharge );
% Q=Q';
%
% Subarea= fopen ( 'Subarea1.txt' , 'r');
% As = fscanf ( Subarea , '%g %g' , [2 inf] );
% fclose ( Subarea );
% As=As';
%
Volume= fopen ( 'Volume1.txt' , 'r');
V = fscanf ( Volume , '%g %g' , [2 inf] );
fclose ( Volume );
V=V';
%
%
% figure(1);
% plot(h(:,1),h(:,2), '-r');
% xlabel('t (min)');
% hold on;
% plot(tspan2,dhdt.*60, '-g');
% h1=legend('water level h, m', 'dh/dt, m/h',2);
% hold off;
%
% figure(2);
% plot (A(:,1), A(:,2), '-b');
% ylabel('Area (m^2)');
% xlabel('Stage (m)');
% axis ([-0.25 0.7  0 2500]);
%
figure(3);
plot (V(:,1), V(:,2), '-b');
ylabel('Inundated volume (m^3)');
xlabel('Time (min)');
%
% figure(4);
```

```
% plot (As(:,1), As(:,2), '-b');
% ylabel('Inundated area (m^2)');
% xlabel('Time (min)');
%
% figure(5);
% plot (Q(:,1), Q(:,2), '-b');
% ylabel('Discharge (m^3/min)');
% xlabel('Time (min)');
%
% for i=1:length(Q);
%     H(i)=h(i,2);
% end;
% H=H';
%
% figure (6);
% plot (Q(:,2),H(:,1));
% ylabel('Stage (m)');
% xlabel ('Discharge (m^3/min)');
% axis ([-1.5 1.5  0 0.45]);
%
'end'
```

7.4Calibration code

```
clear all
close all
clc

%Calibration

% Set points used to calibrate as global variables

global C;

% Set parameters that are not calibrated as global variables

global Z0; % Initial conditions vector
global DataIN; % Concentrations in entering water vector
global K; % Kinetic constants vector
global theta; % Arrhenius constants vector
global T; % Temperature
global P; % Phytoplankton
global B; % Vegetation biomass
global soilthick; % Reactive soil layer thickness
global As; % Inundated area as a function of time
global Sin;
global Q0;
global Q; % Discharge exiting
global Qin; % Discharge entering
% global Vsoil; % Reactive volume of soil
% global L; % Likelihood function

% Read the output of the hydraulic submodel

Discharge = fopen ('Discharge3.txt', 'r');
Q0 = fscanf (Discharge, '%g %g', [2 inf]);
fclose (Discharge);
Q0=Q0';
```

```
Volume = fopen ('Volume3.txt', 'r');
V = fscanf (Volume, '%g %g', [2 inf]);
fclose (Volume);
V=V';

Sub_Area = fopen ('SubArea3.txt', 'r');
As = fscanf (Sub_Area, '%g %g', [2 inf]);
fclose (Sub_Area);
As=As';

Concentrazioni = fopen ( 'Concentrazioni3.txt' , 'r');
C = fscanf ( Concentrazioni , '%g %g' , [5 inf] );
fclose ( Concentrazioni );
C=C';

Phyto = fopen ( 'Phyto.txt' , 'r');
P = fscanf ( Phyto , '%g %g' , [2 inf] );
fclose ( Phyto );
P=P';

Biomass = fopen ( 'Biomass.txt' , 'r');
B = fscanf ( Biomass , '%g %g' , [2 inf] );
fclose ( Biomass );
B=B';

OSSERV = fopen ('osservazioni.txt', 'r');
OSS = fscanf (OSSERV, '%g', [1 inf]);
fclose (OSSERV);
OSS=OSS';


tspan=[1:1:length(Q0)];

%Create two vectors for entering and exiting discharge

for i=1:length(tspan);
    Q0(i,2)=Q0(i,2);
    Q(i,1)=Q0(i,1);
    Q(i,2)=Q0(i,2);
    Qin(i,1)=tspan(i);
end;

Qin(:,2)=zeros(1,length(tspan));

for i=1:length(tspan);
    if Q(i,2)>0;
        Qin(i,2)=Q0(i,2);
        Q(i,2)=0;
    else
        Q(i,2)=abs(Q(i,2));
    end;
end;

theta = 1.01;
soilthick = 0.1; %[m]

B=B(6,2);
P=P(6,2);
```

```
OS=OSS(3,1);


% Read initial ammonia concentration values and transform them in mass values

Data_IN = fopen ('Canal_IN_3.txt', 'r');
DataIN = fscanf (Data_IN, '%g %g', [4 inf]);
fclose (Data_IN);
DataIN=DataIN';

MAin=DataIN(1,2)*V(1,2);
MNin=DataIN(1,3)*V(1,2);
MDin=DataIN(1,4)*V(1,2);

Sin=C(1,5);
Vsoil=110; % [m3] Volume of soil that exchanges nitrogen with water
% MSin=Sin*Vsoil;

V0=0; % [m3] initial volume occupied by water
G0=0; % [mgN/l] Denitrified nitrogen at time t=0
% F0=0; % [mgN/l] Nitrogen uptaken from sediment at time t=0

Temperature = fopen ('Temperature3.txt', 'r');
T = fscanf (Temperature, '%g %g', [2 inf]);
fclose (Temperature);
T=T';

kAU=0.002; % [1/m] ammonia uptake (by vegetation) reaction constant
kAUP=0.01; % [1/m] ammonia uptake (by PON) reaction constant
kNU=5e-06; % [1/m] nitrate uptake (by vegetation) reaction constant
kNUP=0.001; % [1/m] nitrate uptake (by PON) reaction constant
kDEXB=4.5e-06; % [1/m] DON exudation/release/death (by biomass) reaction
constant
kDEXP=1e-6; % [1/m] DON exudation/release/death (by PON) reaction constant

knitr=0.0024; % [1/m] nitrification reaction constant
khydrD=0.0034; % [1/m] DON hydrolysis reaction constant
kdenitr=0.0027; % [1/m] denitrification reaction constant

% kSB=1.73e-4; % [1/m] biomass stocked in sediments
% kSP=0.001; % [1/m] particulated stocked in sediments
%
% kSUB=9.64e-7; % [1/m] Uptake of soil nitrogen by plants
kRA=1e-7; % [1/m] Ammonia release from soil
kRN=1e-7; % [1/m] Nitrate release from soil
kRD=1e-7; % [1/m] DON release from soil

Z0=[V0,MAin, MNin, MDin, G0];
K=[kAU, kAUP, kNU, kNUP, kDEXB, kDEXP, knitr, khydrD, kdenitr, kRA, kRN, kRD];

param = [kAU kNU kDEXB knitr khydrD kdenitr kRD];

r_kAU=[0.0001 0.009];
% r_kAUP=[0.0001 0.1];
r_kNU=[0.000001 0.000009];
% r_kNUP=[0.0001 0.01];
r_kDEXB=[0.000001 0.00009];
% r_kDEXP=[10^-7 10^-5];
```

```
r_knitr=[0.001 0.5];
r_khydrD=[0.0001 0.09];
r_kdenitr=[0.0001 0.09];
% r_kRA=[10^-8 10^-6];
% r_kRN=[10^-8 10^-6];
r_kRD=[10^-8 10^-7];



% Upper and lower bound of parameters

lb=[r_kAU(1) r_kNU(1) r_kDEXB(1) r_knitr(1) r_khydrD(1) r_kdenitr(1) r_kRD(1)];
%      r_kRD(1)];
ub=[r_kAU(2) r_kNU(2) r_kDEXB(2) r_knitr(2) r_khydrD(2) r_kdenitr(2) r_kRD(2)];
%     r_kRD(2)];

% lb=[r_kAU(1) r_knitr(1) r_kdenitr(1)];
% ub=[r_kAU(2) r_knitr(2) r_kdenitr(2)];



% Calculation of the parameters which better fit the observed data
options = optimset('MaxFunEvals',10000,'MaxIter',5000,'Display','iter',
'FunValCheck', 'on');

[param_fit, fval] =
fmincon(@objective_fun_noV,param,[],[],[],[],lb,ub,[],options);

% global Z1

% Parameters fitted
kAU_fit=param_fit(1);
% kAUP_fit=param_fit(2);
kNU_fit=param_fit(2);
% kNUP_fit=param_fit(3);
kDEXB_fit=param_fit(3);
% kDEXP_fit=param_fit(4);
knitr_fit=param_fit(4);
khydrD_fit=param_fit(5);
kdenitr_fit=param_fit(6);
% kRA_fit=param_fit(10);
% kRN_fit=param_fit(11);
kRD_fit=param_fit(7);

'fitted parameters are'
kAU_fit
% kAUP_fit
kNU_fit
% kNUP_fit
kDEXB_fit
% kDEXP_fit
knitr_fit
khydrD_fit
kdenitr_fit
% kRA_fit
% kRN_fit
kRD_fit

% global K_fit
```

```
K_fit = [kAU_fit, kAUP, kNU_fit, kNUP, kDEXB_fit, kDEXP, knitr_fit, khydrD_fit,
kdenitr_fit,...
    kRA, kRN, kRD_fit];

[TIME Z] = ode45(@(t,z)
massbalance_noV(t,z,DataIN,Qin,Q,soilthick,As,Sin,B,P,K_fit,theta,T),tspan,Z0);

Z1=Z; % Z1 contains the concentrations (M(t)/V(t) of ammonia, Nitrate,
DON;M(t)/Vsoil for sediments)
for i=1:length(Z1)
    if Z1(i,1)<=0
        Z1(i,2)=0;
        Z1(i,3)=0;
        Z1(i,4)=0;
        Z1(i,5)=0;
    else
Z1(i,2)=Z1(i,2)./Z1(i,1); % [mg/l] Ammonia concentration
Z1(i,3)=Z1(i,3)./Z1(i,1); % [mg/l] Nitrate concentration
Z1(i,4)=Z1(i,4)./Z1(i,1); % [mg/l] DON concentration
    end
end

for i=1:length(Z1)
    if Z1(i,2)<0
        Z1(i,2)=0;
        Z1(i,3)=0;
        Z1(i,4)=0;
    else
    end
end


figure (1);
plot (TIME, Z1(:,1));
title ('dVdt');

figure (2);
plot (TIME, Z1(:,2),'-r', C(:,1), C(:,2), 'ob');
title ('NH4');
ax=gca;
ax.XGrid = 'off';
ax.YGrid = 'on';
axis ([0 inf 0 inf]);
hold on;
err=0.01*ones(size(C(:,2)));
e = errorbar(C(:,1),C(:,2),err,'o',...
    'MarkerEdgeColor','blue','MarkerFaceColor','w');
e.Color='blue';


figure (3);
plot (TIME, Z1(:,3),'-r', C(:,1), C(:,3), 'ob');
title ('NOx');
ax=gca;
ax.XGrid = 'off';
ax.YGrid = 'on';
axis ([0 inf 0 inf]);
hold on;
err=0.05*ones(size(C(:,3)));
e = errorbar(C(:,1),C(:,3),err,'o',...
```

```
    'MarkerEdgeColor','blue','MarkerFaceColor','w');
e.Color='blue';


figure (4);
plot (TIME, Z1(:,4),'-r', C(:,1), C(:,4), 'ob');
title ('DON');
ax=gca;
ax.XGrid = 'off';
ax.YGrid = 'on';
axis ([0 inf 0 inf]);
hold on;
err=0.1*ones(size(C(:,4)));
e = errorbar(C(:,1),C(:,4),err,'o',...
    'MarkerEdgeColor','blue','MarkerFaceColor','w');
e.Color='blue';


%%

% Ammonia efficiency

num=0;
den=0;
for jj=1:size(C(:,1));
num=num+(C(jj,2)-interp1(TIME,Z1(:,2),C(jj,1)))^2;
den=den+(C(jj,2)-mean(C(:,2)))^2;
end
EFF_A=1-num/den;

% Nitrate efficiency

num=0;
den=0;
for jj=1:size(C(:,1));
num=num+(C(jj,3)-interp1(TIME,Z1(:,3),C(jj,1)))^2;
den=den+(C(jj,3)-mean(C(:,3)))^2;
end
EFF_N=1-num/den;

% DON efficiency

num=0;
den=0;
for jj=1:size(C(:,1));
num=num+(C(jj,4)-interp1(TIME,Z1(:,4),C(jj,1)))^2;
den=den+(C(jj,4)-mean(C(:,4)))^2;
end
EFF_D=1-num/den;


%%
% Corrected Akaike information criterion computation

% Likelihood computation for ammonia

for ii=1:size(C(:,1));
diff(ii)=C(ii,2)-interp1(TIME,Z1(:,2),C(ii,1));
end;
```

```
L(1)=likelihood(diff);

% Likelihood computation for nitrate

for ii=1:size(C(:,1));
diff(ii)=C(ii,3)-interp1(TIME,Z1(:,3),C(ii,1));
end;
L(2)=likelihood(diff);

% Likelihood computation for DON

for ii=1:size(C(:,1));
diff(ii)=C(ii,4)-interp1(TIME,Z1(:,4),C(ii,1));
end;
L(3)=likelihood(diff);


% Total likelihood

Ltot=sum(L(:));

% AICc computation

param=param';

AICc_A=2*L(1)+2*length(param)*length(C(:,1))/(length(C(:,1))-length(param)-1);
AICc_N=2*L(2)+2*length(param)*length(C(:,1))/(length(C(:,1))-length(param)-1);
AICc_D=2*L(3)+2*length(param)*length(C(:,1))/(length(C(:,1))-length(param)-1);

AICc_tot=2*Ltot+2*length(param)*OS/(OS-length(param)-1);


'end'
```

7.5 Objective function for the calibration code

```
function differences = objective_fun_noV(param)

% Call global variables

global C;
global Z0;
global DataIN;
global K;
global theta;
global T;
global P;
global B;
global soilthick;
global As;
global Sin;
global Q0;
global Q;
global Qin;
% global Vsoil;

% tspan definition
```

```
tspan=[1:1:length(Q0)];

% Parameters definition

K=[param(1) K(2) param(2) K(4) param(3) K(6) param(4) param(5)...
    param(6) K(10) K(11) param(7)];
%%
% ODE solution
%

[TIME Z] = ode45(@(t,z)
massbalance_noV(t,z,DataIN,Qin,Q,soilthick,As,Sin,B,P,K,theta,T),tspan,Z0);


% global Z1

Z1=Z; % Z1 contains the concentrations (M(t)/V(t) of ammonia, Nitrate,
DON;M(t)/Vsoil for sediments)
for i=1:length(Z1)
    if Z1(i,1)<=0
        Z1(i,2)=0;
        Z1(i,3)=0;
        Z1(i,4)=0;
        Z1(i,5)=0;
    else
Z1(i,2)=Z1(i,2)./Z1(i,1); % [mg/l] Ammonia concentration
Z1(i,3)=Z1(i,3)./Z1(i,1); % [mg/l] Nitrate concentration
Z1(i,4)=Z1(i,4)./Z1(i,1); % [mg/l] DON concentration
    end
end

for i=1:length(Z1)
    if Z1(i,2)<0
        Z1(i,2)=0;
        Z1(i,3)=0;
        Z1(i,4)=0;
    else
    end
end

% global L

% Ammonia

for ii=1:size(C(:,1));
diff(ii)=C(ii,2)-interp1(TIME,Z1(:,2),C(ii,1));
end;
L(1)=likelihood(diff);


% Nitrate

for ii=1:size(C(:,1));
diff(ii)=C(ii,3)-interp1(TIME,Z1(:,3),C(ii,1));
end;
L(2)=likelihood(diff);
```

```
% DON

for ii=1:size(C(:,1));
diff(ii)=C(ii,4)-interp1(TIME,Z1(:,4),C(ii,1));
end;
L(3)=likelihood(diff);


Ltot=sum(L(:));

differences = Ltot;
```

7.6 Mass balance function for the calibration code

```
function dZdt=massbalance_noV(t,z,DataIN,Qin,Q,soilthick,As,Sin,B,P,K,theta,T)
%
% Parameters definition
%
% Initial conditions

Ain=interp1(DataIN(:,1),DataIN(:,2),t);
Nin=interp1(DataIN(:,1),DataIN(:,3),t);
Din=interp1(DataIN(:,1),DataIN(:,4),t);


% Kinetic constants

kAU=K(1);
kAUP=K(2);
kNU=K(3);
kNUP=K(4);
kDEXB=K(5);
kDEXP=K(6);
knitr=K(7);
khydrD=K(8);
kdenitr=K(9);
% kSB=K(10);
% kSP=K(11);
% kSUB=K(12);
kRA=K(10);
kRN=K(11);
kRD=K(12);

%Change k with T

kAU=kAU*theta^(interp1(T(:,1),T(:,2),t) -20);
kAUP=kAUP*theta^(interp1(T(:,1),T(:,2),t) -20);
kNU=kNU*theta^(interp1(T(:,1),T(:,2),t) -20);
kNUP=kNUP*theta^(interp1(T(:,1),T(:,2),t) -20);
kDEXB=kDEXB*theta^(interp1(T(:,1),T(:,2),t) -20);
kDEXP=kDEXP*theta^(interp1(T(:,1),T(:,2),t) -20);
knitr=knitr*theta^(interp1(T(:,1),T(:,2),t) -20);
khydrD=khydrD*theta^(interp1(T(:,1),T(:,2),t) -20);
kdenitr=kdenitr*theta^(interp1(T(:,1),T(:,2),t) -20);
kRA=kRA*theta^(interp1(T(:,1),T(:,2),t) -20);
kRN=kRN*theta^(interp1(T(:,1),T(:,2),t) -20);
kRD=kRD*theta^(interp1(T(:,1),T(:,2),t) -20);
```

```
% Differential equations:
% Solves for MASS

if t<450;
dVdt = interp1(Qin(:,1),Qin(:,2),t)-interp1(Q(:,1),Q(:,2),t);
else
dVdt = -z(1);
end

if z(1)<=0

dVAdt = -z(2);
dVNdt = -z(3);
dVDdt = -z(4);
DeNitro = -z(5);

else

dVAdt = (interp1(Qin(:,1),Qin(:,2),t))*Ain -(interp1(Q(:,1),Q(:,2),t))*z(2)/z(1)
- kAU*z(2)*B - kAUP*z(2)*P -...
    knitr*z(2) + khydrD*z(4) + kRA*Sin*soilthick*interp1(As(:,1),As(:,2),t);

dVNdt = (interp1(Qin(:,1),Qin(:,2),t))*Nin -
(interp1(Q(:,1),Q(:,2),t))*z(3)/z(1) - kNU*z(3)*B - kNUP*z(3)*P +...
    knitr*z(2) - kdenitr*z(3) + kRN*Sin*soilthick*interp1(As(:,1),As(:,2),t);

dVDdt = (interp1(Qin(:,1),Qin(:,2),t))*Din -(interp1(Q(:,1),Q(:,2),t))*z(4)/z(1)
+ kDEXB*B*(interp1(As(:,1),As(:,2),t)) +...
    kDEXP*P*z(1) - khydrD*z(4) + kRD*Sin*soilthick*(interp1(As(:,1),As(:,2),t));

DeNitro = kdenitr*z(3);

end


dZdt = [dVdt; dVAdt; dVNdt; dVDdt; DeNitro];
```

7.7 Global calibration code

```
clear all
close all
clc

%Calibration

% Set points used to calibrate as global variables

% global C;

% Set parameters that are not calibrated as global variables

global Z0; % Initial conditions vector
% global DataIN; % Concentrations in entering water vector
global K; % Kinetic constants vector
% global theta; % Arrhenius constants vector
```

```
% global T; % Temperature
% global P; % Phytoplankton
% global B; % Vegetation biomass
% global soilthick; % Reactive soil layer thickness
% global As; % Inundated area as a function of time
% global Sin;
% global Q0;
% global Q; % Discharge exiting
% global Qin; % Discharge entering
% global Vsoil; % Reactive volume of soil
% global L; % Likelihood function

%Initial conditions

MAin=0;
MNin=0;
MDin=0;
V0=0; % [m3] initial volume occupied by water
G0=0; % [mgN/l] Denitrified nitrogen at time t=0
% F0=0; % [mgN/l] Nitrogen uptaken from sediment at time t=0


kAU=0.0041; % [1/m] ammonia uptake (by vegetation) reaction constant
kAUP=0.01; % [1/m] ammonia uptake (by PON) reaction constant
kNU=5.00e-06; % [1/m] nitrate uptake (by vegetation) reaction constant
kNUP=0.001; % [1/m] nitrate uptake (by PON) reaction constant
kDEXB=4.50e-06; % [1/m] DON exudation/release/death (by biomass) reaction
constant
kDEXP=1e-6; % [1/m] DON exudation/release/death (by PON) reaction constant

knitr=0.0024; % [1/m] nitrification reaction constant
khydrD=0.0034; % [1/m] DON hydrolysis reaction constant
kdenitr=0.0027; % [1/m] denitrification reaction constant

% kSB=1.73e-4; % [1/m] biomass stocked in sediments
% kSP=0.001; % [1/m] particulated stocked in sediments
%
% kSUB=9.64e-7; % [1/m] Uptake of soil nitrogen by plants
kRA=0; % [1/m] Ammonia release from soil
kRN=0; % [1/m] Nitrate release from soil
kRD=1e-7; % [1/m] DON release from soil

Z0=[V0, MAin, MNin, MDin, G0];
K=[kAU, kAUP, kNU, kNUP, kDEXB, kDEXP, knitr, khydrD, kdenitr, kRA, kRN, kRD];

param = [kAU kNU kDEXB knitr khydrD kdenitr kRA kRN kRD];

r_kAU=[0.0001 0.09];
% r_kAUP=[0.0001 0.1];
r_kNU=[0.000001 0.000009];
% r_kNUP=[0.0001 0.01];
r_kDEXB=[0.000001 0.00009];
% r_kDEXP=[10^-7 10^-5];
r_knitr=[0.001 0.5];
r_khydrD=[0.0001 0.09];
r_kdenitr=[0.0001 0.09];
r_kRA=[0 10^-7];
r_kRN=[0 10^-7];
r_kRD=[10^-8 10^-6];
```

```
% Upper and lower bound of parameters

lb=[r_kAU(1) r_kNU(1) r_kDEXB(1) r_knitr(1) r_khydrD(1) r_kdenitr(1) r_kRA(1)...
    r_kRN(1) r_kRD(1)];

ub=[r_kAU(2) r_kNU(2) r_kDEXB(2) r_knitr(2) r_khydrD(2) r_kdenitr(2) r_kRA(2)...
    r_kRN(2) r_kRD(2)];


% Calculation of the parameters which better fit the observed data
options = optimset('MaxFunEvals',10000,'MaxIter',5000,'Display','iter',
'FunValCheck', 'on');

[param_fit, fval] =
fmincon(@objective_fun_long,param,[],[],[],[],lb,ub,[],options);


% Parameters fitted
kAU_fit=param_fit(1);
% kAUP_fit=param_fit(2);
kNU_fit=param_fit(2);
% kNUP_fit=param_fit(3);
kDEXB_fit=param_fit(3);
% kDEXP_fit=param_fit(4);
knitr_fit=param_fit(4);
khydrD_fit=param_fit(5);
kdenitr_fit=param_fit(6);
kRA_fit=param_fit(7);
kRN_fit=param_fit(8);
kRD_fit=param_fit(9);

'fitted parameters are'
kAU_fit
% kAUP_fit
kNU_fit
% kNUP_fit
kDEXB_fit
% kDEXP_fit
knitr_fit
khydrD_fit
kdenitr_fit
kRA_fit
kRN_fit
kRD_fit

numfiles=7;

for j=1:numfiles
    if j==2
    else
   j;
   nomefile=['Discharge' sprintf('%g',j) '.txt'];
   fi=fopen(nomefile);

   Q0 = fscanf ( fi , '%g %g' , [2 inf] );
   fclose ( fi );
   Q0=Q0';
```

```
   nomefile2=['Volume' sprintf('%g',j) '.txt'];
   fi=fopen(nomefile2);

   V = fscanf ( fi , '%g %g' , [2 inf] );
   fclose ( fi );
   V=V';

   nomefile3=['SubArea' sprintf('%g',j) '.txt'];
   fi=fopen(nomefile3);

   As = fscanf ( fi , '%g %g' , [2 inf] );
   fclose ( fi );
   As=As';

   nomefile4=['Concentrazioni' sprintf('%g',j) '.txt'];
   fi=fopen(nomefile4);

   C = fscanf ( fi , '%g %g' , [5 inf] );
   fclose ( fi );
   C=C';


Phyto = fopen ( 'Phyto_cali.txt' , 'r');
P = fscanf ( Phyto , '%g %g' , [2 inf] );
fclose ( Phyto );
P=P';

Biomass = fopen ( 'Biomass_cali.txt' , 'r');
B = fscanf ( Biomass , '%g %g' , [2 inf] );
fclose ( Biomass );
B=B';


Sin=C(1,5);
B=B(j,2);
P=P(j,2);

theta = 1.01;
soilthick = 0.1;

tspan=[1:1:length(Q0)];


   for i=1:length(tspan);
    Q0(i,2)=Q0(i,2);
    Q(i,1)=Q0(i,1);
    Q(i,2)=Q0(i,2);
    Qin(i,1)=tspan(i);
   end;

Qin(:,2)=zeros(1,length(tspan));

    for i=1:length(tspan);
    if Q(i,2)>0;
        Qin(i,2)=Q0(i,2);
        Q(i,2)=0;
    else
        Q(i,2)=abs(Q(i,2));
    end;
```

```
    end;


   nomefile5=['Canal_IN_' sprintf('%g',j) '.txt'];
   fi=fopen(nomefile5);

   DataIN = fscanf ( fi , '%g %g' , [4 inf] );
   fclose ( fi );
   DataIN=DataIN';

   nomefile6=['Temperature' sprintf('%g',j) '.txt'];
   fi=fopen(nomefile6);

   T = fscanf ( fi , '%g %g' , [2 inf] );
   fclose ( fi );
   T=T';

% global K_fit

K_fit = [kAU_fit, kAUP, kNU_fit, kNUP, kDEXB_fit, kDEXP, knitr_fit, khydrD_fit,
kdenitr_fit,...
      kRA_fit, kRN_fit, kRD_fit];

[TIME Z] = ode45(@(t,z)
massbalance_noV(t,z,DataIN,Qin,Q,soilthick,As,Sin,B,P,K_fit,theta,T),tspan,Z0);

Z1=Z; % Z1 contains the concentrations (M(t)/V(t) of ammonia, Nitrate,
DON;M(t)/Vsoil for sediments)
for i=1:length(Z1)
    if Z1(i,1)<=0
        Z1(i,2)=0;
        Z1(i,3)=0;
        Z1(i,4)=0;
        Z1(i,5)=0;
    else
Z1(i,2)=Z1(i,2)./Z1(i,1); % [mg/l] Ammonia concentration
Z1(i,3)=Z1(i,3)./Z1(i,1); % [mg/l] Nitrate concentration
Z1(i,4)=Z1(i,4)./Z1(i,1); % [mg/l] DON concentration
    end
end

for i=1:length(Z1)
    if Z1(i,2)<0
        Z1(i,2)=0;
        Z1(i,3)=0;
        Z1(i,4)=0;
    else
    end
end


% Ammonia efficiency

num=0;
den=0;
for jj=1:size(C(:,1));
num=num+(C(jj,2)-interp1(TIME,Z1(:,2),C(jj,1)))^2;
den=den+(C(jj,2)-mean(C(:,2)))^2;
end
```

```
NUM_A(j)=num;
DEN_A(j)=den;

% Nitrate efficiency

num=0;
den=0;
for jj=1:size(C(:,1));
num=num+(C(jj,3)-interp1(TIME,Z1(:,3),C(jj,1)))^2;
den=den+(C(jj,3)-mean(C(:,3)))^2;
end
NUM_N(j)=num;
DEN_N(j)=den;


% DON efficiency

num=0;
den=0;
for jj=1:size(C(:,1));
num=num+(C(jj,4)-interp1(TIME,Z1(:,4),C(jj,1)))^2;
den=den+(C(jj,4)-mean(C(:,4)))^2;
end
NUM_D(j)=num;
DEN_D(j)=den;

%%
% Corrected Akaike information criterion computation

% Likelihood computation for ammonia

for ii=1:size(C(:,1));
diff(ii)=C(ii,2)-interp1(TIME,Z1(:,2),C(ii,1));
end;
L_A(j)=likelihood(diff);

% Likelihood computation for nitrate

for ii=1:size(C(:,1));
diff(ii)=C(ii,3)-interp1(TIME,Z1(:,3),C(ii,1));
end;
L_N(j)=likelihood(diff);

% Likelihood computation for DON

for ii=1:size(C(:,1));
diff(ii)=C(ii,4)-interp1(TIME,Z1(:,4),C(ii,1));
end;
L_D(j)=likelihood(diff);


clearvars Q As V C T DataIN Qin QO Z Z1 tspan

    end

end

%Global efficiencies
```

```
NUM_A_tot=sum(NUM_A(:));
NUM_N_tot=sum(NUM_N(:));
NUM_D_tot=sum(NUM_D(:));

DEN_A_tot=sum(DEN_A(:));
DEN_N_tot=sum(DEN_N(:));
DEN_D_tot=sum(DEN_D(:));

EFF_A_tot=1-NUM_A_tot/DEN_A_tot;
EFF_N_tot=1-NUM_N_tot/DEN_N_tot;
EFF_D_tot=1-NUM_D_tot/DEN_D_tot;


% Total likelihood

L_A_tot=sum(L_A(:));
L_N_tot=sum(L_N(:));
L_D_tot=sum(L_D(:));

L=L_A_tot+L_N_tot+L_D_tot;

% AICc computation

param=param';

AICc=2*L+2*length(param)*(105/(105-length(param)-1));



'end'
```

7.8 Objective function for the global calibration code

```
function differences = objective_fun_long(param)

% Call global variables

% global C;
global Z0;
% global DataIN;
global K;
% global theta;
% global T;
% global P;
% global B;
% global soilthick;
% global As;
% global Sin;
% global Q0;
% global Q;
% global Qin;
% global Vsoil;
```

```
theta = 1.01;
soilthick = 0.1; %[m]
Vsoil=110;

numfiles=7;

for j=1:numfiles
    if j==2
    else
   j;
   nomefile=['Discharge' sprintf('%g',j) '.txt'];
   fi=fopen(nomefile);

   Q0 = fscanf ( fi , '%g %g' , [2 inf] );
   fclose ( fi );
   Q0=Q0';

   nomefile2=['Volume' sprintf('%g',j) '.txt'];
   fi=fopen(nomefile2);

   V = fscanf ( fi , '%g %g' , [2 inf] );
   fclose ( fi );
   V=V';

   nomefile3=['SubArea' sprintf('%g',j) '.txt'];
   fi=fopen(nomefile3);

   As = fscanf ( fi , '%g %g' , [2 inf] );
   fclose ( fi );
   As=As';

   nomefile4=['Concentrazioni' sprintf('%g',j) '.txt'];
   fi=fopen(nomefile4);

   C = fscanf ( fi , '%g %g' , [5 inf] );
   fclose ( fi );
   C=C';


Phyto = fopen ( 'Phyto_cali.txt' , 'r');
P = fscanf ( Phyto , '%g %g' , [2 inf] );
fclose ( Phyto );
P=P';

Biomass = fopen ( 'Biomass_cali.txt' , 'r');
B = fscanf ( Biomass , '%g %g' , [2 inf] );
fclose ( Biomass );
B=B';

% Denitro = fopen ( 'dati_denitro.txt' , 'r');
% DEN = fscanf ( Denitro , '%g' , [1 inf] );
% fclose ( Denitro );
% DEN=DEN';


Sin=C(1,5);
B=B(j,2);
P=P(j,2);
% DEN=DEN(j);
```

```
tspan=[1:1:length(Q0)];


   for i=1:length(tspan);
    Q0(i,2)=Q0(i,2);
    Q(i,1)=Q0(i,1);
    Q(i,2)=Q0(i,2);
    Qin(i,1)=tspan(i);
    end;

Qin(:,2)=zeros(1,length(tspan));

    for i=1:length(tspan);
    if Q(i,2)>0;
        Qin(i,2)=Q0(i,2);
        Q(i,2)=0;
    else
        Q(i,2)=abs(Q(i,2));
    end;
    end;


   nomefile5=['Canal_IN_' sprintf('%g',j) '.txt'];
   fi=fopen(nomefile5);

   DataIN = fscanf ( fi , '%g %g' , [4 inf] );
   fclose ( fi );
   DataIN=DataIN';

   nomefile6=['Temperature' sprintf('%g',j) '.txt'];
   fi=fopen(nomefile6);

   T = fscanf ( fi , '%g %g' , [2 inf] );
   fclose ( fi );
   T=T';

% Parameters definition

K=[param(1) K(2) param(2) K(4) param(3) K(6) param(4) param(5)...
    param(6) param (7) param(8) param(9)];
%%
% ODE solution
%

[TIME Z] = ode45(@(t,z) massbalance_noV
(t,z,DataIN,Qin,Q,soilthick,As,Sin,B,P,K,theta,T),tspan,Z0);


% global Z1

Z1=Z; % Z1 contains the concentrations (M(t)/V(t) of ammonia, Nitrate,
DON;M(t)/Vsoil for sediments)
for i=1:length(Z1)
    if Z1(i,1)<=0
        Z1(i,2)=0;
        Z1(i,3)=0;
        Z1(i,4)=0;
        Z1(i,5)=0;
```

```
    else
Z1(i,2)=Z1(i,2)./Z1(i,1); % [mg/l] Ammonia concentration
Z1(i,3)=Z1(i,3)./Z1(i,1); % [mg/l] Nitrate concentration
Z1(i,4)=Z1(i,4)./Z1(i,1); % [mg/l] DON concentration
    end
end

for i=1:length(Z1)
    if Z1(i,2)<0
        Z1(i,2)=0;
        Z1(i,3)=0;
        Z1(i,4)=0;
    else
    end
end

% global L

% Ammonia

for ii=1:size(C(:,1));
diff(ii)=C(ii,2)-interp1(TIME,Z1(:,2),C(ii,1));
end;
L(1)=likelihood(diff);


% Nitrate

for ii=1:size(C(:,1));
diff(ii)=C(ii,3)-interp1(TIME,Z1(:,3),C(ii,1));
end;
L(2)=likelihood(diff);


% DON

for ii=1:size(C(:,1));
diff(ii)=C(ii,4)-interp1(TIME,Z1(:,4),C(ii,1));
end;
L(3)=likelihood(diff);


LIKE(j)=sum(L(:));


clearvars Q As V C T DataIN Qin QO Z Z1 tspan

    end

end

Ltot=sum(LIKE(:));

differences = Ltot;
```

7.9 Likelihood function

```
function like = likelihood(diff) % returns -ln(likelihood)
%
% function computing the NEGATIVE LIKELIHOOD FUNCTION
% for element i on vector of residuals diff
%
% variance

sigma=sqrt(sum(diff.^2)/length(diff));

% individual likelihoods

individ_L = exp(-0.5*(diff./sigma).^2) / sqrt(2*pi*sigma^2);
log_ind_L = log(individ_L);
log_L = sum(log_ind_L); % ln-likelihood

like = - log_L; % negative log likelihood
```

7.10 Long scale model

```
clear all
close all
clc

% Read the output of the hydraulic submodel

Discharge = fopen ('Discharge_mean.txt', 'r');
Q0 = fscanf (Discharge, '%g %g', [2 inf]);
fclose (Discharge);
Q0=Q0';

Volume = fopen ('Volume_mean.txt', 'r');
V = fscanf (Volume, '%g %g', [2 inf]);
fclose (Volume);
V=V';

Sub_Area = fopen ('SubArea_mean.txt', 'r');
As = fscanf (Sub_Area, '%g %g', [2 inf]);
fclose (Sub_Area);
As=As';

Sediment = fopen ( 'Sedimenti.txt' , 'r');
SED = fscanf ( Sediment , '%g %g' , [2 inf] );
fclose ( Sediment );
SED=SED';

SEDIM = fopen ('sedimento.txt', 'r');
S = fscanf (SEDIM, '%g %g', [3 inf]);
fclose (SEDIM);
S=S';

Temperature2 = fopen ( 'Temperature_long.txt' , 'r');
Temp = fscanf ( Temperature2 , '%g %g' , [2 inf] );
fclose ( Temperature2 );
Temp=Temp';
```

```
Phyto = fopen ( 'Phyto.txt' , 'r');
Phy = fscanf ( Phyto , '%g %g' , [2 inf] );
fclose ( Phyto );
Phy=Phy';

Biomass = fopen ( 'Biomass.txt' , 'r');
Bio = fscanf ( Biomass , '%g %g' , [2 inf] );
fclose ( Biomass );
Bio=Bio';

CONC_IN = fopen ( 'Initial_conc.txt' , 'r');
C_IN = fscanf ( CONC_IN , '%g %g' , [4 inf] );
fclose ( CONC_IN );
C_IN=C_IN';

tspan=[1:1:length(Q0)];

%Create two vectors for entering and exiting discharge

for i=1:length(tspan);
    Q0(i,2)=Q0(i,2);
    Q(i,1)=Q0(i,1);
    Q(i,2)=Q0(i,2);
    Qin(i,1)=tspan(i);
end;

Qin(:,2)=zeros(1,length(tspan));

for i=1:length(tspan);
    if Q(i,2)>0;
        Qin(i,2)=Q0(i,2);
        Q(i,2)=0;
    else
        Q(i,2)=abs(Q(i,2));
    end;
end;
%%

for i=1:12


MAin=C_IN(i,2)*V(1,2);
MNin=C_IN(i,3)*V(1,2);
MDin=C_IN(i,4)*V(1,2);
DataIN=[C_IN(i,2); C_IN(i,3); C_IN(i,4)];


Sin=SED(i,2);
Vsoil=110; % [m3] Volume of soil that exchanges nitrogen with water
% MSin=Sin*Vsoil;

V0=0; % [m3] initial volume occupied by water
G0=0; % [mgN/l] Denitrified nitrogen at time t=0
% F0=0; % [mgN/l] Nitrogen uptaken from sediment at time t=0

T=Temp(i,2);

%%
```

```
kAU=1.0162e-4; % [1/m] ammonia uptake (by vegetation) reaction constant
kAUP=0.01; % [1/m] ammonia uptake (by PON) reaction constant
kNU=1.2540e-6; % [1/m] nitrate uptake (by vegetation) reaction constant
kNUP=0.001; % [1/m] nitrate uptake (by PON) reaction constant
kDEXB=2.0984e-6; % [1/m] DON exudation/release/death (by biomass) reaction
constant
kDEXP=1e-6; % [1/m] DON exudation/release/death (by PON) reaction constant

knitr=0.0069; % [1/m] nitrification reaction constant
khydrD=1.0058e-4; % [1/m] DON hydrolysis reaction constant
kdenitr=0.0148; % [1/m] denitrification reaction constant

% kSB=1.73e-4; % [1/m] biomass stocked in sediments
% kSP=0.001; % [1/m] particulated stocked in sediments
%
% kSUB=9.64e-7; % [1/m] Uptake of soil nitrogen by plants
% kRA=1e-7; % [1/m] Ammonia release from soil
% kRN=1e-8; % [1/m] Nitrate release from soil
kRD=1.1874e-7; % [1/m] DON release from soil

theta = 1.01;
soilthick = 0.1; %[m]

B=Bio(i,2);
P=Phy(i,2);

%%

Z0=[V0,MAin, MNin, MDin, G0];
K=[kAU, kAUP, kNU, kNUP, kDEXB, kDEXP, knitr, khydrD, kdenitr, kRD];

[TIME Z] = ode45(@(t,z)
massbalance_long(t,z,DataIN,Qin,Q,soilthick,As,Sin,B,P,K,theta,T),tspan,Z0);

Z1=Z;% Z1 contains the concentrations (M(t)/V(t) of ammonia, Nitrate,
DON;M(t)/Vsoil for sediments)

for n=1:length(Z1)
    if Z1(n,1)<=0
        Z1(n,2)=0;
        Z1(n,3)=0;
        Z1(n,4)=0;
        Z1(n,5)=0;
    else
Z1(n,2)=Z1(n,2)./Z1(n,1); % [mg/l] Ammonia concentration
Z1(n,3)=Z1(n,3)./Z1(n,1); % [mg/l] Nitrate concentration
Z1(n,4)=Z1(n,4)./Z1(n,1); % [mg/l] DON concentration
    end
end

for n=1:length(Z1)
    if Z1(n,2)<0
        Z1(n,2)=0;
        Z1(n,3)=0;
        Z1(n,4)=0;
    else
    end
end
```

```
% Fluxes obtained on a single cycle (integral computation)
% Mass=integral(Q(t)*C(t))
%
% integration extremes
t1=1; % [min] lower integration bound
t2=360; % [min] upper integration bound


% Ammonia flux in [g]
ain=@(Qin,DataIN,tt) interp1(Qin(:,1),Qin(:,2),tt)*DataIN(1);
F_MAin(i)=quadgk(@(tt)ain(Qin,DataIN,tt),t1,t2); % [gN/tc]

% Nitrate flux in
nin=@(Qin,DataIN,tt) interp1(Qin(:,1),Qin(:,2),tt)*DataIN(2);
F_MNin(i)=quadgk(@(tt)nin(Qin,DataIN,tt),t1,t2); % [gN/tc]

% DON flux in
din=@(Qin,DataIN,tt) interp1(Qin(:,1),Qin(:,2),tt)*DataIN(3);
F_MDin(i)=quadgk(@(tt)din(Qin,DataIN,tt),t1,t2); % [gN/tc]

% Ammonia flux out
if i==6 || i==7
    F_MAout(i)=0;
else
nout=@(Q,Z1,tt) interp1(Q(:,1),Q(:,2),tt).*interp1(Q(:,1),Z1(:,2),tt);
F_MAout(i)=quadgk(@(tt)nout(Q,Z1,tt),t1,t2);
end

% Nitrate flux out
nout=@(Q,Z1,tt) interp1(Q(:,1),Q(:,2),tt).*interp1(Q(:,1),Z1(:,3),tt);
F_MNout(i)=quadgk(@(tt)nout(Q,Z1,tt),t1,t2); % [gN/tc]

% DON flux out
dout=@(Q,Z1,tt) interp1(Q(:,1),Q(:,2),tt).*interp1(Q(:,1),Z1(:,4),tt);
F_MDout(i)=quadgk(@(tt)dout(Q,Z1,tt),t1,t2); % [gN/tc]

% Nitrified nitrogen
F_MGout(i)=max(Z1(:,5)); % [gN]


end

F_MA = (F_MAin-F_MAout); % [gN/tc]
F_MN = (F_MNin-F_MNout); % [gN/tc]
F_MD = (F_MDin-F_MDout); % [gN/tc]

F_oneTE = F_MA + F_MN + F_MD; % [gN/tc]

A_MAX=2331.12; % [m^2]

F_MAin_month=F_MAin*60; % [gN/month]
F_MAout_month=F_MAout*60; % [gN/month]
F_MNin_month=F_MNin*60; % [gN/month]
F_MNout_month=F_MNout*60; % [gN/month]
F_MDin_month=F_MDin*60; % [gN/month]
F_MDout_month=F_MDout*60; % [gN/month]
F_MGout_month=F_MGout*60; % [gN/month]

NET_NIT = F_MNin_month - F_MNout_month; % [gN/month]
```

```
TRENDtot_IN = F_MAin_month + F_MNin_month + F_MDin_month; % [gN/month]
TRENDtot_OUT = F_MAout_month + F_MNout_month + F_MDout_month; % [gN/month]
TRENDtot=TRENDtot_IN-TRENDtot_OUT; % [gN/month]

names = {'J';'F';'M';'A'; 'M';'J';'J';'A';'S';'O';'N';'D';''};

figure (1);
plot (1:1:12, F_MAin_month/A_MAX, 'b-o','MarkerFaceColor',[1,1,1]);
hold on;
plot (1:1:12,  F_MAout_month/A_MAX, 'r-o','MarkerFaceColor',[1,1,1]);
set(gca,'xtick',[1:13],'xticklabel',names);
ax=gca;
ax.XGrid = 'off';
ax.YGrid = 'on';
axis ([0 13 0 0.06]);
legend ('N-NH4 input','N-NH4 output','Location','north');
xlabel ('month');
ylabel ('Flux (gN/m^2 month)');
set(gca,'xTickLabel',names);


figure (2);
plot (1:1:12, F_MNin_month/A_MAX, 'b-o','MarkerFaceColor',[1,1,1]);
hold on;
plot (1:1:12,  F_MNout_month/A_MAX, 'r-o','MarkerFaceColor',[1,1,1]);
set(gca,'xtick',[1:13],'xticklabel',names);
ax=gca;
ax.XGrid = 'off';
ax.YGrid = 'on';
axis ([0 13 0.0 0.9]);
legend ('N-NO3 input','N-NO3 output','Location','north');
xlabel ('month');
ylabel ('Flux (gN/m^2 month)');
set(gca,'xTickLabel',names);


figure (3);
plot (1:1:12, F_MDin_month/A_MAX, 'b-o','MarkerFaceColor',[1,1,1]);
hold on;
plot (1:1:12,  F_MDout_month/A_MAX, 'r-o','MarkerFaceColor',[1,1,1]);
set(gca,'xtick',[1:13],'xticklabel',names);
ax=gca;
ax.XGrid = 'off';
ax.YGrid = 'on';
axis ([0 13 0.0 0.35]);
legend ('DON input','DON output','Location','north');
xlabel ('month');
ylabel ('Flux (gN/m^2 month)');
set(gca,'xTickLabel',names);


figure (4);
plot (1:1:12, TRENDtot_IN/A_MAX , 'b-o','MarkerFaceColor',[1,1,1]);
hold on;
plot (1:1:12, TRENDtot_OUT/A_MAX, 'r-o','MarkerFaceColor',[1,1,1]);
set(gca,'xtick',[1:13],'xticklabel',names);
ax=gca;
ax.XGrid = 'off';
ax.YGrid = 'on';
```

```
axis ([0 13 0 1.2]);
legend ('TDN input','TDN output','Location','north');
xlabel ('month');
ylabel ('Flux (gN/m^2 month)');
set(gca,'xTickLabel',names);


figure (5);
plot (1:1:12, TRENDtot/A_MAX, 'b-o','MarkerFaceColor',[1,1,1]);
set(gca,'xtick',[1:13],'xticklabel',names);
ax=gca;
ax.XGrid = 'off';
ax.YGrid = 'on';
axis ([0 13 0 0.70]);
xlabel ('month');
ylabel ('Flux (gN/m^2 month)');
set(gca,'xTickLabel',names);


figure (6);
plot (1:1:12, F_MGout_month/A_MAX , 'b-o','MarkerFaceColor',[1,1,1]);
hold on;
plot (1:1:12, NET_NIT/A_MAX, 'r-o','MarkerFaceColor',[1,1,1]);
set(gca,'xtick',[1:13],'xticklabel',names);
ax=gca;
ax.XGrid = 'off';
ax.YGrid = 'on';
axis ([0 13 0 0.9]);
legend ('Actual denitrification','Potential denitrification [(N-NO3 IN) - (N-NO3
OUT)]','Location','north');
xlabel ('month');
ylabel ('Flux (gN/m^2 month)');
set(gca,'xTickLabel',names);


% Fluxes of biomass and sediments

Bio1=[Bio(12,2); Bio(:,2)]; % [gN/m^2 mese]
Sed1=[SED(12,2); SED(:,2)]; % [gN/m^3 mese]
for i=1:12;
MB(i)=(Bio1(i+1)-Bio1(i))*A_MAX; % [gN/mese]
MS(i)=(Sed1(i+1)-Sed1(i))*Vsoil; % [gN/mese]
end;

MB_corr=MB/A_MAX;
MS_corr=MS/A_MAX;

figure (7);
plot (1:1:12, MB_corr , 'b-o','MarkerFaceColor',[1,1,1]);
set(gca,'xtick',[1:13],'xticklabel',names);
ax=gca;
ax.XGrid = 'off';
ax.YGrid = 'on';
axis ([0 13 -1.5 2.5]);
set(gca,'yTick',-1.5:0.5:2.5);
xlabel ('month');
ylabel ('Flux (gN/m^2 month)');
set(gca,'xTickLabel',names);

figure (8);
```

```
plot (1:1:12, MS_corr , 'b-o','MarkerFaceColor',[1,1,1]);
set(gca,'xtick',[1:13],'xticklabel',names);
ax=gca;
ax.XGrid = 'off';
ax.YGrid = 'on';
axis ([0 13 -50 30]);
% set(gca,'yTick',-0.25:0.05:0.15);
xlabel ('month');
ylabel ('Flux (gN/m^2 month)');
set(gca,'xTickLabel',names);

% Total fluxes computation

% Total mass exchanged in one year during a tidal cycle [kg]


MTAin=sum(F_MAin_month(:))/A_MAX; % [gN] Ammonia flux entering
MTNin=sum(F_MNin_month(:))/A_MAX; % [gN] Nitrate flux entering
MTDin=sum(F_MDin_month(:))/A_MAX; % [gN] DON flux entering
MTAout=sum(F_MAout_month(:))/A_MAX; % [gN] Ammonia flux exiting -> this flux is
practically zero
MTNout=sum(F_MNout_month(:))/A_MAX; % [gN] Nitrate flux exiting
MTDout=sum(F_MDout_month(:))/A_MAX; % [gN] DON flux exiting
MTGout=sum(F_MGout_month(:))/A_MAX; % [gN] Nitrogen gas exiting
MTS=sum(MS(:)); % [gN] Sediments
MTB=sum(MB(:)); % [gN] Biomass

% Net Ammonia, Nitrate, DON fluxes exchanged in one year [gN/y]
deltaA=MTAin-MTAout; % [gN] Ammonia retained in the salt marsh
deltaN=MTNin-MTNout; % [gN] Nitrate retained in the salt marsh
deltaD=MTDin-MTDout; % [gN] DON retained in the salt marsh

deltaTOT=deltaA + deltaN + deltaD; % [gN]

% A_MAX=max(As(:,2)); % [m^2]


for i=1:12
TRENDtot_in_MQ(i)=((TRENDtot_IN(i))/A_MAX)+0.12+S(i,2);
TRENDtot_out_MQ(i)=((TRENDtot_OUT(i))/A_MAX);
end

TRENDtot_corr = TRENDtot_in_MQ -TRENDtot_out_MQ;

CAPAC=deltaTOT; % [gN/m^2]
CAPAC_corr=sum(TRENDtot_corr(:)); % [gN/m^2]


figure (9);
plot (1:1:12, TRENDtot_in_MQ, 'b-o','MarkerFaceColor',[1,1,1]);
hold on;
plot (1:1:12, TRENDtot_out_MQ, 'r-o','MarkerFaceColor',[1,1,1]);
set(gca,'xtick',[1:13],'xticklabel',names);
ax=gca;
ax.XGrid = 'off';
ax.YGrid = 'on';
axis ([0 13 0 2]);
% set(gca,'ytick',[8.6:0.1:9.8]);
legend ('Total N INPUT','Total N OUTPUT','Location','north');
```

```
xlabel ('month');
ylabel ('Flux (gN/m^2 month)');
set(gca,'xTickLabel',names);

figure (10);
plot (1:1:12, TRENDtot_corr , 'b-o','MarkerFaceColor',[1,1,1]);
set(gca,'xtick',[1:13],'xticklabel',names);
ax=gca;
ax.XGrid = 'off';
ax.YGrid = 'on';
axis ([0 13 0.6 1.5]);
xlabel ('month');
ylabel ('Flux (gN/m^2 month)');
set(gca,'xTickLabel',names);

'end'
```

7.11 Mass balance function for the long scale model

```
function dZdt=massbalance_long(t,z,DataIN,Qin,Q,soilthick,As,Sin,B,P,K,theta,T)
%
% Parameters definition
%
% Initial conditions

Ain=DataIN(1);
Nin=DataIN(2);
Din=DataIN(3);


% Kinetic constants

kAU=K(1);
kAUP=K(2);
kNU=K(3);
kNUP=K(4);
kDEXB=K(5);
kDEXP=K(6);
knitr=K(7);
khydrD=K(8);
kdenitr=K(9);
% kSB=K(10);
% kSP=K(11);
% kSUB=K(12);
% kRA=K(10);
% kRN=K(11);
kRD=K(10);

%Change k with T

kAU=kAU*theta^(T-20);
kAUP=kAUP*theta^(T-20);
kNU=kNU*theta^(T-20);
kNUP=kNUP*theta^(T-20);
kDEXB=kDEXB*theta^(T-20);
kDEXP=kDEXP*theta^(T -20);
knitr=knitr*theta^(T -20);
khydrD=khydrD*theta^(T -20);
```

```
kdenitr=kdenitr*theta^(T -20);
% kRA=kRA*theta^(T -20);
% kRN=kRN*theta^(T -20);
kRD=kRD*theta^(T -20);

% Differential equations:
% Solves for MASS

if t<450;
dVdt = interp1(Qin(:,1),Qin(:,2),t)-interp1(Q(:,1),Q(:,2),t);
else
dVdt = -z(1);
end

if z(1)<=0

dVAdt = -z(2);
dVNdt = -z(3);
dVDdt = -z(4);
DeNitro = -z(5);

else

dVAdt = (interp1(Qin(:,1),Qin(:,2),t))*Ain -(interp1(Q(:,1),Q(:,2),t))*z(2)/z(1)
- kAU*z(2)*B - kAUP*z(2)*P -...
    knitr*z(2) + khydrD*z(4);% + kRA*Sin*soilthick*interp1(As(:,1),As(:,2),t);

dVNdt = (interp1(Qin(:,1),Qin(:,2),t))*Nin -
(interp1(Q(:,1),Q(:,2),t))*z(3)/z(1) - kNU*z(3)*B - kNUP*z(3)*P +...
    knitr*z(2) - kdenitr*z(3);% + kRN*Sin*soilthick*interp1(As(:,1),As(:,2),t);

dVDdt = (interp1(Qin(:,1),Qin(:,2),t))*Din -(interp1(Q(:,1),Q(:,2),t))*z(4)/z(1)
+ kDEXB*B*(interp1(As(:,1),As(:,2),t)) +...
    kDEXP*P*z(1) - khydrD*z(4) + kRD*Sin*soilthick*(interp1(As(:,1),As(:,2),t));

DeNitro = kdenitr*z(3);

end


dZdt = [dVdt; dVAdt; dVNdt; dVDdt; DeNitro];
```

7.12 Numerical data of samples concentrations

Values signed with “<0.01” are considered as zero, because they have a concentration lower than the one that the spectrophotometer can detect.

7.12.1 April 2017

	SURFACE OF THE CHANNEL			
	$N\text{-}NH_4^+$	$N\text{-}NO_3^-$	*DON*	$P\text{-}PO_4^{3-}$
11:15	0.05	0.13	0.74	0.02
14:30	0.02	0.09	0.46	0.01
16:45	0.04	0.08	0.52	0.01

	BOTTOM OF THE CHANNEL			
	$N\text{-}NH_4^+$	$N\text{-}NO_3^-$	*DON*	$P\text{-}PO_4^{3-}$
11:20	0.06	0.33	0.49	0.01
14:30	0.07	0.03	0.57	<0.01
16:45	0.05	0.03	0.58	0.01

	SALT MARSH CREEK			
	$N\text{-}NH_4^+$	$N\text{-}NO_3^-$	*DON*	$P\text{-}PO_4^{3-}$
11:10	0.11	0.69	0.32	0.03
12:10	0.09	0.41	0.48	0.01
13:00	0.06	0.26	0.40	<0.01
13:45	0.04	0.15	0.33	0.01
14:50	0.04	0.01	0.60	0.01
15:45	0.03	0.04	0.52	0.01
16:25	0.03	0.11	0.53	0.01
17:00	0.04	0.21	0.40	0.01

7.12.2 May 2017

	SURFACE OF THE CHANNEL			
	$N\text{-}NH_4^+$	$N\text{-}NO_3^-$	*DON*	$P\text{-}PO_4^{3-}$
10:53	0.08	0.02	0.67	0.01
13:23	0.02	0.12	0.59	0.02
15:53	0.05	0.09	0.77	0.02

	BOTTOM OF THE CHANNEL			
	$N\text{-}NH_4^+$	$N\text{-}NO_3^-$	*DON*	$P\text{-}PO_4^{3-}$
11:00	0.05	0.13	0.63	0.06
13:23	0.03	0.11	0.51	0.01
16:00	0.14	0.15	0.54	0.02

	SALT MARSH CREEK			
	$N\text{-}NH_4^+$	$N\text{-}NO_3^-$	*DON*	$P\text{-}PO_4^{3-}$
11:22	0.13	0.12	1.70	0.03
12:20	0.07	0.41	0.66	0.03
12:30	0.09	0.41	0.56	0.03
13:05	0.07	0.37	0.58	0.02
13:15	0.06	0.34	0.68	0.03
13:55	0.01	0.14	0.93	0.02
15:25	0.05	0.06	1.24	0.05

7.12.3 June 2016

	SURFACE OF THE CHANNEL		
	$N\text{-}NH_4^+$	$N\text{-}NO_3^-$	*DON*
13.19	0.18	1.16	0.38
14.14	0.20	0.96	1.03
15.34	0.07	0.30	0.45
16.18	0.07	0.40	0.40
16.54	0.08	0.32	0.41
17.33	0.17	0.22	0.33
18.07	0.13	0.25	0.11
18.23	0.08	0.24	0.32
18.34	0.13	0.27	0.42

	SALT MARSH CREEK		
	$N\text{-}NH_4^+$	$N\text{-}NO_3^-$	*DON*
14.28	0.16	1.03	0.76
15.41	0.08	0.67	0.51
16.23	0.11	0.65	0.54
16.59	0.11	0.65	0.56
17.39	0.17	0.50	0.44
18.12	0.11	0.53	0.43
18.28	0.12	0.58	0.03
18.42	0.08	0.46	0.56

7.12.4 June 2017

	SURFACE OF THE CHANNEL			
	$N\text{-}NH_4^+$	$N\text{-}NO_3^-$	*DON*	$P\text{-}PO_4^{3-}$
11:44	0.03	0.36	1.06	0.01
15:53	<0.01	0.02	0.71	0.01
17:50	<0.01	0.03	0.77	0.01

	BOTTOM OF THE CHANNEL			
	$N\text{-}NH_4^+$	$N\text{-}NO_3^-$	*DON*	$P\text{-}PO_4^{3-}$
11:57	0.02	0.46	0.44	0.02
15:56	<0.01	0.02	0.60	0.01
17:57	<0.01	0.03	0.54	0.01

	SALT MARSH CREEK			
	$N\text{-}NH_4^+$	$N\text{-}NO_3^-$	*DON*	$P\text{-}PO_4^{3-}$
12:58	0.01	0.31	0.95	0.02
13:30	0.02	0.21	0.85	0.01
14:30	0.01	0.06	1.11	0.00
15:28	0.01	0.05	0.98	0.01
16:37	<0.01	0.07	1.08	0.01
17:27	<0.01	0.01	1.91	0.02

7.12.5 July 2017

	SURFACE OF THE CHANNEL			
	$N\text{-}NH_4^+$	$N\text{-}NO_3^-$	*DON*	$P\text{-}PO_4^{3-}$
12:47	<0.01	0.06	0.52	0.01
16:13	<0.01	0.08	0.53	0.01
18:27	<0.01	<0.01	0.55	0.01

	BOTTOM OF THE CHANNEL			
	$N\text{-}NH_4^+$	$N\text{-}NO_3^-$	*DON*	$P\text{-}PO_4^{3-}$
12:51	<0.01	<0.01	0.63	0.02
16:11	<0.01	0.01	0.62	0.01
18:25	<0.01	0.03	0.30	0.01

	SALT MARSH CREEK			
	$N\text{-}NH_4^+$	$N\text{-}NO_3^-$	*DON*	$P\text{-}PO_4^{3-}$
12:28	0.01	0.42	0.61	0.01
13:20	<0.01	0.14	0.75	0.01
14:32	<0.01	0.01	0.66	0.01
15:35	<0.01	0.00	0.74	0.01
16:39	<0.01	0.01	0.67	0.01
17:25	<0.01	0.01	0.72	0.01
18:15	<0.01	0.00	0.42	0.01

7.12.6 August 2015

	SURFACE OF THE CHANNEL		
	$N\text{-}NH_4^+$	$N\text{-}NO_3^-$	*DON*
10.15	0.03	0.05	0.64
13.11	0.01	0.01	0.69
15.50	0.01	0.03	1.17

	SALT MARSH CREEK		
	$N\text{-}NH_4^+$	$N\text{-}NO_3^-$	*DON*
10:12	0.06	0.22	0.44
11:00	0.01	0.19	0.54
11:50	0.01	0.15	0.85
12:50	0.01	0.14	0.84
14:51	0.02	0.11	1.01
15:40	0.01	0.03	0.92
15:50	0.01	0.03	1.17

7.12.7 September 2017

	SURFACE OF THE CHANNEL			
	$N\text{-}NH_4^+$	$N\text{-}NO_3^-$	*DON*	$P\text{-}PO_4^{3-}$
10:46	0.01	0.29	0.38	0.01
13:28	0.01	0.04	0.64	0.01
16:02	0.01	0.10	0.38	0.01

	BOTTOM OF THE CHANNEL			
	$N\text{-}NH_4^+$	$N\text{-}NO_3^-$	*DON*	$P\text{-}PO_4^{3-}$
10:48	0.02	0.21	0.51	0.01
13:27	0.01	0.04	0.61	0.01
16:00	0.01	0.11	0.38	0.01

	SALT MARSH CREEK			
	$N\text{-}NH_4^+$	$N\text{-}NO_3^-$	*DON*	$P\text{-}PO_4^{3-}$
10:50	0.04	0.44	0.46	0.01
11:42	0.01	0.25	0.36	0.01
12:28	0.02	0.07	0.61	0.01
13:28	0.02	0.02	0.53	0.01
14:16	0.02	0.02	0.53	0.01
15:15	0.02	0.01	0.62	0.01
15:52	0.02	<0.01	0.42	0.01

7.12.8 October 2017

	SURFACE OF THE CHANNEL			
	$N\text{-}NH_4^+$	$N\text{-}NO_3^-$	*DON*	$P\text{-}PO_4^{3-}$
09:45	0.02	0.27	0.36	0.01
11:50	0.01	0.24	0.30	0.01
14:11	<0.01	0.36	0.34	0.01

	BOTTOM OF THE CHANNEL			
	$N\text{-}NH_4^+$	$N\text{-}NO_3^-$	*DON*	$P\text{-}PO_4^{3-}$
09:50	0.02	0.30	0.31	0.01
11:47	0.01	0.24	0.30	0.01
14:13	0.01	0.41	0.18	0.01

	SALT MARSH CREEK			
	$N\text{-}NH_4^+$	$N\text{-}NO_3^-$	*DON*	$P\text{-}PO_4^{3-}$
09:45	0.02	0.45	0.44	0.02
10:33	0.02	0.36	0.42	0.01
11:17	0.01	0.28	0.40	0.01
11:55	0.01	0.24	0.33	<0.01
12:55	0.01	0.27	0.39	0.01
13:54	0.01	0.20	0.37	0.01